Abstract

A *Wolbachia* Nuclease and Its Binding Partner Provide a Novel Mechanism for Cytoplasmic Incompatibility

Hongli Chen

2020

Wolbachia are maternally inherited obligate bacterial endosymbionts that infect nearly half of all arthropod species, a success largely due to their ability to selfishly manipulate host reproduction to favor infected females. Cytoplasmic incompatibility (CI), a phenomenon where *Wolbachia* infection renders male insects sterile when they mate with uninfected females, is the most common type of these manipulations. Since matings between infected females and infected (the "Rescue" cross) or uninfected males are both fully compatible, *Wolbachia* infection provides a selective advantage to infected females who in turn help the bacteria propagate in a population through the infected female germline.

For decades, *Wolbachia* and CI have been utilized as a strategy to control agricultural pests and reduce the spread of vector-borne human diseases. The most promising application involves using *Wolbachia* in mosquito population control through either sterilizing male mosquitoes or using a population replacement method that exploits *Wolbachia*'s ability to provide the host with resistance to mosquito-borne viruses. Release of *Wolbachia*-infected mosquitos is EPA-approved in 20 states in the United States with the most recent large-scale release being conducted in Miami in an effort to reduce the population of *Aedes aegypti*, a mosquito vector for Zika virus.

CI embryos showed abnormal phenotypes during early developmental stages, generally resulting in embryonic death before hatching in many insect species. The incompatibility between *Wolbachia*-infected sperm and uninfected egg is due to the asynchronous development of male and female pronuclei at the early stage of mitosis after fertilization. The earliest observable embryonic defect from an incompatible CI cross between infected male and uninfected female is a delayed deposition of maternal H3.3 and H4 histone in the paternal pronuclei immediately after protamine removal. Paternal activation of cell cycle kinase Cdk1 and nuclear envelope breakdown are delayed. The consequence is improper condensation of male chromosomes that fail to segregate during anaphase, causing chromatin bridging and shearing of paternal DNA that generally lead to embryonic lethality.

Despite the success of *Wolbachia* in mosquito control, the molecular mechanism of CI had long eluded identification. The discovery of the *Wolbachia* two-gene *cif* (CI factor) operons as the main contributor of CI marks a major step in understanding its molecular mechanism. Within each *cif* operon, the downstream gene is annotated as the B gene while the upstream gene is annotated as the A gene. These operons were further divided into two groups based on the enzymatic activity of the B proteins; a *cid* (CI-inducing deubiquitylase) type which encodes deubiquitylases and a *cin* (CI-inducing nuclease) type which encodes nucleases. Significant progress has been made in recent years on understanding the genetic and molecular relevance of the *cid* genes on *Wolbachia*-induced CI. Expression of the *cid* operon in transgenic male *Drosophila melanogaster* induces CI-like postzygotic male sterility through interference with embryonic nuclear division. Transgenic expression of *cidA* gene in female flies can

rescue both transgenic CI and natural CI caused by male flies infected with *Wolbachia*. A large-scale population genomic screen of *Culex* mosquitoes linked crossing-type diversity in CI among mosquitoes infected with different *w*Pip *Wolbachia* strains to genetic variations in the *cid* operon, further highlighting the important role of the *cid* genes in CI.

The facts that some CI-inducing *Wolbachia* strains, such as the *w*No strain that infects *Drosophila simulans*, contain only *cin* but not *cid* type operons and that neither operon is present in *w*Au, a close relative of *w*Mel that does not induce CI, suggested that the *cin* type operon should also be able to induce CI independent of the *cid* operon. Recent genetic analyses have uncovered natural variation in both *cid* and *cin* loci that correlates with CI in different *Wolbachia*-infected *Drosophila* species. While this supports previous speculations on the possible function of the *cin* operon in CI, the ability of these genes to cause CI had not been experimentally tested. Similarly, while there are distant sequence similarities between CinB and the PD-(D/E)xK superfamily of nucleases, no nuclease activity has been demonstrated. In this thesis work, I show that CinB has DNase activity. Mutation of putative active-site residues in either CinB PD-(D/E)xK domain abolishes activity *in vitro* and renders the resulting protein nontoxic to *Saccharomyces cerevisiae*. Most importantly, the *cin* operon induces a CI-like phenotype in transgenic flies, and expression of *cinA* alone in females is sufficient for rescue of transgenic CI. Therefore, the *cin* type nuclease operon provides a biochemically distinct mechanism for CI and its presence likely accounts for the ability of many *Wolbachia* strains to induce CI in their hosts despite not carrying an intact *cid* operon.

A *Wolbachia* Nuclease and Its Binding Partner Provide a Novel Mechanism for Cytoplasmic Incompatibility

A Dissertation

Presented to the Faculty of the Graduate School

of

Yale University

in Candidacy for the Degree of

Doctor of Philosophy

by

Hongli Chen

Dissertation Director: Mark Hochstrasser

May 2020

Table of Contents

List of Tables and Figures

Chapter III

Chapter IV

Chapter V

Acknowledgments

I would first like to thank Mark Hochstrasser for his expert advice and mentorship in my PhD education. I want to thank former lab members John Beckmann and Judith Ronau for their mentorship and support during my first three years in the lab, Jason Berk and Mengwen Zhang for the weekly discussion during our subgroup meetings, and also all my fellow lab members for creating a welcoming and collaborative working environment. I would also like to thank my thesis committee members Drs. John Carlson and Christian Schlieker for providing me with constructive feedback and suggestions as well as letting me use their lab space and instruments. Lastly, I want to thank my beloved wife Jin for her constant support and encourage throughout my education and my life.

Chapter I: Introduction to *Wolbachia* and Cytoplasmic Incompatibility (CI)

i. *Wolbachia* and Its Reproductive Manipulations

Wolbachia pipientis are Gram-negative obligate intracellular bacteria that infect insects, mites, crustaceans, and filarial nematodes. They are α–proteobacteria of the order *Rickettsiales*, a diverse group of mostly intracellular bacteria. Since first discovered in *Culex pipiens* mosquitoes nearly a century ago, *Wolbachia* has been found in every insect order and up to two-thirds of all insect species (Hilgenboecker *et al.*, 2008). The success of *Wolbachia* infection is in part due to their ability to manipulate host reproduction to selectively favor infected females. Since *Wolbachia* are transmitted by vertical transmission through the infected female germline, the reproductive advantage *Wolbachia* provides to an infected female hosts enhances its own ability to propagate in an insect population (Hoffmann, Turelli and Harshman, 1990; Bressac and Rousset, 1993; Turelli and Hoffmann, 1995; Clark, Jan and Jan, 1997; Hoffmann, Hercus and Dagher, 1998).

Wolbachia-induced host manipulations include parthenogenesis, feminization of genetic males, male killing, and cytoplasmic incompatibility (Serbus *et al.*, 2008). Among these reproductive manipulations, cytoplasmic incompatibility (CI) is the most frequently found phenotype in insects. CI is a phenomenon where mating between infected males and uninfected females causes severe developmental defects in the early stages of embryogenesis, which often results in embryonic lethality (Laven, 1953; Yen and Barr, 1973; Werren, Baldo and Clark, 2008). While uninfected females can only produce viable offspring with uninfected males, infected females are capable of

producing fully viable progeny with either infected or uninfected males (**Figure 1**) (Beckmann *et al.*, 2019b).

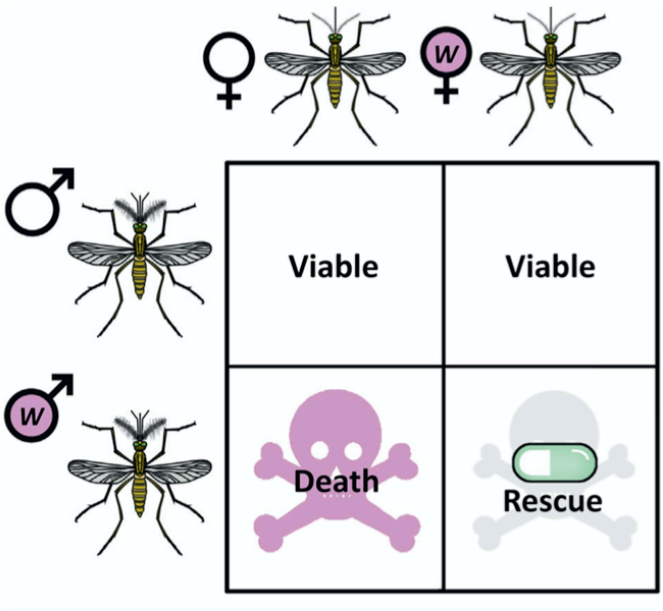

Figure 1. Illustration of cytoplasmic incompatibility. Infected females can produce viable offspring with both infected and uninfected males, whereas uninfected females can produce viable progeny only if they mate with uninfected males. Abbreviation: w, *Wolbachia*-infected. Figure adapted from Beckmann *et al*., 2019b.

CI embryos show abnormal phenotypes during early developmental stages, generally resulting in embryonic death before hatching in many insect species (Riparbelli *et al.*, 2012). The incompatibility between *Wolbachia*-infected sperm and uninfected egg is due to the asynchronous development of male and female pronuclei at the early stage of mitosis after fertilization. In normal embryonic development, following the initial nuclear envelope breakdown of male and female pronuclei, protamine proteins used to package the paternal DNA are removed and nucleosomes are assembled using maternally supplied core histones and the histone variant H3.3 (Loppin *et al.*, 2005; Balhorn, 2007; Tirmarche *et al.*, 2014; Loppin, Dubruille and Horard, 2015). The male and female pronuclei migrate towards one another. Both sets of chromosomes are replicated, condensed and then separated at anaphase creating two diploid daughter cells.

In CI embryos, the earliest detectable developmental defect is the abnormal deposition of H3.3 and H4 histone in male pronuclei following normal protamine removal from paternal DNA (Landmann *et al.*, 2009). Paternal activation of cell cycle kinase Cdk1 and nuclear envelope breakdown are delayed (Tram and Sullivan, 2002). Prolonged retention of DNA replication factor proliferating cell nuclear antigen (PCNA) was also observed in the male pronuclei, a possible indication of progression into mitosis with incompletely replicated DNA (Landmann *et al.*, 2009). The consequence is improper condensation of male chromosomes that fail to segregate during anaphase, causing chromatin bridging and shearing of paternal DNA (Reed and Werren, 1995; Lassy and Karr, 1996; Callaini, Dallai and Riparbelli, 1997; Tram *et al.*, 2006). Excess centrosomes unassociated with the maternal and paternal nuclei as well as mitotic spindles lacking centrosomes are also often observed in CI embryos, possibly a direct

outcome of delayed nuclei development and abnormal chromosome condensation (Lassy and Karr, 1996; Callaini, Dallai and Riparbelli, 1997; de Saint Phalle and Sullivan, 1998). In recent years, a group of *Wolbachia* genes called *cif* genes has been identified and shown to be the key genetic elements in *Wolbachia*-related CI. Detailed evidence supporting *cif* genes as the CI factors will be discussed in a later section of the Introduction.

Other *Wolbachia*-induced reproductive phenotypes are less common than CI. *Wolbachia*-related parthenogenesis occurs in species such as mites, wasps and thrips (Stouthamer, Luck and Hamilton, 1990; Weeks and Breeuwer, 2001; Arakaki, Miyoshi and Noda, 2001). Most of these species have haplodiploid sex determination where unfertilized eggs develop into haploid males while fertilized eggs develop into diploid females. In *Wolbachia*-induced parthenogenesis, meiosis is followed by fusion of the two nuclei from the first mitotic division, resulting in restoration of diploidy and development of diploid females which unlike males are able to transmit *Wolbachia* to their offspring (Stouthamer and Kazmer, 1994; Stouthamer, Breeuwer and Hurst, 1999). Another *Wolbachia*-related host manipulation is feminization. The exact mechanism for *Wolbachia*-induced feminization of genetic males still remains unclear (Asgharian *et al.*, 2014). Feminizing *Wolbachia* strains have been characterized in several arthropod species and most heavily studied in the common pill bug *Armadillidium vulgare* (Cordaux et al., 2004; Badawi, Greve and Cordaux, 2015). Only two insect species, *Eurema hecabe* and *Zyginidia pullulan*, are currently known to be feminized by *Wolbachia* (Hiroki *et al.*, 2002; Negri *et al.*, 2008).

Wolbachia has also been described to cause male killing in several arthropod orders (Fialho and Stevens, 2000; Jiggins *et al.*, 2001; Dyer and Jaenike, 2004; Zeh, Zeh and Bonilla, 2005). Male-killing occurs mainly during early embryogenesis resulting in more resources for the surviving female offspring. In *Ostrinia scapulalis*, male killing occurs when genetic males become feminized and die during the larval stage in the presence of *Wolbachia* (Kageyama *et al.*, 2002; Kageyama and Traut, 2004). In *Drosophila bifasciata*, *Wolbachia*-induced male killing is associated with defective chromatin condensation, chromosome segregation and mitotic spindle organization in the early development of male embryos, leading to embryonic death before hatching (Riparbelli *et al.*, 2012). Recent evidence suggests the phage gene *wmk* from the *w*Mel *Wolbachia* strain could be a candidate for *Wolbachia*-related male killing. Transgenic expression of *w*Mel *wmk* gene in *D. melanogaster* caused a lower male-to-female sex ratio in the offspring and an increase in abnormal cytology in male embryos (Perlmutter *et al.*, 2019; Perlmutter, Meyers and Bordenstein, 2020). However, since *w*Mel is not known to naturally cause male killing, further genomic analyses and transgenic fly studies are needed to identify if similar *wmk* genes exist in male-killing *Wolbachia* strains that infect *Drosophila*, such as *w*Bif and *w*Rec (Hurst *et al.*, 2000; Sasaki, Kubo and Ishikawa, 2002; Jaenike, 2007; Richardson *et al.*, 2016).

ii. Application of *Wolbachia* in Vector-Borne Disease Control

A primary target for mosquito-borne disease control is *Aedes aegypti*. This type of mosquito prefers tropical and subtropical regions of the world where they live and breed near or within human habitats **(**Flores and O'Neill, 2018). With rapid urban growth and the convenience of global air travel, the pandemics of mosquito-transmitted viral diseases have increased significantly over the past few decades (Gubler, 2002). For example, the incidence of dengue fever has grown over 30-fold during this period, now becoming the world's most common mosquito-borne virus (Pang, Mak and Gubler, 2017). Dengue virus is estimated to infect 390 million people per year, of which about 100 million would manifest significant clinical severity (Bhatt *et al.*, 2013).

Chikungunya, an arbovirus originated in sub-Saharan Africa, has also recently expanded its geographic range and spread into new areas around the world (Powers *et al.*, 2000). Since a reported emergence of chikungunya in the coastal area of Kenya in 2004, the virus has spread to different regions of Africa (Chretien *et al.*, 2007), Asia, several islands in the Indian Ocean (Hochedez *et al.*, 2006; Lanciotti *et al.*, 2007; Taubitz *et al.*, 2007) and temperate areas in Europe (Rezza *et al.*, 2007; Grandadam *et al.*, 2011) and reached the Americas in 2013 (Leparc-Goffart *et al.*, 2014; Mayer, Tesh and Vasilakis, 2017). Zika virus is another mosquito-borne arbovirus that has been rapidly introduced to areas where it was not previously reported. After its first outbreak on the Island of Yap in Micronesia in 2007, the Zika virus reached French Polynesia in 2013 causing another major epidemic **(**Ioos *et al.*, 2014; Mayer, Tesh and Vasilakis, 2017). In the following years, the virus spread to Thailand (Buathong *et al.*, 2015), other South Pacific regions

such as Easter Island (Musso, Nilles and Cao-Lormeau, 2014) and eventually reached the Americas with a major outbreak in Brazil in 2015 (Musso, 2015; Zanluca *et al.*, 2015).

A subset of vector control focuses on reducing the spread of mosquito-borne viruses by direct suppression of the mosquito population or modification of the mosquitoes to make them resistant to the pathogens. The approaches used to suppress mosquito population work by reducing mosquito bite rates, thus lowering virus transmission and risk of disease. Although the assumption certainly is true if a mosquito population is completely eliminated, more evidence is required to evaluate the effect when mosquito population is only partially suppressed (Wilson *et al.*, 2015; Bowman, Donegan and McCall, 2016; Flores and O'Neill, 2018). Currently, one promising approach in reducing mosquito population involve rearing and releasing large numbers of male mosquitoes that cannot produce viable offspring when mating with wild females. These methods include the sterile insect technique (SIT) and incompatible insect technique (IIT).

Traditionally, SIT involves irradiating or chemically treating male insects to sterilize them (Bushland, Lindquist and Knipling, 1955). When these males are released and mate with wild females, they cannot produce viable offspring, leading to a decrease in the wild mosquito population. A major limitation of SIT is that irradiation and chemical treatment can reduce the fitness of the treated males, rendering them less reproductively competitive comparing to the wild males. IIT, a version of SIT that utilizes *Wolbachia* to effectively sterilize males, can overcome the fitness costs associated with the traditional SIT methods. In IIT, *Wolbachia*-infected males are released into a mosquito population to mate with uninfected wild females. Due to CI,

such matings between *Wolbachia*-infected males and uninfected females would produce few offspring, leading to a decrease in mosquito population size. The main concern about IIT is that accidental release of infected females during sex sorting might cause the *Wolbachia*-infected mosquitoes to replace the field mosquito population, due to CI, and thus prevent future population suppression through IIT.

IIT also shares many limitations with SIT. Since both methods require continual release of large numbers of males into the wild mosquito population, effective rearing/sex-sorting facilities are required to constantly produce large amounts of male mosquitoes. Migration of mosquitoes from untreated neighboring areas can also limit the long-term effectiveness of these methods. Other major concerns of IIT include introgression of unfavorable genetic alleles into the mosquito population and development of population resistance against the sterilization or embryo-killing mechanisms.

The first field trial of IIT utilizing *Wolbachia*, which achieved complete elimination of a wild *Culex quinquefasciatus* population, was conducted in Burma in 1967 (Laven, 1967). More recently, *Wolbachia*-infected male *Aedes polynesiensis* mosquitoes were released in French Polynesia, resulting in a significant decrease in mosquito egg hatch rate in the treated area (O'Connor *et al.*, 2012). In the United States, release of *Wolbachia*-infected mosquitoes is EPA-approved in 20 states and Washington D.C. In 2016, release of male *Aedes albopictus* mosquitoes infected by *Wolbachia* in Lexington, Kentucky over a 17-week period caused significant reduction in both the number of adult females and egg hatch rates (Mains *et al.*, 2016).

The latest release of *Wolbachia*-infected mosquitoes in the United States was conducted in Miami, Florida in 2019 where researchers released male *Aedes aegypti* mosquitoes infected by *Wolbachia* over the course of six months in response to heightened concern of Zika virus transmission, leading to a significant decrease in both the egg hatch rate and number of adult mosquitoes (Mains *et al.*, 2019). Organizations such as the World Mosquito Program (formerly known as the Eliminate Dengue Program) for years have also been using *Wolbachia*-infected mosquitoes to control mosquito population in order to reduce the spread of mosquito-borne diseases in Australia, Indonesia, Brazil, and many other places around the world (O'Neill, 2018; O'Neill *et al.*, 2018).

The combination of SIT and IIT has also proven to be effective in mosquito population suppression. Treating *Wolbachia*-infected mosquitoes with low-level irradiation will sterilize females while leaving males generally unaffected (Arunachalam and Curtis, 1985; Shahid and Curtis, 1987; Zhang *et al.*, 2015a; Zhang *et al.*, 2015b). Therefore, females that might escape during sex sorting and be released into the field would not be able to produce viable offspring, eliminating the risk of population replacement. A recent field study conducted in Guangzhou, China using the combined SIT-IIT approach; millions of factory-reared male mosquitoes were released and achieved near elimination of field *A. albopictus* populations (Zheng *et al.*, 2019).

In contrast to the population reduction approach using *Wolbachia*-induced CI, the population modification method exploits the ability of *Wolbachia* to protect host insects from pathogenic viruses. Since *Wolbachia* was first discovered to protect host *Drosophila melanogaster* from Drosophila C virus, many laboratory studies have shown that

Wolbachia infection can prevent the transmission of various viruses (Teixeira, Ferreira and Ashburner, 2008), particulary RNA viruses such as dengue (Walker *et al.*, 2011; Blagrove *et al.*, 2012), chikungunya (Moreira *et al.*, 2009), Zika and West Nile virus (Joubert and O'Neill, 2017), by inhibiting pathogen replication in the host insect (Hedges *et al.*, 2008; Kambris *et al.*, 2009; Walker *et al.*, 2011). This ability of *Wolbachia* to provide pathogen resistance coupled with CI allows an alternative strategy for controlling mosquito-borne viruses. Due to the reproductive advantage in *Wolbachia*-infected females and *Wolbachia*'s ability to transmit vertically through female germlines, releasing both male and female mosquitoes infected by *Wolbachia* would allow *Wolbachia* infection to spread throughout a wild population, thus reducing the probability of the mosquitoes transmitting viruses to humans.

A major advantage of this approach over SIT or IIT is that the method requires the release of far fewer mosquitoes and, once *Wolbachia* infection is established in the wild population, it is expected to be maintained at a high frequency indefinitely (Turelli, 2010; Hoffmann *et al.*, 2011). As a result, the *Wolbachia*-based population replacement strategy has much lower cost than the population suppression approach. Many field studies have proven the effectiveness in spreading *Wolbachia* infection throughout wild mosquito populations. In Australia, since the initial release of *w*Mel-infected *A. aegypti* in 2011 by the World Mosquito Program, the frequency of the *w*Mel *Wolbachia* strain has been maintained at rate of 90% or greater (Hoffmann *et al.*, 2011; Hoffmann *et al.*, 2014). However, the effectiveness of this approach in suppressing viral transmissions remains unclear. An ongoing field trial in Yogyakarta, Indonesia is expected to provide

evidence on the degree of disease reduction through the use of the *Wolbachia* population replacement method (Flores and O'Neill, 2018).

Lastly, another potential strategy of using *Wolbachia* in mosquito control is by creating a gene-drive system utilizing genomic editing to increase the odds of the drive system to be passed onto offspring. Recent study showed that in laboratory settings, CRISPR-Cas9 could be used to spread anti-*Plasmodium falciparum* effector genes m2A10-m1C3 into an *Anopheles stephensi* population (Gantz and Bier, 2015; Gantz *et al.*, 2015). Subsequent work also exploited CRISPR-Cas9 gene-drive system for population suppression in *Anopheles gambiae* by either targeting female reproduction or creating sex-ratio distortion (Hammond *et al.*, 2016; Galizi *et al.*, 2016). The effectiveness of gene-drive systems in mosquito-borne disease control has yet to be tested in field studies. Several concerns about the gene-drive approach include the difficulty in receiving public support in releasing transgenic organisms into the wild, potential risk of spreading the gene-drive system into neighboring populations, and the possibility for viruses to develop mutations over time that can render them resistant to the transgenes.

iii. Discovery of CI Factors and A Note on Nomenclature

Despite the success of *Wolbachia* in reducing mosquito-borne viruses and agricultural pest control, the molecular mechanisms of *Wolbachia*-induced CI have long eluded identification. Since CI is caused by improper condensation and segregation of chromosomes from *Wolbachia*-infected male sperm, it was thought that *Wolbachia* must somehow modify the sperm and such modification has to take place during spermatogenesis because the bacteria are removed from mature sperm (Bressac and Rousset, 1993). The fact that sperm from *Wolbachia*-infected males induce CI and embryonic lethality only in uninfected but not infected embryos could be explained by a toxin-antidote model wherein the sperm from the infected male carries the toxin and the egg from the infected female carries the *Wolbachia*-derived antidote. Driven by these hypotheses, a proteomic analysis was conducted on sperm and ovaries collected from *w*Pip *Wolbachia*-infected *Culex pipiens*. Peptides of a *Wolbachia* protein, now called CidA, were identified by mass spectrometry in both sperm and ovaries of *w*Pip-infected mosquitoes but were absent from mosquitoes not infected by *Wolbachia* (Beckmann and Fallon, 2013). Further genetic analysis revealed that *cidA* is part of a two-gene operon, which we now call *cidA*-*cidB*, and there coexists a paralogous operon in the same *w*Pip *Wolbachia* genome termed *cinA*-*cinB* (**Figure 2**).

The first evidence demonstrating that genes in either the *cid* or *cin* operons can behave as toxin-antidote pairs came from transgenic studies in yeast. Using *Saccharomyces cerevisiae* as a model system, expression of *cidB* or *cinB* caused a temperature-dependent growth defect at 37°C that can be rescued when the cognate *A* genes (*cidA* or *cinA*, respectively) were co-expressed, suggesting that the *A* genes in each

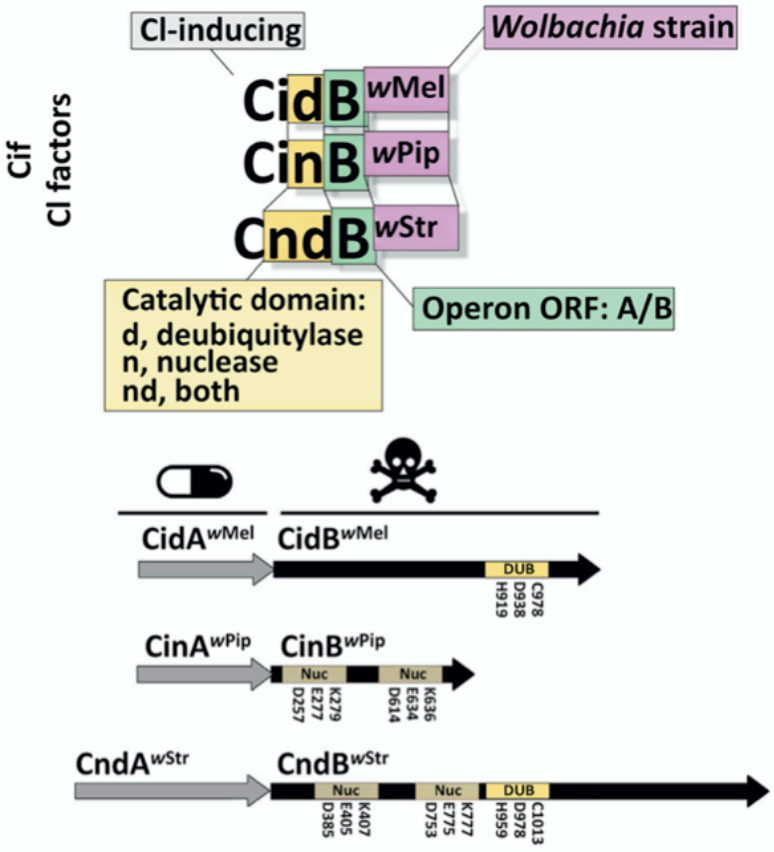

Figure 2. A nomenclature proposal and schematic view of putative cytoplasmic incompatibility operon structures. In this naming system, the *cif* (and Cif) terms designate CI genes (and proteins) in general, while genes from specific operon categories are named according to the enzymatic activity of the putative toxin. The first and second genes within each operon are denoted *A* and *B*, respectively, and the *Wolbachia* strain is indicated as a superscript when relevant. The structure of several CI operons is shown to illustrate this system; active-site residues are labeled. Abbreviation: ORF, open reading frame. Figure adapted from Beckmann *et al*., 2019b.

operon are likely the antidote genes while the *B* genes are toxin-encoding genes (Beckmann, Ronau and Hochstrasser, 2017). *In vitro* binding experiments also showed that the two proteins within each operon bind tightly to one another in a cognate-specific manner, a common feature among type II toxin-antitoxin systems in free-living bacteria (Beckmann, Ronau and Hochstrasser, 2017; Yamaguchi, Park and Inouye, 2011).

Subsequent studies in transgenic *D. melanogaster* confirmed the role of the *cid* operon in *Wolbachia*-induced CI and rescue. Transgenic expression of $cid^{w\text{Pip}}$ or $cid^{w\text{Mel}}$ in uninfected male fruit flies recapitulate CI embryonic lethality and cytological defects when mated with wild-type uninfected females (Beckmann, Ronau and Hochstrasser, 2017; LePage *et al.*, 2017). Importantly, female flies transgenic for $cidA^{w\text{Mel}}$ can rescue CI when crossed with either wild-type *w*Mel-infected males or uninfected males transgenic for *cidA*-$cidB^{w\text{Mel}}$, indicating that the *cid* operon is capable of inducing both CI and rescue (LePage *et al.*, 2017; Shropshire *et al.*, 2018; Shropshire and Bordenstein, 2019; Beckmann *et al.*, 2019c). However, the notion of *cidB* as the sole gene remains uncertain as transgenic expression of $cidB^{w\text{Mel}}$ alone in male flies was unable to induce CI when crossed with wild-type uninfected females.

Before further discussion on the biochemistry and genetics of these CI-inducing operons, it is important to note that there are currently two different CI gene nomenclatures coexisting in the literature. One nomenclature system proposed naming the CI operons based on the enzymatic function of the proteins encoded by the *B* genes and using *cif*, short for CI factors, only to designate CI genes in general (Beckmann, Ronau and Hochstrasser, 2017; Beckmann *et al.*, 2019b; Beckmann *et al.*, 2019a). The B protein in *cid* type operon, short for CI-inducing deubiquitylase (DUB), has been

confirmed to have DUB activity *in vitro* when it is expressed recombinantly; moreover, mutating the DUB active site abrogates toxicity in yeast and flies (Beckmann, Ronau and Hochstrasser, 2017). Prior to the work presented in this thesis, the nuclease function of the B protein in *cin*-type operon, short for CI-inducing nuclease, was only proposed based on its weak protein sequence homology to other known nucleases.

The second nomenclature system names all CI-related genes as *cif* regardless of the biochemical functions of the proteins encoded by the CI operons (LePage *et al.*, 2017; Shropshire *et al.*, 2019). Bordenstein and colleagues argued that it was premature to name the nuclease-type operons *cin* since it had not been shown that these operons caused CI or that CinB had nuclease activity. They further argued that the B proteins are potentially polyvalent, suggesting that other putative protein domains aside from the DUB or the nuclease domains could contribute to their CI-related functions. However, in both nomenclature systems, the upstream gene in each operon is denoted as the *A* gene (*cifA, cidA* or *cinA*), while the downstream gene is denoted as the *B* gene (*cifB*, *cidB*, or *cinB*). In this thesis work, we use the first nomenclature system in which "*cif*" is used only when discussing CI genes generally and the more specific "*cid*" or "*cin*" names when the enzymatic function of particular toxins is known or strongly predicted. The relevant *Wolbachia* strain is denoted by a superscript (**Figure 2**) (Beckmann *et al.*, 2019b).

iv. Biochemistry and Genetics of CI Factors

The discovery of the *Wolbachia cif* genes marked a major step in understanding the molecular mechanisms of CI. Prior to the work presented in this thesis, most research had focused on understanding the biochemistry and relevance of *cid*-type operons in inducing CI and its underlying mechanism. Little was known about the *cin* operon. Protein sequence analysis suggested that CidB protein contains a C-terminal Ulp1-like (ubiquitin-like protein-specific protease 1) domain (Beckmann, Ronau and Hochstrasser, 2017). Ulp1 is a cysteine protease that catalyzes the deconjugation of the small ubiquitin-related modifier (SUMO) from proteins (Li and Hochstrasser, 1999; Hickey, Wilson and Hochstrasser, 2012).

Interestingly, recombinant CidB protein showed no SUMO protease activity but instead, reacted with the ubiquitin-based suicide inhibitor ubiquitin vinyl methyl ester (UbVME) and exhibited activity towards ubiquitin-AMC and polyubiquitin chains with isopeptide linkages. Active site cysteine-to-alanine mutation renders CidB unreactive toward UbVME. These results suggested that CidB is a DUB, a group of enzymes that specifically remove ubiquitin from ubiquitin-modified proteins (Ronau, Beckmann and Hochstrasser, 2016; Beckmann, Ronau and Hochstrasser, 2017).

A follow-up study aimed to uncover the molecular mechanism of *cid*-induced CI using an *in vitro* affinity purification approach found that the catalytic inactive CidB protein interacts with both karyopherin-α (Kap-α), a nuclear import receptor, and the P32 histone chaperone from *Drosophila melanogaster* protein extracts (Beckmann *et al.*, 2019c). Transgenic expression of these two proteins in uninfected female *D. melanogaster* partially suppressed CI when crossed with wild type males infected by

*w*Mel *Wolbachia*. Overexpression of yeast Kap-α (Srp1) also suppressed CidB toxicity in yeast. However, it is still unclear how exactly Kap-α and P32 are involved in the molecular mechanism of CI. Ubiquitylation of Kap-α might be important for promoting nuclear import of key proteins involved in protamine-histone exchange. It is also possible that protein interaction between CidB and P32 could allow the DUB to deubiquitylate certain histone components, resulting in impaired histone deposition.

A large-scale population genomic screen of *Culex* mosquitoes correlated crossing-type diversity in CI among mosquitoes infected with different *w*Pip strains to genetic variation in the *cidA*-*cidB*^{wPip} operon (Bonneau *et al.*, 2018a). The intensity of CI embryonic defects was also correlated specifically with variations in the *cidB* gene in the genome of the *w*Pip strain hosted by the male mosquitoes (Bonneau *et al.*, 2018b). A follow-up genetic analysis using *w*Pip strains from North Italy also linked *cidB* variants to CI phenotypes but found no association between *cidA* variants and CI diversity (Bonneau *et al.*, 2019). These results together provide genetic evidence highlighting the important role of the *cid* genes in CI and support the model that *cidB* is the CI-inducing toxin in *cid*.

Another set of *Wolbachia cif* factors hypothesized to contribute to CI is the two-gene *cin* operon, named after the putative nuclease domains in the CinB protein suggested by protein sequence analysis (Beckmann, Ronau and Hochstrasser, 2017). The same genomic screen found that the *cin* operon genes were monomorphic among the incompatible *w*Pip strains, suggesting that CI in *C. pipiens* are only related to *cid* but not *cin* operons **(**Bonneau *et al.*, 2018a). However, the fact that some CI-inducing *Wolbachia* strains, such as the *w*No strain that infects *Drosophila simulans*, contain only *cin* but not

cid operons and that neither operon is present in *w*Au, a close relative of *w*Mel that does not induce CI, suggested that the *cin* operon might also be able to induce CI independently of the *cid* operon (Sutton *et al.*, 2014; Lindsey *et al.*, 2018). As was true for CidB, CinB was shown to inhibit growth when expressed in yeast (Beckmann, Ronau and Hochstrasser, 2017).

Recent genomic analyses have also uncovered natural variation in both *cid* and *cin* loci that correlates with CI in different *Wolbachia*-infected *Drosophila* species (Cooper *et al.*, 2019; Meany *et al.*, 2019). While this supports previous speculations on the possible function of the *cinA-cinB* operon in CI, the ability of these genes to cause CI has not been experimentally tested. Similarly, while there are distant sequence similarities between CinB and the PD-(D/E)xK superfamily of nucleases, no nuclease activity has been demonstrated. In this thesis work, I show that CinB has DNase activity. Mutation of putative active-site residues in either of two CinB PD-(D/E)xK domains present in CinB abolishes activity *in vitro* and renders the resulting protein nontoxic to yeast. Most importantly, the *cinA-cinB*$^{w\mathrm{Pip}}$ operon induces a CI-like phenotype in transgenic flies, and *cinA*$^{w\mathrm{Pip}}$ is sufficient for rescue of transgenic CI. Therefore, the *cinA-cinB* nuclease operon provides a biochemically distinct mechanism for CI and its presence likely accounts for the ability of many *Wolbachia* strains to induce CI in their hosts despite not carrying an intact *cidA-cidB* gene pair. A majority of the work presented in this thesis has been previous published in four peer-reviewed journals (Beckmann *et al.*, 2019b; Beckmann *et al.*, 2019a; Chen *et al.*, 2019; Beckmann *et al.*, 2019c).

Chapter II: Materials and Methods

Sequence Alignment and Structure Prediction. Multiple sequence alignments of CinB orthologs from several *Wolbachia* strains and known PD-(D/E)xK nucleases were generated using the Clustal Omega Multiple Sequence Alignment program from EMBL-EBI followed by manual adjustment (Kanz *et al.*, 2005). Secondary structure predictions and alignments of the protein sequences were performed using the PSIPRED Protein Sequence Analysis Workbench program (Jones, 1999). Structure prediction of CinB^{wPip} was done using the RaptorX Structure Prediction server with a few unstructured regions removed in the displayed figure (Wang *et al.*, 2016).

Western Immunoblotting. The following antibodies were used: mouse anti-FLAG M2 (Sigma, 1:10,000); mouse 16B12 anti-HA (Covance, 1:1000), mouse anti-PGK (Molecular Probes, 1:20,000), and HRP-conjugated sheep anti-mouse NA931V (GE Healthcare, 1:10,000). Protein samples were resolved by SDS-PAGE and transferred to PVDF membranes (Millipore) for immunoblotting. Proteins were visualized by HRP-based chemiluminescence (Mruk and Cheng, 2011).

Purification of Proteins for *In Vitro* Nuclease Assays and ITC. Full-length CinB, catalytically inactive CinB mutants (K279A, K636A, and KK279/636AA), CidB$_{1-761}$(V686E/R688K), and CinA were expressed as glutathione-S-transferase (GST) fusions from the pGEX6P1 vector in Rosetta DE3 (Novagen) *E. coli* as previously described (Beckmann, Ronau and Hochstrasser, 2017). To reduce the likelihood of CinB

copurficiation with DNA, we used a protocol to isolate DNA-free protein described by Epling *et al* (Epling *et al.*, 2015). 2 L of back-diluted bacterial cultures were grown to OD_{600} = 0.5 in LB medium containing ampicillin at 37 °C followed by induction of protein expression with 0.3 mM isopropyl-β-D-thiogalactoside (IPTG) at 18 °C overnight. Cells were harvested by centrifugation, resuspended in a buffer containing 50 mM Tris pH 8, 250 mM NaCl, 10% glycerol, 2 mM β-mercaptoethanol, and lysed on ice via French press. The lysate was clarified by centrifugation at 50,000 x g for 1 hr at 4°C (Thermo Sorvall Lynx 600 F20-12x50 LEX). Nucleic acids were separated from protein upon the addition of 1M (final concentration) sodium chloride to the clarified lysate, followed by precipitation of nucleic acids by addition of 0.3% (final concentration) of a solution composed of 10% polyethylenemine in 10% hydrochloric acid. After centrifugation (5,000 rpm, 15 min), the supernatant was treated with 70% ammonium sulfate to remove excess PEI by precipitation of the protein. The protein was centrifuged at 50,000 x g for 1 hr at 4°C and the pellet was resuspended in PBS supplemented with 400 mM KCl. The protein was further purified via GST affinity chromatography and size-exclusion chromatography as described previously (Beckmann, Ronau and Hochstrasser, 2017). All proteins were concentrated using Amicon Ultra centrifuge filter units and stored at -80°C in 25 mM Tris-HCl, pH7.5, 150 mM NaCl, and 4 mM dithiothreitol (DTT).

Isothermal Titration Calorimetry. Isothermal titration calorimetry (ITC) experiments were carried out at 25°C using a NanoITC (TA Instruments). First, $CinA^{wPip}$ and $CinB^{wPip}$ were dialyzed extensively against a buffer of 50 mM HEPES pH 7.4 over the course of two days with 3-4 buffer exchanges. To determine the binding affinity of CinB

for CinA, 500 µM CinA was loaded into the syringe and titrated into a 50 µM solution of CinB. A total of 22 injections (2 µl/injection) were performed over the course of the experiment with a spacing of 300 seconds between injections to ensure a return to baseline prior to the next injection. The data were baseline corrected using NITPIC and analyzed in SEDPHAT using the one-site (A+B → AB) binding model. The figure was prepared in GUSSI, which was downloaded from the MBR Software Page (http://biophysics.swmed.edu/MBR/software.html) (Roe and Cheatham, 2013; Keller *et al.*, 2012; Houtman *et al.*, 2007).

***In Vitro* Nuclease Assay.** All *in vitro* nuclease activity assays were performed with full-length CinB$^{w\text{Pip}}$ (1-733) with or without CinA$^{w\text{Pip}}$ (1-446). For DNase and RNase activity assays, 1 µM CinB or CinB mutant proteins was incubated in a reaction buffer containing 20 mM HEPES (pH 8.0), 5 mM $MgCl_2$, 2.5% sucrose, 150 mM NaCl, 0.001% Triton X-100, and 2 mM DTT with 15 nM of either linearized or supercoiled pBluescript SK+, 500 nM single-stranded or double-stranded Cy5-labeled DNA (70-mer: Cy5-GCAATTCGATCGTTGACATCTCGCGTGCTCGGTCAATCGGCAGATGCGGAGT GAAGTTCCAACGTTCGGC, previously used for ssDNA cleavage analysis (Komori *et al.*, 2000); 45-mer: Cy5-GGGTCAACGTGGGCAAAGATGTCCTAGCAAGCCAGAAT TCGGCAG, which was tested with the online calculator OligoCalc to confirm that the sequence should not form any strong hairpins; and the respective complements to generate dsDNA) or 500 ng of either yeast tRNA (Thermo Fischer) or *D. melanogaster* total RNA (Bogart and Andrews, 2006). In reactions where CinA was present, 10 µM CinA was used.

All reactions were carried out at 25 °C for 90 min and quenched by adding EDTA to a final concentration of 10 mM unless otherwise noted.

For reactions using linear or circular pBluescript SK+ vector or RNA, samples were run in agarose gels with a range of concentrations between 0.8 and 2.0% containing 0.4 μg/mL ethidium bromide in 1x TAE buffer at 100 V for 40-60 min and imaged on a Syngene G:box with GeneTools software. For reactions using Cy5-labeled oligodeoxynucleotides, samples were run in 9% TBE polyacrylamide native gels at 100 V for 45-60 min and imaged on Typhoon FLA 7000 with Typhoon FLA 7000 control software.

Yeast Methods. The yeast growth assays shown were done in the BY4741 strain (Brachmann *et al.*, 1998). The 2-micron plasmid pYES2 (URA3) utilizes a *GAL1* promoter and a *CYC1* terminator and was used for galactose-inducible *cinB* expression in yeast. Standard site-directed mutagenesis was used to create point mutations in CinB. For yeast growth assays, cultures were grown overnight at 30 °C in glucose minimal medium (SD) lacking uracil. Cultures were spotted in six-fold serial dilution from an initial concentration of 0.2 OD_{600} on solid minimal SD media lacking uracil and containing either 2% glucose or galactose. Plates were then left at 30, 34, and 36 °C for 2-3 days.

For immunoblotting, cells were grown overnight in either glucose (non-inducing) or galactose (inducing) media lacking uracil, diluted to 0.2 OD_{600} the next morning and left to grow at 30 °C until reaching 0.8-1.0 OD_{600} at which point the equivalent of 2-3 OD_{600} units of cells were harvested, washed and resuspended in 1 mL cold water followed by the addition of 150 μL of a 2 N NaOH/1 M β-mercaptoethanol solution (Kushnirov, 2000).

Cells were vortexed vigorously for 20 s, incubated on ice for 15 min, and pelleted. Pellets were resuspended in 1x SDS-PAGE sample buffer and heated at 100 °C for 3 min before immunoblot analyses.

Yeast High-Copy Suppressor Screens. The high-copy suppressor screen was performed in the BY4741 yeast strain. Flag-CinB^{wPip} was cloned into the pRS416GAL1 (CEN) plasmid with a galactose-inducible promoter and a *URA3* selection cassette. Plasmids from a yeast high-copy genomic tiling library utilizing a *LEU2* selection cassette were transformed into yeast expressing Flag-CinB^{wPip} using a standard lithium acetate transformation method (Jones *et al.*, 2008; Gietz and Schiestl, 2007). Transformed cells were plated directly on selective media containing either galactose or glucose and incubated at 37°C. If first plated on glucose media, cells were then allowed to grow at 37°C for 3 days followed by replica-plating onto galactose-containing selective media. After plating on selective media containing galactose, colonies were allowed to grow for 3-5 days before they were picked and re-streaked onto a fresh selective media. Plasmids were extracted from yeast by standard phenol/chloroform extraction followed by ethanol precipitation and electroporated into electrocompetent Top10F' *E. coli* cells for better plasmid recovery (Hoffman and Winston, 1987). Each plasmid was then sequenced to identify its yeast genomic insert and also retransformed back into yeast expressing Flag-CinB^{wPip} to confirm suppression.

Drosophila Hatch Rate and Cytology Analyses. Each CI candidate gene (*cinA*, *cinB*, *cinB-K636A*, *cinA-T2A-cinB*) was inserted into the pUASp-attB vector by standard cloning

techniques without codon optimization. In brief, the open reading frames of the genes were amplified by PCR and cloned into the pBluescript SK+ vector followed by restriction digestion and re-ligation of the genes into the pUASp-attB vector. All plasmids were verified by fully sequencing the inserted genes before they were sent to BestGene, Inc. for microinjection of *D. melanogaster* embryos (Beckmann, Ronau and Hochstrasser, 2017). Fly background #9744 was chosen for all gene constructs for site-directed attP/B integration on the 3rd chromosome by PhiC31 integrase with the exception that background #9723 was chosen for site-specific integration of *cinA* on the 2nd chromosome (Groth *et al.*, 2004). Drosophila DNA was purified by homogenizing 30 flies (infected or uninfected by *Wolbachia*) and recovering DNA with phenol/chloroform extraction (Livak, 1984; Beckmann and Fallon, 2012; Beckmann, Ronau and Hochstrasser, 2017). Integrations were confirmed independently by PCR amplifying the candidate genes.

D. melanogaster stocks were verified to be uninfected with native *Wolbachia* isolates by PCR amplification of $cidA^{w\text{Mel}}$ gene. The MTD-Gal4 line from the Bloomington stock center was found to be infected by *w*Mel and was treated by addition of 20 μg/ml tetracycline to the growth medium for three generations. Once the infection was confirmed to be cleared by PCR amplification of the $cidA^{w\text{Mel}}$ gene, flies were reared on untreated media for at least three additional generations to allow for mitochondrial recovery (Chatzispyrou *et al.*, 2015). Both uninfected and *w*No-infected *D. simulans* were also verified by PCR amplification of $cinB^{w\text{No}}$ gene. Flies were reared on standard cornmeal-based solid media and maintained at room temperature. During virgin female collection, stocks were maintained at 18 °C overnight and room temperature the following day. All transgenic flies were maintained as homozygous lines.

Parental flies were generated by crossing either NGT-Gal4 or MTD-Gal4 virgin females with *cin* transgenic males (Rorth, 1998; Petrella, Smith-Leiker and Cooley, 2007). Only the males emerging between 0 and 30 h from these crosses were collected and used in CI analyses (Yamada *et al.*, 2007). All flies used in both hatch rate and cytological analyses were aged for 2-4 days. Hatch-rate analysis was performed and embryos for cytological analyses were prepared as previously described (Beckmann, Ronau and Hochstrasser, 2017; LePage *et al.*, 2017). In the hatch-rate analysis, one male and one virgin female were placed in a 100-mL polypropylene bottle with the bottom punctured for aeration. An apple juice agar plate (made by adding 26.1 g of dextrose, 13.03 g of sucrose, 9.9 g of agar, 12 mL of 1.25 N NaOH and 203 mL of apple juice to 242 mL of de-ionized water followed by autoclaving) with a small amount of yeast paste smeared in the center of the plate was taped at the bottle opening. Bottles were placed in an incubator at 25 °C overnight. The next morning the agar plates were replaced with freshly yeasted plates which were collected after another 24 h incubation at 25 °C. Both sets of plates were incubated at 25 °C for a total of 48 h before embryo counting. The numbers from the two sets of plates were pooled, and the counting was not blinded. Any crosses with fewer than ten total embryos laid were removed from hatch rate analysis.

To prepare embryos for cytological analyses, ~100 males and ~300 virgin females were placed in a 100 mL plastic cup and allowed to mate for two days at 25 °C with a freshly yeasted apple juice agar plate replaced every day. After two days, a freshly yeasted apple juice agar plate was provided and removed after 1 h. Embryos were then incubated at 25 °C for another hour to ensure each embryo has undergone 1-2 h development. These were then collected, dechorionated, washed in embryo wash buffer (0.6% NaCl, 0.04%

Trition X-100) and fixed immediately in a small scintillation vial containing 5 mL heptane and 5 mL methanol followed by shaking vigorously for 30 s (Sullivan, Ashburner and Hawley, 2000). De-vitellinated embryos were collected, washed three times with methanol, and stored overnight at 4 °C. The old methanol was then removed and replaced with 250 μL of fresh methanol and 750 μL PBTA (1x PBS, 1% BSA, 0.05% Triton X-100, 0.02% sodium azide). After inverting the tube a few times, the solution was replaced with 500 μL PBTA to rehydrate the embryos. PBTA was then replaced with 200 μL of 10 mg/ml RNase A and incubated at 37 °C for 2 h. The RNase was then removed, and the embryos were washed several times with PBS followed by a final wash of PBS-azide. The samples were stained with either Hoechst 33342 at 1:1000 in PBTA or 1 μg/ml propidium iodide. Stained embryos were mounted on glass slides and sealed under cover slips by nail polish. Imaging was done either on a Zeiss Axioskop microscope with AxioCam MRm camera using 10X and 40X objective lenses or a Zeiss LSM 880 Airyscan/NLO confocal microscope with internal PMT using a 20X objective lens. Software used to capture and analyze the images were AxioVision Rel. 4.8 or Zen (blue edition), respectively.

Statistical Analyses. All statistical analyses were done in GraphPad Prism 7. Hatch rate analyses were performed by either using one-way ANOVA with pairwise comparison after removal of outliers identified by ROUT method with Q = 1%, or unpaired two-tailed Mann-Whitney *U* test. Pairwise χ^2 test was used in cytological analyses to compare normal and defect cytological phenotypes.

Chapter III: *In Vitro* Biochemistry of CinA and CinB Proteins

Note: Portions of this chapter were published in Chen, H., Ronau, J. A., Beckmann, J. F. and Hochstrasser, M. (2019) 'A Wolbachia nuclease and its binding partner provide a distinct mechanism for cytoplasmic incompatibility', Proceedings of the National Academy of Sciences, 116(44), pp. 22314-22321.

i. Introduction

The *cinA-cinB*$^{w\text{Pip}}$ operon was first hypothesized to be another potential CI-inducing genes pair due to its paralogous relationship to the *cidA-cidB* operon identified in the initial proteomic analysis of *C. pipiens* spermathecae isolated following insemination by *w*Pip-infected males (Beckmann and Fallon, 2013). That study found that the *Wolbachia* CidA protein was present in the sperm of *w*Pip-infected *C. pipiens* and absent from the uninfected mosquitoes. Protein sequence analysis suggested that CinB encodes a putative DUF1703 putative nuclease domain within the PD-(D/E)xK nuclease superfamily (Knizewski *et al.*, 2007; Beckmann and Fallon, 2013). Interestingly, the DUF1703 domain is also found in another selfish genetic element named Medea (Maternal-Effect Dominant Embryonic Arrest) that is involved in a different reproductive manipulation phenomenon in *Tribolium castaneum* (Lorenzen *et al.*, 2008). Here we report additional sequence analysis suggesting that CinB has a second PD-(D/E)xK nuclease domain located at the N-terminus of the protein in addition to the previously reported C-terminal nuclease fold. Furthermore, using recombinant CinB$^{w\text{Pip}}$

protein, we showed that, for the first time, CinB is indeed a nuclease whose nuclease activity requires both of its PD-(D/E)xK nuclease domains to be active.

ii. Sequence Alignments and Structural Predictions

PD-(D/E)xK nucleases constitute a large and diverse group of enzymes that share little sequence similarity despite retaining a common core structural fold and conserved catalytic residues. CinB has putative PD-(D/E)xK domains located near both the N- and C-termini of the protein (**Figure 3**). Sequence and secondary structure alignments revealed that these domains have homology to other PD-(D/E)xK nucleases such as archaeal Holliday junction resolvase (Nishino *et al.*, 2001; Knizewski *et al.*, 2007) and are conserved across the so-called type II and type III *Wolbachia cif* operons, which lack the DUB domain (**Figure 4**) (Gillespie *et al.*, 2018; Lindsey *et al.*, 2018). Secondary structure predictions by PSIPRED (Jones, 1999) and protein structure prediction by RaptorX (Wang *et al.*, 2016) suggest both the N-terminal and C-terminal nuclease domains (NTND and CTND) share a conserved αββββαβ fold where the two α-helices are predicted to sandwich a four-stranded β-sheet, a conserved feature in almost all PD-(D/E)xK nucleases (**Figure 4 and Figure 5**) (Steczkiewicz *et al.*, 2012).

Similar to other PD-(D/E)xK nucleases, both CinB nuclease domains also contain a highly conserved set of catalytic residues (**highlighted in Figure 4 and Figure 5**) (Pingoud *et al.*, 2005; Knizewski *et al.*, 2007; Steczkiewicz *et al.*, 2012). In most PD-(D/E)xK nucleases, the negatively charged aspartate and glutamate residues help coordinate up to three metal ions that serve as Lewis acids to stabilize the transition state, while lysine functions as a general base for deprotonation of the nucleophilic water

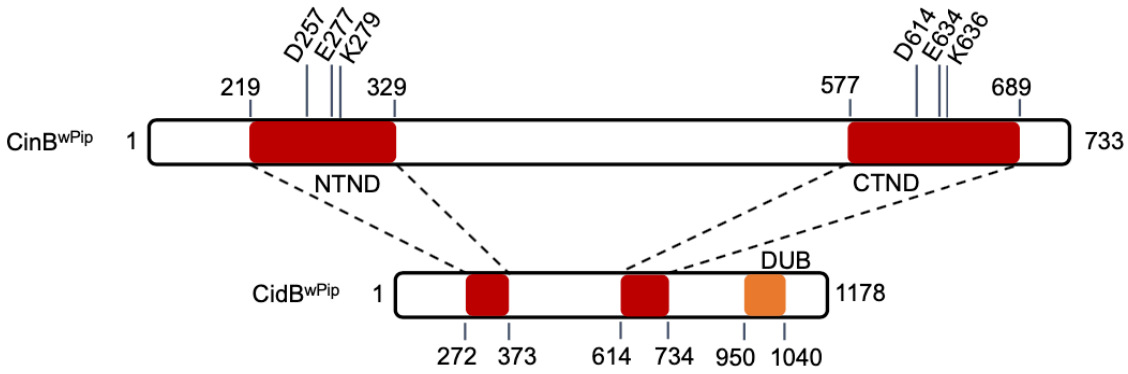

Figure 3. The NTND and CTND of CinB^{wPip} with their predicted catalytic aspartate, glutamate and lysine residues labeled. CidB^{wPip} also has two predicted PD-(D/E)xK nuclease folds upstream of its deubiquitylase domain; these are related to the dual nuclease domains in CinB^{wPip} but lack two or three of the three predicted core catalytic residues.

Figure 4. Protein sequence and secondary structure alignments of the NTND and CTND of CinB from various *Wolbachia* strains as well as several known PD-(D/E)xK nucleases. Predicted α-helical residues are labeled H and residues predicted to be part of β-sheets are labeled E. The numbers of excluded residues are shown in parentheses. The last residues numbers are shown at the end of each sequence. Catalytic D-E-K residues are highlighted in black. Residues in red are conserved among all three groups. Residues in gray are conserved within the respective groups.

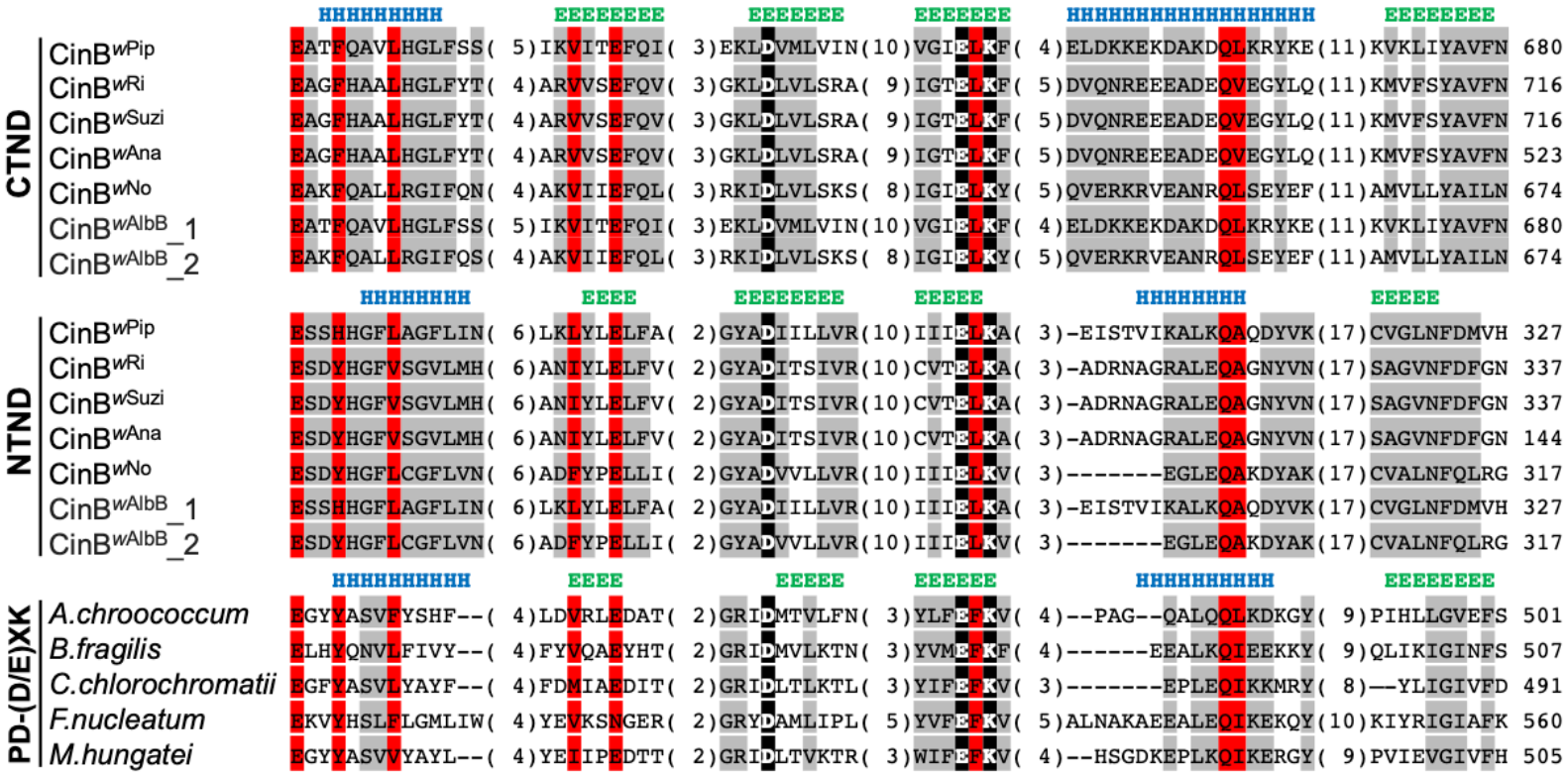
CTND
CinB wPip
CinB wRi
CinB wSuzi
CinB wAna
CinB wNo
CinB wAlbB_1
CinB wAlbB_2
NTND
CinB wPip
CinB wRi
CinB wSuzi
CinB wAna
CinB wNo
CinB wAlbB_1
CinB wAlbB_2
PD-(D/E)XK
A.chroococcum
B.fragilis
C.chlorochromatii
F.nucleatum
M.hungatei

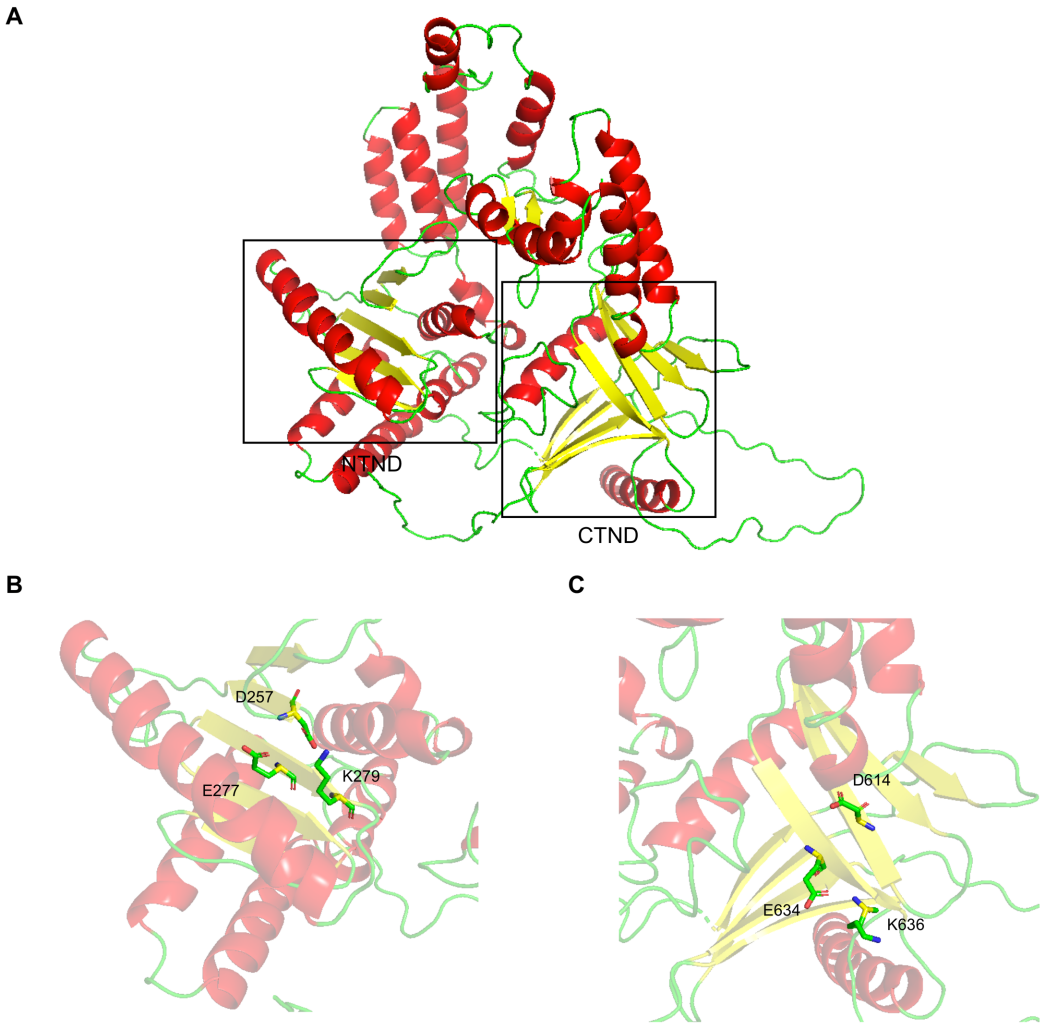

Figure 5. Predicted protein structure of CinB^{wPip} by RaptorX (A) with zoomed in views to highlight the catalytic triads of the CinB^{wPip} NTND (B) and CTND (C). Structure 2EWF was determined to be the best template with p-value of 2.16e-03 and an overall uGDT (GDT) score of 138 (18).

molecule (**Figure 6**) (Pingoud *et al.*, 2005; Knizewski *et al.*, 2007). Interestingly, CidB also contains two potential PD-(D/E)xK folds upstream of its catalytic deubiquitylase (DUB) domain with significant sequence similarities to the NTND and CTND of CinB, respectively (**Figure 3**). However, these domains in CidB lack residues predicted to be essential for catalytic activity (Gillespie *et al.*, 2018).

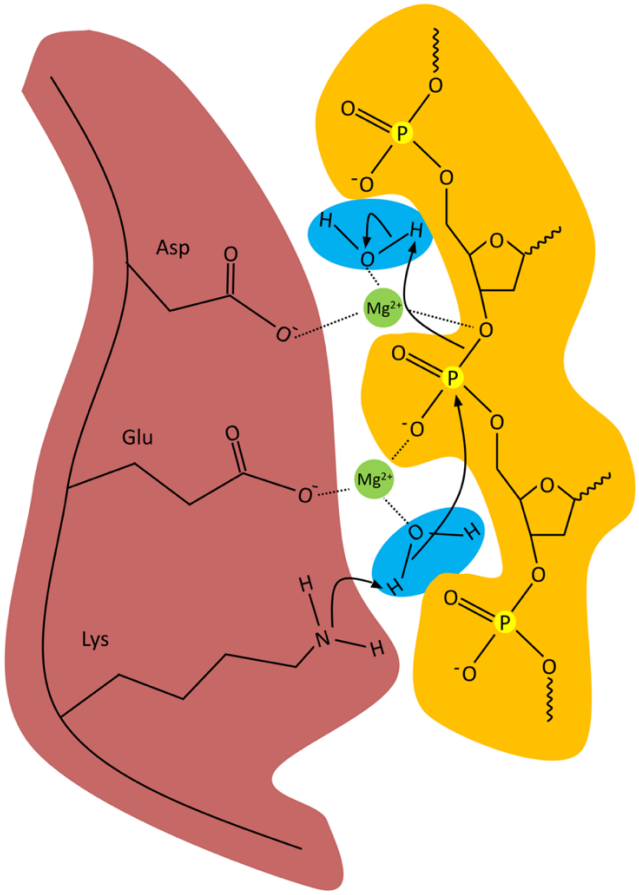

Figure 6. A model for a two-ion mechanism of phosphodiester bond cleavage by PD-(D/E)xK nucleases. The catalytic aspartate and glutamate help in coordinating two Mg^{2+} ions that stabilize two neighboring water molecules and also interact with the oxygen atoms in the phosphodiester bond during the transition state of catalysis. The lysine deprotonates one of the water molecules to create a hydroxide ion that serves as the nucleophile to attack the phosphate group. Lastly, the 3' hydroxyl becomes the leaving group and picks up a hydrogen atom from the adjacent water molecule to complete the reaction. The color of the scheme is as follows: catalytic site of the nuclease in burgundy, DNA in amber with phosphorus in yellow, water molecules in blue, and magnesium ions in green.

iii. *In Vitro* Nuclease Activity of CinB Protein

To test if CinB has nuclease activity, we purified recombinant CinB^{wPip} using polyethylenemine to separate DNA from the protein (**Figure 7**) (Epling *et al.*, 2015). CinB^{wPip} degraded both linearized and circular dsDNA plasmids (**Figure 8-10**). The DNase was activated by magnesium or manganese ions but not calcium and was active over a broad range of pHs (**Figures 11 and 12**). We further examined the nuclease activity of CinB against shorter ssDNA and dsDNA substrates and found it cleaves both forms of DNA (either 45 or 70 residues in length; **Figures 13 and 14**). Importantly, the catalytic CTND (K636A) or NTND (K279A) mutations each abolished DNase activity (**Figures 8, 13, 15 and 16**). By contrast, the purified CidB^{wPip} DUB protein did not exhibit DNase activity even after reinstating key catalytic residues in the CTND of CidB^{wPip} (**Figure 17**). We also tested the nuclease activity of CinB^{wPip} against several different DNA structures, which included both four-way and three-way junctions, but found no substrate preference towards any of the structures tested (**Figure 18**) (Komori *et al.*, 2000).

We further tested whether CinB^{wPip} could cleave RNA substrates but did not detect activity against either yeast tRNA or a *Drosophila* total RNA extract under our conditions (**Figure 19**). Thus, CinB is a DNase capable of cleaving both ssDNA and dsDNA. Its activity might be higher against specific DNA sequences or structures, but we have not yet been able to identify such substrates. These *in vitro* experiments support the idea of CinB as a nuclease that requires both PD-(D/E)xK domains for its activity.

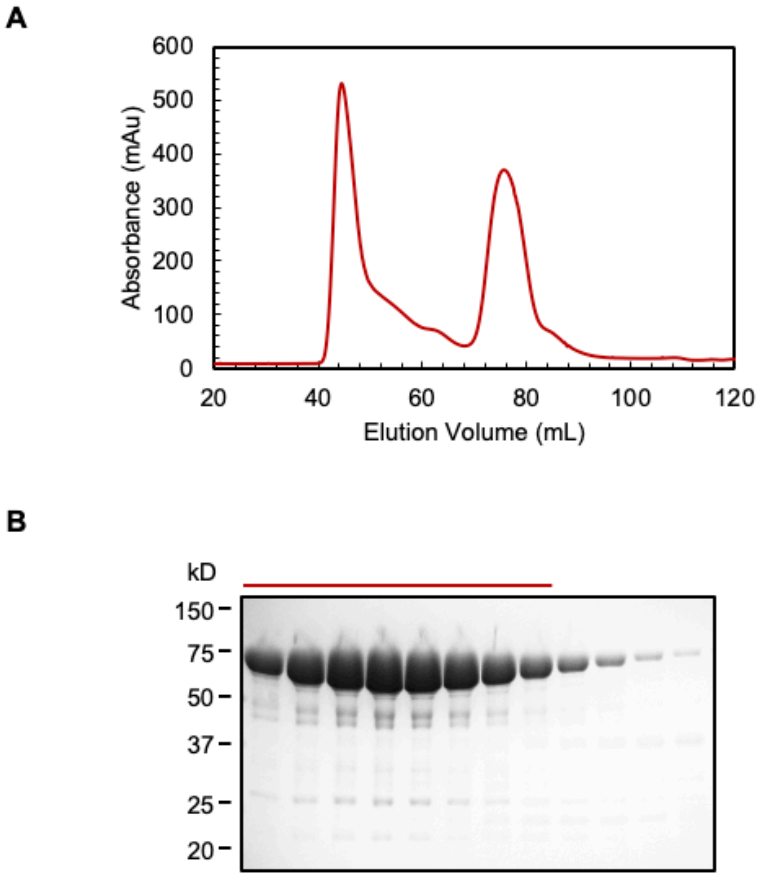

Figure 7. An example of purification of full-length recombinant CinB^{wPip}. (A) Chromatogram of CinB^{wPip} purification by size-exclusion chromatography using HiLoad 16/600 Superdex 200 PG column. The first peak between 40 ml and 50 ml elution volume represents the void peak and the second peak between 70 ml and 80 ml elution volume represents CinB^{wPip}. (B) SDS-PAGE gel of the samples collected in the second peak from size-exclusion chromatography. Lanes highlighted represents the fractions that were pooled, concentrated and used as the purified CinB^{wPip} in *in vitro* nuclease assays. Protein purification was done with Judith Ronau.

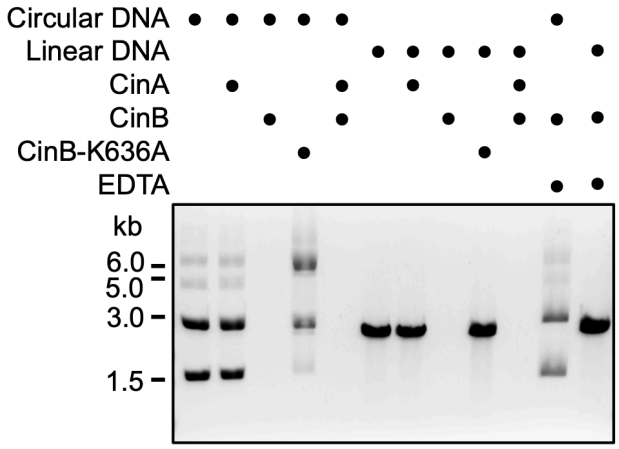

Figure 8. CinB^{wPip} cleaved both circular and linearized pBluescript SK+ plasmids. In all reactions, 1 μM CinB^{wPip} was incubated with 15 nM DNA for 90 min. In reactions where CinA^{wPip} was present, 10 μM CinA^{wPip} and 1 μM CinB^{wPip} were incubated on ice for 30 min to allow complex formation before adding to substrate. To stop the reactions, EDTA was added to a 2x molar excess over Mg^{2+}. Samples were run in a 0.8% agarose gel, and the gel was stained with ethidium bromide.

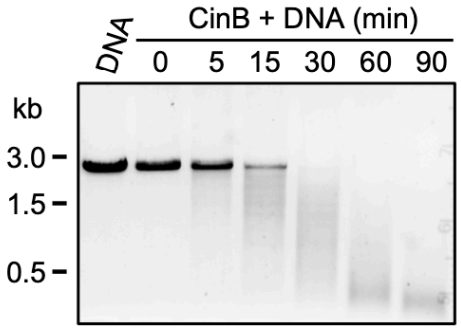

Figure 9. Time-course experiment showing CinB^{wPip} activity against linearized pBluescript SK+ plasmid. In all reactions, 1 μM CinB^{wPip} was incubated with 15 nM DNA. To stop the reactions, EDTA was added to a 2x molar excess over Mg^{2+}. Samples were run in a 0.8% agarose gel, and the gel was stained with ethidium bromide.

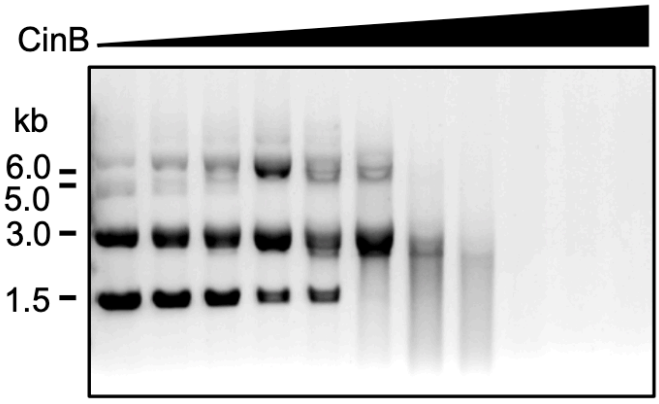

Figure 10. DNase activity of CinB^{wPip} against purified pBluescript SK+ plasmid, which includes both linear, relaxed circular, and supercoiled forms, with various concentrations of the protein. All forms appear to be susceptible to cleavage, as also seen in **Figure 8**. Lanes starting from the left: 0, 20, 50, 100, 200, 500 nM, 1, 2, 5, 10, 25, 50 μM. In all reactions, 1 μM CinB^{wPip} was incubated with DNA for 90 min. To stop the reactions, EDTA was added to a 2x molar excess over Mg^{2+}. Samples were run in a 0.8% agarose gel, and the gel was stained with ethidium bromide.

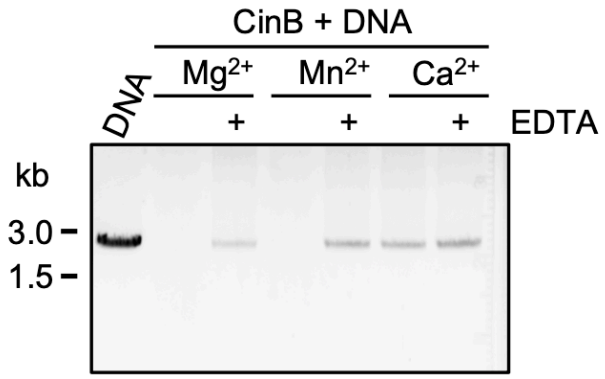

Figure 11. Mg^{2+} and Mn^{2+}, but not Ca^{2+}, support the DNase activity of $CinB^{wPip}$. In all reactions, 1 μM $CinB^{wPip}$ was incubated with 15 nM DNA for 90 min in the present of 5 mM divalent cations. To stop the reactions, EDTA was added to each reaction to a final concentration of 10 mM. Samples were run in a 0.8% agarose gel, and the gel was stained with ethidium bromide.

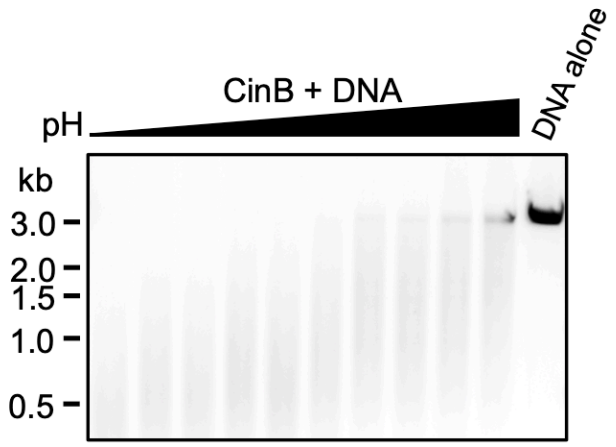

Figure 12. DNase activity of CinB^{wPip} is weakly pH-dependent. Reaction pH was between 6.0 (left lane) and 10.5 (right lane) with 0.5 increments between adjacent lanes. In all reactions, 1 μM CinB^{wPip} was incubated with 15 nM DNA for 90 min. To stop the reactions, EDTA was added to a 2x molar excess over Mg^{2+}. Samples were run in a 0.8% agarose gel, and the gel was stained with ethidium bromide.

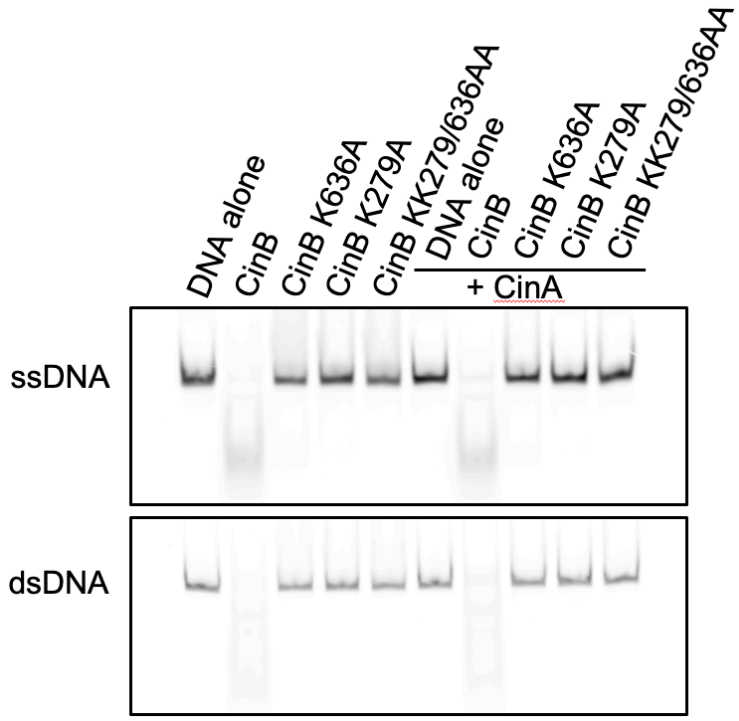

Figure 13. CinB^{wPip} cleaved both single- and double-stranded 70-mer DNAs. CinB^{wPip} at 1 μM was incubated with 0.5 μM Cy5-labeled DNA for 90 min. Reactions were set up as described in **Figure 8**. Samples were run in a 9% polyacrylamide/TBE gel and imaged on Typhoon FLA 7000.

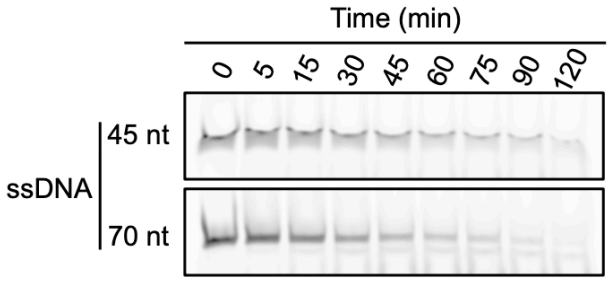

Figure 14. Time-course experiment showing CinB^{wPip} cleavage of 45-nucleotide or 70-nucleotide Cy5-labeled single-stranded DNA. CinB^{wPip} at 1 μM was incubated with 0.5 μM Cy5-labeled DNA. Reactions were set up as described in **Figure 8**. Samples were run in a 9% polyacrylamide/TBE gel and imaged on Typhoon FLA 7000.

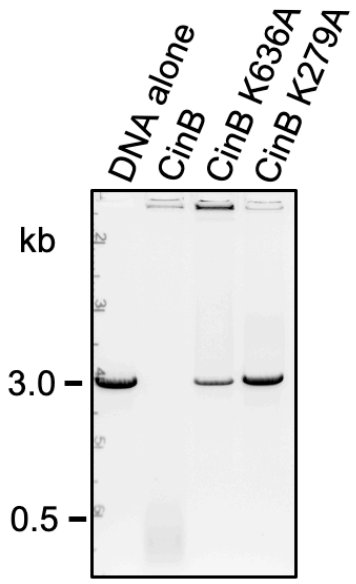

Figure 15. Mutation of either K636 or K279 eliminated CinB^{wPip} cleavage of linearized pBluescript SK+ (~3 kb). The mutant proteins appeared to still bind DNA based on the signal remaining in the loading wells (top). In all reactions, 1 μM CinB^{wPip} was incubated with 15 nM DNA for 90 min. To stop the reactions, EDTA was added to a 2x molar excess over Mg^{2+}. Samples were run in a 0.8% agarose gel, and the gel was stained with ethidium bromide.

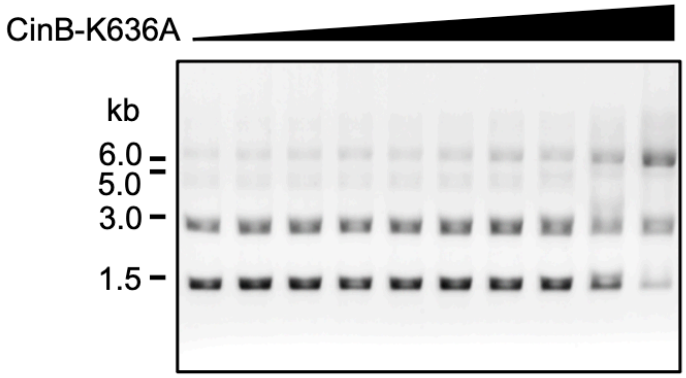

Figure 16. Catalytic K636A mutation eliminated DNase activity in CinB^{wPip} except at the highest concentrations, which might represent low levels of contaminating *E. coli* nucleases. Lanes starting from the left: 0, 20, 50, 100, 200, 500 nM, 1, 2, 5, 10, 25, 50 μM. In all reactions, 1 μM CinB^{wPip} K636A was incubated with DNA for 90 min. To stop the reactions, EDTA was added to a 2x molar excess over Mg^{2+}. Samples were run in a 0.8% agarose gel, and the gel was stained with ethidium bromide.

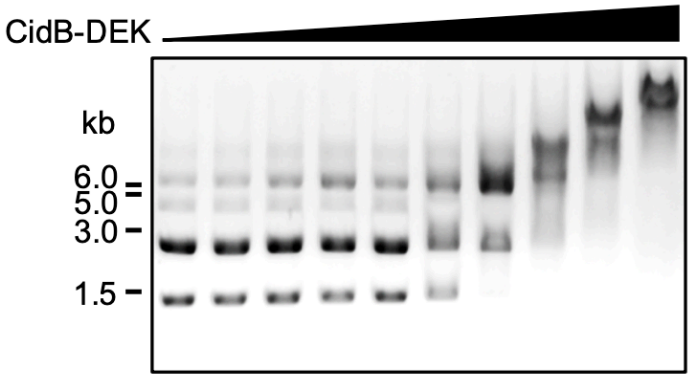

Figure 17. CidB^{wPip} protein, even with a potentially reactivated CTND through a double point mutation (V686E, R688K), did not display nuclease activity but did display a weak DNA-binding activity based on the reduced mobility of the substrate DNA at high protein concentrations. Lanes starting from the left: 0, 20, 50, 100, 200, 500 nM, 1, 2, 5, 10, 25, 50 μM. In all reactions, 1 μM CidB^{wPip} was incubated with DNA for 90 min. To stop the reactions, EDTA was added to a 2x molar excess over Mg^{2+}. Samples were run in a 0.8% agarose gel, and the gel was stained with ethidium bromide.

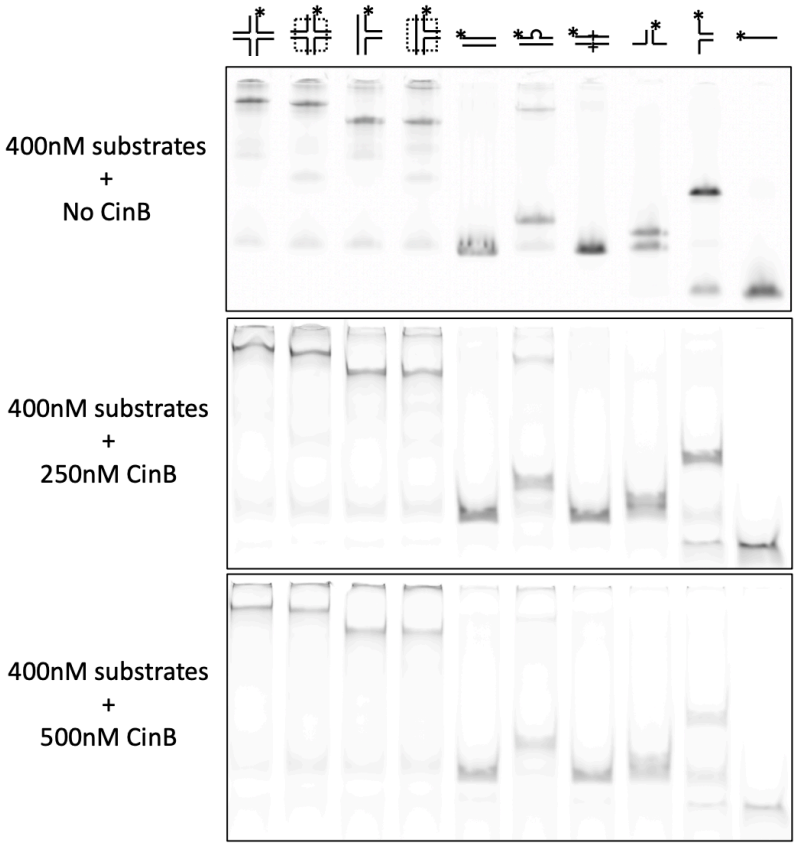

Figure 18. CinB$^{w\text{Pip}}$ showed no obviously increased activity against various structured DNA substrates. Ten substrates were used in this assay (from left to right: four-way junction, four-way junction with homologous cores, three-way junction, three-way junction with homologous cores, duplex, loop-out, mismatch, half-duplex 1, half-duplex 2, and single stranded DNA). Reactions were set up as described in **Figure 8**. Samples were run in a 9% polyacrylamide/TBE gel and imaged on Typhoon FLA 7000.

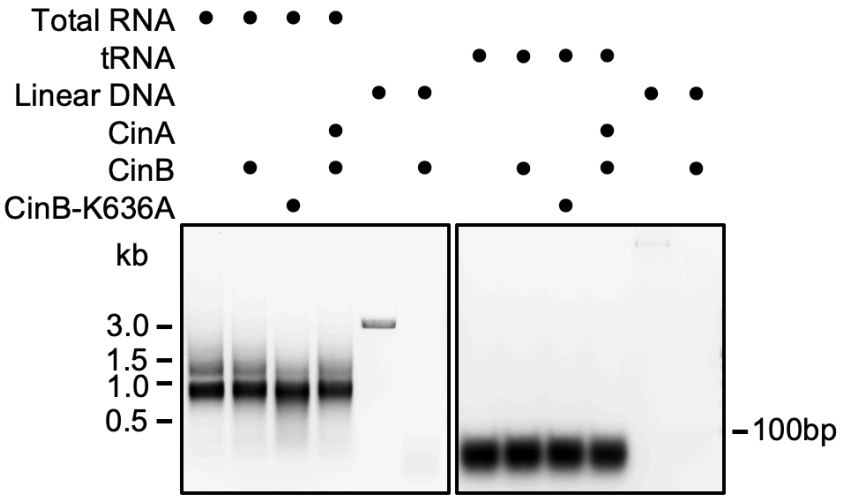

Figure 19. CinB^{wPip} showed no RNase activity against either total RNA extract from *D. melanogaster* or yeast tRNA. 500 ng of RNA were used in each reaction. Linearized pBluescript SK+ was used as a positive control for nuclease activity. Reactions were set up as described in **Figure 8**. Samples were run in a 0.8% agarose gel, and the gel was stained with ethidium bromide.

iv. Protein-Protein Interaction Between CinA and CinB

An important aspect of the toxin-antidote model of CI is the binding specificity between the protein pairs within each *cif* operon as suggested by our previous affinity pull-down experiments (Beckmann, Ronau and Hochstrasser, 2017). Here we used isothermal titration calorimetry (ITC) to determine quantitatively the affinity between CinA^{wPip} and CinB^{wPip}. ITC revealed a K_d of 25 ± 1.3 nM, demonstrating strong binding between the cognate pair (**Figure 20**). We tested whether the tight association of CinA with CinB would inhibit CinB nuclease activity. Pre-incubation of CinB^{wPip} with excess CinA^{wPip} did not reduce DNase activity in our *in vitro* assays, suggesting that CinA rescues cells from CinB-induced toxicity through a distinct mechanism, e.g., cellular re-localization (**Figures 8 and 13**). This observation was not surprising inasmuch as co-incubation of CidA^{wPip} and CidB^{wPip} also did not limit the DUB activity of CidB^{wPip} (Beckmann, Ronau and Hochstrasser, 2017).

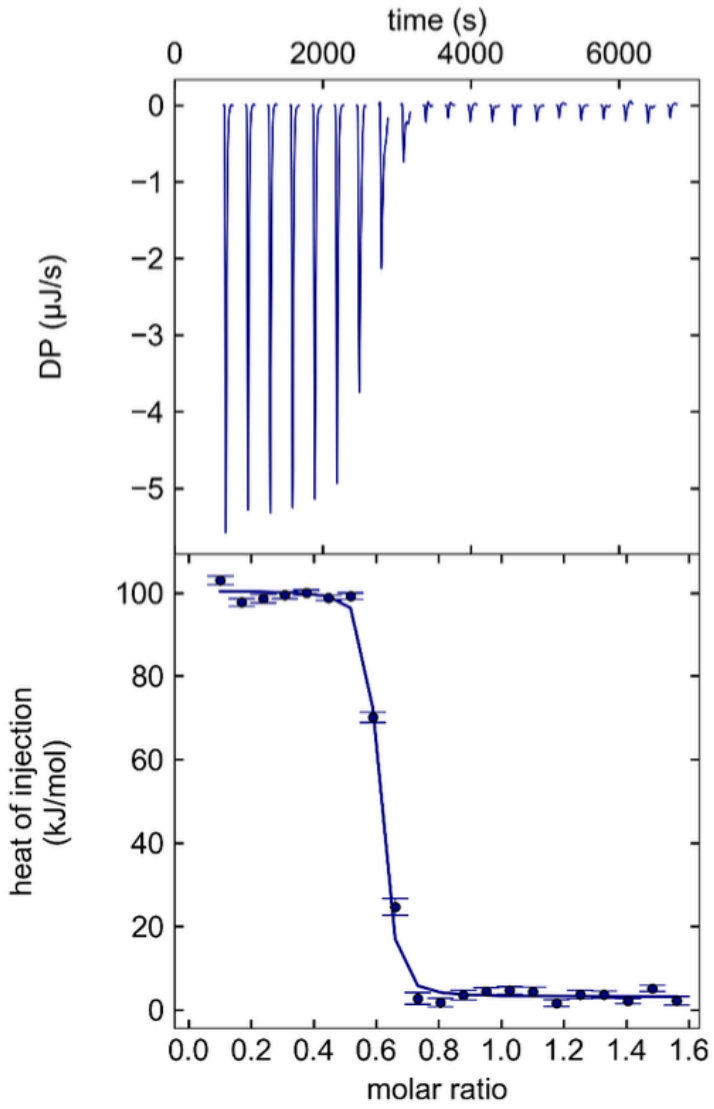

Figure 20. The ITC binding isotherm for binding of CinA$^{w\text{Pip}}$ to CinB$^{w\text{Pip}}$ yielded a $\boldsymbol{K_d}$ of 25 ± 1.3 nM. This tight interaction provides support to the hypothesis that the cognate pair exists as a toxin-antidote system. Top panel shows raw injection data over time while the bottom panel shows integrated heats over the course of the reaction (n = 3). Experiment was performed by Judith Ronau.

v. Discussion

Recent studies have revealed the central role of the *cidA-cidB* operon in both CI induction and rescue (Beckmann, Ronau and Hochstrasser, 2017; LePage *et al.*, 2017; Shropshire *et al.*, 2018; Shropshire and Bordenstein, 2019; Beckmann *et al.*, 2019c). CidB is a DUB, and this enzymatic activity is crucial for its ability to promote CI. Previous findings led to the hypothesis that the *cinA-cinB* locus, with a pair of genes paralogous to *cidA-cidB*, might also be involved in *Wolbachia*-induced CI despite lacking a known DUB domain. Here we have shown that CinB is a nuclease, specifically a DNase. It remains possible that the apparent lack of RNase activity reflects the absence of a crucial cofactor or appropriate reaction conditions. The DNA-cleaving activity we have detected is of broad specificity but weak, at least under the conditions tested. An unregulated, highly active nuclease would likely be harmful to *Wolbachia*; we note that expression of CinB in *E. coli* is not obviously deleterious to growth. It is possible that the enzyme is more potent against particular DNA sequences or structures. For example, during the exchange of protamine for histones that occurs in the male pronucleus in the nascent zygote, transiently uncoated paternal DNA may be prone to forming cruciforms or other structures that are preferred substrates for CinB. Among the earliest signs of CI are chromosome condensation defects in the male pronucleus (Callaini, Dallai and Riparbelli, 1997; Landmann *et al.*, 2009).

Both the NTND and CTND of CinB are highly conserved across many *Wolbachia* strains. Interestingly, our *in vitro* enzyme analysis suggests the nuclease activity of CinB requires both of its nuclease domains to be active. It is possible that the two domains feature a mechanism where one domain is involved in substrate recognition while the

other is responsible for the actual phosphodiester bond cleavage. Another possibility is that both nuclease domains recognize and cleave DNA substrates in a cooperative manner such that mutation in one nuclease domain is sufficient to inhibit the overall function of the protein. Many PD-(D/E)xK nucleases function as homodimers, which also brings together a pair of PD-(D/E)xK domains (Knizewski *et al.*, 2007). Structural analysis will be needed to gain a deeper understanding of the exact CinB reaction mechanism.

Chapter IV: Analysis of the *w*Pip *cin* Operon in *Saccharomyces cerevisiae*

Note: Portions of this chapter were published in Chen, H., Ronau, J. A., Beckmann, J. F. and Hochstrasser, M. (2019) 'A Wolbachia nuclease and its binding partner provide a distinct mechanism for cytoplasmic incompatibility', Proceedings of the National Academy of Sciences, 116(44), pp. 22314-22321.

i. Introduction

The first evidence suggesting that *cifA* and *cifB* genes form a toxin-antidote pair came from expression of these genes in yeast *S. cerevisiae*. Expressing either CidB^{wPip} or CinB^{wPip} in yeast induces a temperature-sensitive growth defect that can only be rescued when the cognate A protein from the same *w*Pip *Wolbachia* strain is co-expressed (Beckmann, Ronau and Hochstrasser, 2017**)**. The yeast lethality and rescue phenotypes were also later recapitulated using the *cidA-cidB* genes from the *w*Ha strain of *Wolbachia* (Beckmann *et al.*, 2019c). Catalytic protease domain cysteine-to-alanine mutation in CidB^{wPip} or a D-E-K catalytic triad triple mutation to alanines in the CinB^{wPip} C-terminal nuclease domain eliminated the proteins' toxicity in yeast (Beckmann, Ronau and Hochstrasser, 2017). Here we report that single amino acid to alanine mutation in either the N-terminal or C-terminal nuclease domains in CinB^{wPip} is sufficient in inhibiting its toxicity in yeast. This result, together with our *in vitro* enzymatic analysis, suggests that CinB is a nuclease toxin that requires two active nuclease domains.

A recent high-copy suppressor screen utilizing a yeast genomic tiling library identified karyopherin-α, a nuclear import receptor, as a strong suppressor of the toxicity

of CidB^{wPip} in yeast, providing useful insights on the molecular mechanism of CI caused by *cid* operon (Beckmann *et al.*, 2019c). Here we report our preliminary data on a similar suppressor screen looking for potential suppressors of CinB^{wPip}-induced toxicity in yeast. Lastly, our ITC experiment indicated strong protein-protein interaction between CinA^{wPip} and CinB^{wPip}. However, CinA binding did not inhibit the nuclease activity of CinB *in vitro*, suggesting that the rescue effect of CinA is likely caused by some other mechanism. One possibility is that CinA binding re-localizes CinB nuclease leaving it inaccessible to its target substrate. Here we also report some of our preliminary data on the localization of CinA and CinB in yeast along with our future directions.

ii. *Cin* Operon Expression in Yeast

To determine if the toxicity of CinB^{wPip} expression in yeast is due to its nuclease activity, we generated a panel of mutants with mutations in catalytic residues of either the NTND or CTND. Simultaneously changing all three CTND catalytic residues to alanines (3A) or individually (D614A, E634A or K636A) was sufficient for eliminating the CinB-induced growth defect (**Figure 21A**). Mutation of the corresponding NTND catalytic residues also eliminated CinB^{wPip}-induced toxicity, suggesting that the toxin function of CinB^{wPip} requires both nuclease domains to be active (**Figure 21B**). Changes in protein levels due to the mutations in either domain cannot account for the loss of temperature-dependent lethality (**Figures 22-24**). Interestingly, CinB seemed to undergo proteolytic cleavage in yeast cells, creating two fragments. While the N-terminal fragment is stable, the C-terminal fragment appeared to undergo further degradation in cells and thus could not be detected by Western blot analysis (**Figure 23 and Figure 24**). Nonetheless, these

results together with our enzymatic analysis are consistent with the hypothesis that both N- and C-terminal nuclease domains are important for the function of CinB toxin.

A

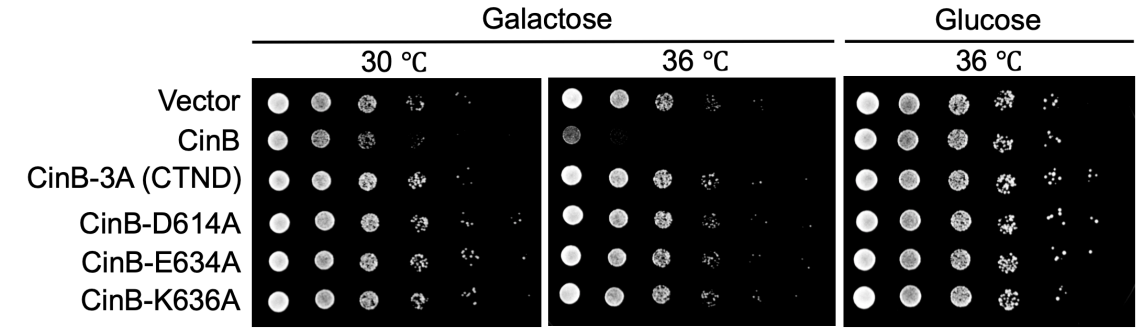

B

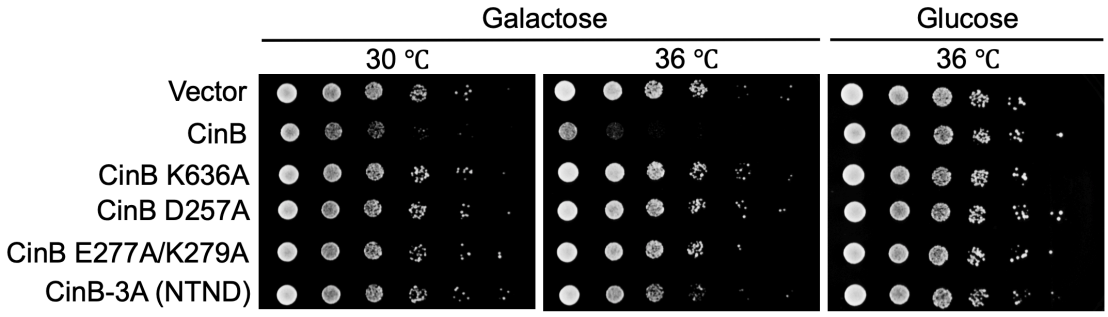

Figure 21. CinB$^{w\text{Pip}}$ toxicity in the *S. cerevisiae* BY4741 strain. All genes were N-terminally FLAG-tagged and cloned into pYES2, a galactose-inducible expression vector. Six-fold serial dilutions were conducted and yeast were allowed to grow for two days before imaging. Expression of wild-type CinB caused a temperature-dependent grow defect. Such growth defects were not observed in yeast expressing CinB with predicted inactivating point mutations in either the CTND (A) or NTND (B). All serial dilutions were done in triplicate with independent transformants.

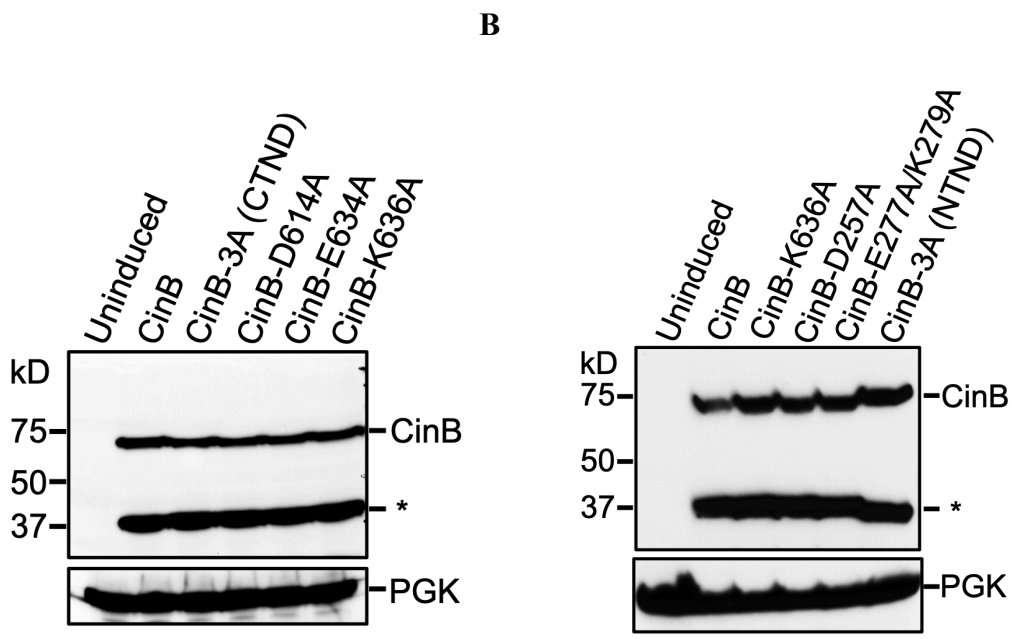

Figure 22. Relative expression levels of WT and mutant CinB proteins in yeast. Equivalent numbers of yeast based on OD_{600} were lysed, and the lysates were resolved by SDS-PAGE and immunoblotted for CinB by α-FLAG antibody; PGK served as a loading control. A fraction of CinB is proteolytically cleaved in yeast and the N-terminal fragment is labeled with an asterisk. (see **Figures 23 and 24**).

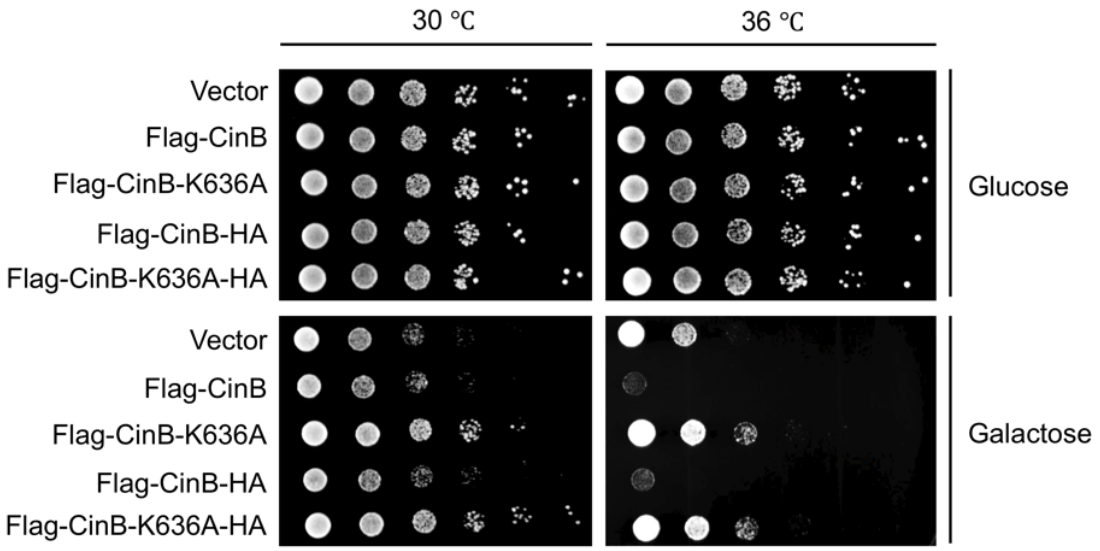

Figure 23. Effect of doubly tagged Flag-CinB^{wPip}-HA on *S. cerevisiae* (BY4741) growth. Growth assay was performed as **Figure 21**. Expression of Flag-CinB^{wPip}-HA induced the same temperature-sensitive grow defect as the singly tagged Flag-CinB^{wPip}. The growth defect was abolished when yeast expressed the mutated derivative, Flag-CinB^{wPip}-K636A-HA, suggesting the C-terminal HA tag did not interfere with the toxin-like function of CinB.

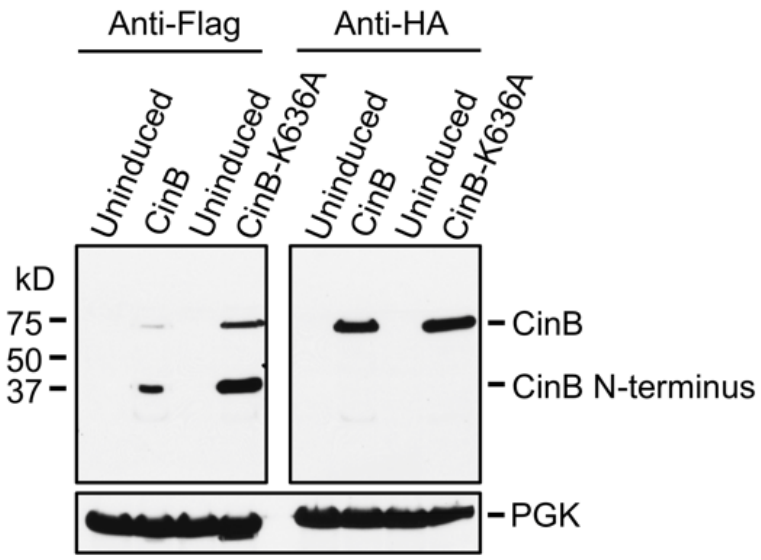

Figure 24. Western blot analysis of yeast expressing either Flag-CinB$^{w\text{Pip}}$-HA or the catalytic K636A mutant derivative, confirming that the inactivating mutation did not reduce the expression level of CinB. The protein undergoes an apparent proteolytic cleavage in yeast cells, as suggested by a N-terminal species at ~37 kDa in the anti-Flag blot. However, a C-terminal fragment of CinB was not seen in anti-HA blot, indicating that this fragment, if indeed synthesized, might have been further degraded.

iii. CinB Suppressor Screen Utilizing a Yeast Genomic Tiling Library (Preliminary Findings)

The fact that nuclease activity of CinB is responsible for its toxicity in yeast led us to hypothesize that the growth defect caused by CinB might be due to CinB-induced DNA damage, resulting in genomic instability. Using a yeast high-copy genomic tiling library, we sought to identify yeast genes that can suppress CinB^{wPip}-induced growth lethality, hoping to gain insight into the molecular mechanism behind its function. The screen was performed in two conditions. In one condition, after transformation of the genomic library, colonies were allowed to form before the expression of CinB^{wPip} was induced by galactose. Unfortunately, this condition resulted in possible homologous recombination of the *URA3* selection marker between the two plasmids used in the screen, leading to a high number of false-positive results (**Table 1**). In the second screening condition, CinB^{wPip} expression was induced right after the transformation of the library plasmids by plating directly onto galactose. Suppressor plasmids recovered under this more stringent condition showed no homologous recombination of *URA3* marker (**Table 2**). The screen was performed only once under each condition. Future work involves doing the screen in triplicate under the more stringent conditions followed by subcloning the individual genes from each candidate plasmid to identify the responsible suppressor.

Table 1. Yeast suppressor plasmids identified under the condition where after the transformation of genomic tiling plasmids colonies were allowed to grow for a few days before the expression of CinB^{wPip} was induced by galactose. Candidate suppressor plasmids were sequenced to verify if homologous recombination of *URA3* occurred between the library plasmids and pRS416gal1.

Notes	# of Replicates	Plasmid	Genes on the Plasmid										
	1	**YGPM3c12**	[ORC2]*	TRM7	YBR062C	YBR063C	YBR064W	ECM2	NRG2				
False positive, URA3 HR	1	**YGPM10l11**	[NTH2]*	RER2	COQ1	FMP44	RCR1	UGA2	[DSF2]&				
	1	**YGPM6n14**	[YDL038C]*	BSC1	YDL036C	[GPR1]&	[YDL034W]*						
	1	**YGPM15p09**	[EXG2]*	tS(AGA)D2	YDR261W-A	[YDR261W-B]*							
	1	**YGPM17g10**	[PPZ2]&	YDR437W	YDR438W	LRS4	DOT1	APT2	YDR442W	[SSN2]&			
URA3	6	**YGPM25o01**	[GEA2]&	URA3	YEL020C-B	TIM9	RPR1	YEL020C	MMS21	YEL018C-A	EAF5	PMP2	GTT3
	1	**YGPM17b12**	[YEL007W]&	YEL006W	VAB2	YEA4	GIM4	WBP1	YEL001C	[MNN1]*			
False positive, URA3 HR	1	**YGPM8b10**	YFR054C	YFR056C	YFR055W								
	1	**YGPM23o11**	[SAP155]&	ERJ5	YFR042W	YFR043C	YFR044C	YFR045W	CNN1	BNA6	RMD8		
	1	**YGPM11o01**	[SUT1]&	YIP5	YGL160W	YGL159W	tL(CAA)G1	[RCK1]*					
	1	**YGPM6p14**	YHL041W	ARN1	YHL039W	[CBP2]&							
	1	**YGPM4o16**	[YHL009W-B]&	YHL008C	[STE20]&								
	1	**YGPM26a12**	[AMA1]&	YGR226C	DIE2	YGR228W	SMI1	BNS1	PHB2	NAS6	[PHO81]&		
	1	**YGPM23g05**	[TPO2]*	YGR139W	CBF2	VPS62	BTN2	tA(AGC)G	[SKN1]*				
False positive, URA3 HR	1	**YGPM7f04**	[YHR029C]*	SLT2	RRM3	YHR032W	YHR032W-A	YHR032C-A	YHR033W	[PIH1]			
	1	**YGPM4h24**	[KRR1]*	FYV5	[YCL058W-A]	YCL057C-A	PRD1	YCL056C	KAR4	SPB1	[PBN1]		
	1	**YGPM33c06**	[ECM37]*	PAN6	TID3	SSL2	YIL142C-A	[CCT2]*					
False positive, URA3 HR	1	**YGPM23l22**	[PDR11]*	YIL012W	TIR3	DOT5	EST3	tD(GUC)I2	FAA3	URM1	[NAS2]&		
No URA3	1	**YGPM5a13**	[THI11]*	YJR157W	[HXT16]*								
No URA3	1	**YGPM16p04**	[HXT16]&	SOR1	MPH3								
False positive, URA3 HR	2	**YGPM31g23**	[NAP1]*	FMP46	[TRK2]*								
No URA3	1	**YGPM7h13**	[ASK1]*	SFK1	YKL050C	CSE4	ELM1	[YKL047W]*					
No URA3	2	**YGPM9k15**	[YKR104W]&	YKR105C	YKR106W								
No URA3	1	**YGPM28h19**	[DYN1]*	RHO4	[TRM2]*								
No URA3	1	**YGPM31d09**	[APL2]*	OCT1	YKL133C	RMA1	YKL131W	SHE2	[MYO3]&				
No URA3	2	**YGPM26o18**	[PUT1]&	tD(GUC)L1	YLR143W	ACF2	RMP1	SPE4	SMD3	[PEP3]*			
False positive, URA3 HR	1	**YGPM2k14**	[TSL1]&	YML099W-A	ARG81	TAF13	VPS9	YML096W	[RAD10]&				
No URA3	2	**YGPM19a15**	[VIP1]&	YLR410W-B	YLR410W-A	CTR3	YLR412W	YLR412C-A	[YLR413W]*				
No URA3	1	**YGPM11j12**	[YLR455W]&	YLR456W	NBP1	YLR458W	GAB1	YLR460C	PAU4				
No URA3	1	**YGPM13n21**	[CTL1]*	YMR181C	RGM1	YMR182W-A	RUF3	SSO2	YMR184W	[YMR185W]*			
No URA3	1	**YGPM31i14**	[CAF120]&	YNL277W-A	MET2	YNL276C	YNL275W	YNL274C	[TOF1]*				
No URA3	1	**YGPM30h17**	[POL2]	ORC5	YNL260C	[ATX1]							
No URA3	1	**YGPM24c17**	[CHS6]&	SAP185	YJL097W	MRPL49	[BCK1]*						
No URA3	1	**YGPM11f05**	[NGL2]*	MRPL33	MSU1	HSH155	[ABZ2]*						
No URA3	1	**YGPM30h01**	[YOL070C]*	[NUF2]	HST1	RTG1	RIB2	INP54	MET22	[HUS1]&			
No URA3	1	**YGPM20l15**	[IFM1]	YOL022C	tG(GCC)O2	[DIS3]&							
No URA3	1	**YGPM11g16**	[YNR070W]&										
No URA3	1	**YGPM5j03**	[FAP1]*	YNL022C	HDA1	ARK1	YNL019C	YNL018C	YNL017C	tI(AAU)N2	[PUB1]*		
False positive, URA3 HR	1	**YGPM32n14**	[MKK1]&	[YOR231C-A]*	MGE1	KIN4	RPL33B	YOR235W	snR17a	DFR1	HES1	[YOR238W]*	
No URA3	1	**YGPM32k08**	[YOR389W]&	YOR390W	HSP33	YOR392W	ERR1	YOR394W	YOR394C-A	[YOR396W]*			
No URA3	1	**YGPM17m17**	[YPL279C]	YPL278C	YPL277C	YPL276W	YPL275W	[SAM3]*					
No URA3	2	**YGPM12f04**	[YPL257W-B]&	YPL257W	CLN2	BBP1	[HFI1]*						
No URA3	1	**YGPM3p13**	[TCO89]&	PPQ1	tE(UUC)P	CBC2	CUP9	YPL176C	[SPT14]*				
No URA3	1	**YGPM30i12**	[QCR2]&	AQY1	HPA2	OPT2	YPR195C						
No URA3	1	**YGPM11h18**	[YRF1-7]*	YPL282C	[ERR2]								

Table 2. Yeast suppressor plasmids identified under the condition where CinB^{wPip} expression was induced right after the transformation of the library plasmids. None of the candidate suppressors obtained under this condition had homologous recombination of *URA3* occurred between the library plasmids and pRS416gal1.

# of Replicates	Plasmid	Genes on the Plasmid								
1	**YGPM3j18**	[YER139C]*	YER140W	COX15	MAG1	DDI1	[UBP5]&			
1	**YGPM27a24**	[HOS4]&	COX5B	YIL110W	SEC24	YIL108W	[PFK26]&			
1	**YGPM16i22**	[INP51]*	YIL001W	SGN1	MPH1	YIR003W	[DJP1]			
1	**YGPM17j20**	[RIO2]	RTT106	YNL205C	SPS18	YNL203C	SPS19	PSY2	[YNL200C]	
1	**YGPM32b05**	FET4								
1	**YGPM25f07**	[HOL1]&								
2	**YGPM32e11**	[MDH2]*	YOL125W	YOL124C	HRP1	SMF1	[RPS19A]&			
1	**YGPM24h05**	[MSH2]&	HAL9	MPD2	YOL087C	YOL086W-A	[ADH1]&			
1	**YGPM18c02**	[DBP5]*	STD1	RAT1	RSB1	YOR050C	YOR051C	YOR052C	YOR053W	[VHS3]&
1	**YGPM7m21**	[YOR142W-B]&	THI80	[ELG1]&						
1	**YGPM19l07**	tP(UGG)O3	YOR345C	REV1	PYK2	PUT4	[CIN1]*			

iv. Localization of CinA and CinB in Yeast (Preliminary Findings)

To determine the localization of CinA/B^{wPip} and CidA/B^{wPip} in yeast, we tagged CinA^{wPip} and CidA^{wPip} with mCherry and tagged CinB^{wPip} and CidB^{wPip} with eGFP. N-terminal mCherry or eGFP fusions disrupted the proper toxin-antidote behavior of both *cif* operons in yeast (**Figures 25 and 26**). In contrast, C-terminal mCherry and eGFP fusions behave similarly to the untagged proteins in toxicity and rescue assays (**Figure 27 and Figure 28**). However, preliminary data indicated that the expression levels of these proteins in yeast were too low to be detected by live-cell microscopic imaging. Future directions involve either genomic integration of these genes for more consistent protein expression or doing immunofluorescence imaging with fixed yeast cells. We created 3xFlag-tagged CinB^{wPip} and HA-tagged CinA^{wPip} in yeast plasmids and showed that these tags did not disturb the toxin-antidote behavior between CinB and CinA, and thus are suitable to use for immunofluorescent imaging (**Figure 29**).

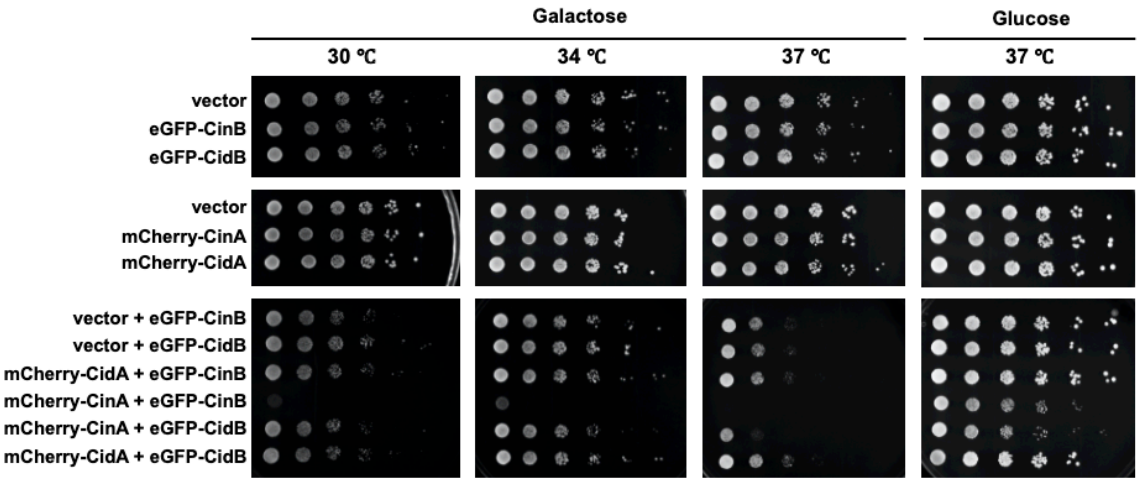

Figure 25. Effect of N-terminal fluorescent protein fusion of Cif^{wPip} on *S. cerevisiae* (BY4741) growth. Growth assay was performed as **Figure 21**. All CifA^{wPip} proteins are N-terminal mCherry fusions while all CifB^{wPip} proteins are N-terminal eGFP fusions. The eGFP fusion CifBs lost their ability to induce temperature dependent growth lethality in yeast. Co-expression of mCherry-CinA^{wPip} with either eGFP-CinB^{wPip} or eGFP-CidB^{wPip} induced growth defect, which was not observed if the proteins are untagged, suggesting the N-terminal fluorescent protein fusions created artificial phenotypes that are related to the protein tags.

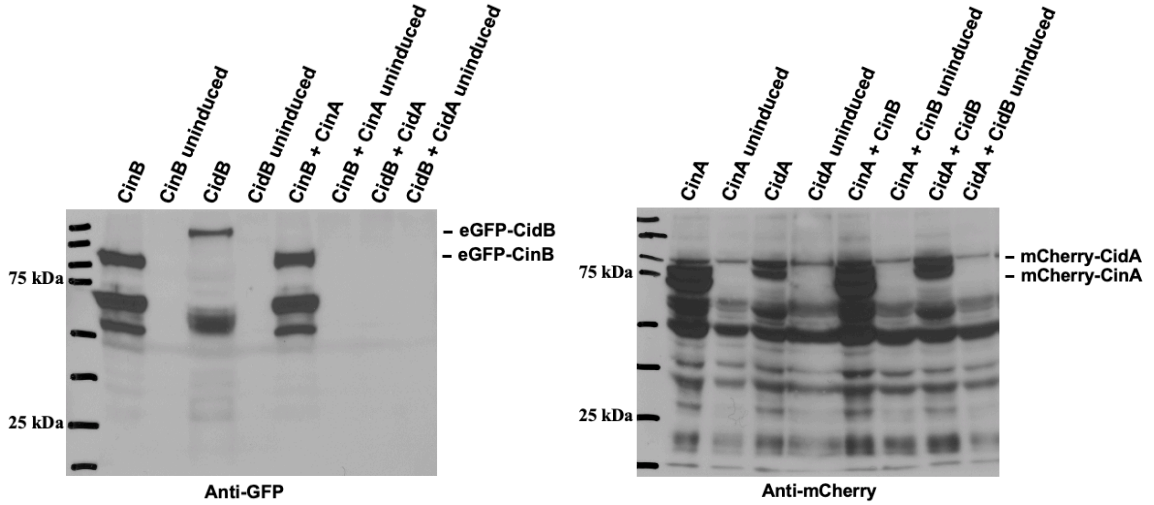

Figure 26. Western blot analysis of yeast expressing either eGFP-CifB^{wPip} (left) or mCherry-CifA^{wPip} (right). Uninduced samples were grown in glucose media and served as negative controls. Equivalent numbers of yeast based on OD_{600} were lysed, and the lysates were resolved by SDS-PAGE and immunoblotted for either CifB by anti-GFP (left) or CifA by anti-mCherry (right) antibodies. The expected sizes for eGFP-CidB and eGFP-CinB are about 161 kDa and 107 kDa, respectively. And the expected sizes for mCherry-CidA and mCherry-CinA are 84 kDa and 78 kDa, respectively.

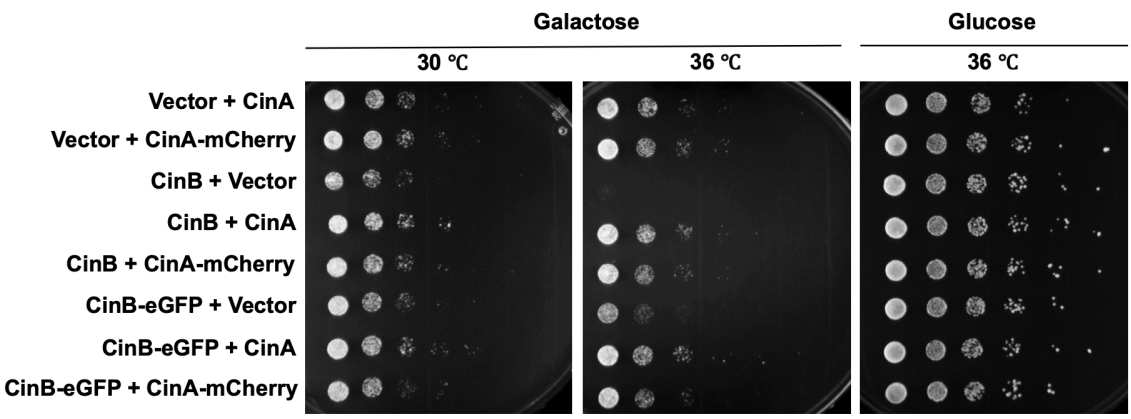

Figure 27. Effect of C-terminal fluorescent protein fusion of Cin$^{w\text{Pip}}$ on *S. cerevisiae* (BY4741) growth. Growth assay was performed as **Figure 21**. CinA and CinB without fluorescent protein fusion are N-terminally Flag-tagged. Though weaker than Flag-CinB, CinB-eGFP fusion protein still possesses toxicity at 36°C. Furthermore, CinA-mCherry fusion is able to rescue yeast from growth defect induced by either Flag-CinB or CinB-eGFP fusion, indicating that the rescue behavior of CinA was not altered by the C-terminal mCherry tag.

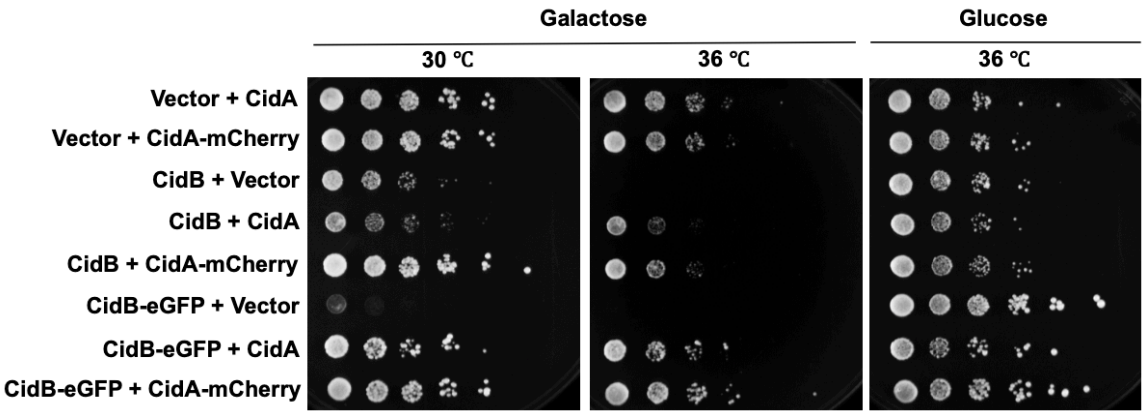

Figure 28. Effect of C-terminal fluorescent protein fusion of Cid^{wPip} on *S. cerevisiae* (BY4741) growth. Growth assay was performed as **Figure 21**. CidA and CidB without fluorescent protein fusion are N-terminally Flag-tagged. CidB-eGFP fusion showed slightly stronger toxicity at 37°C compared to Flag-CidB. CidA-mCherry fusion is able to rescue yeast from growth defect induced by either Flag-CidB or CidB-eGFP fusion, indicating that the rescue behavior of CidA was not altered by the C-terminal mCherry tag.

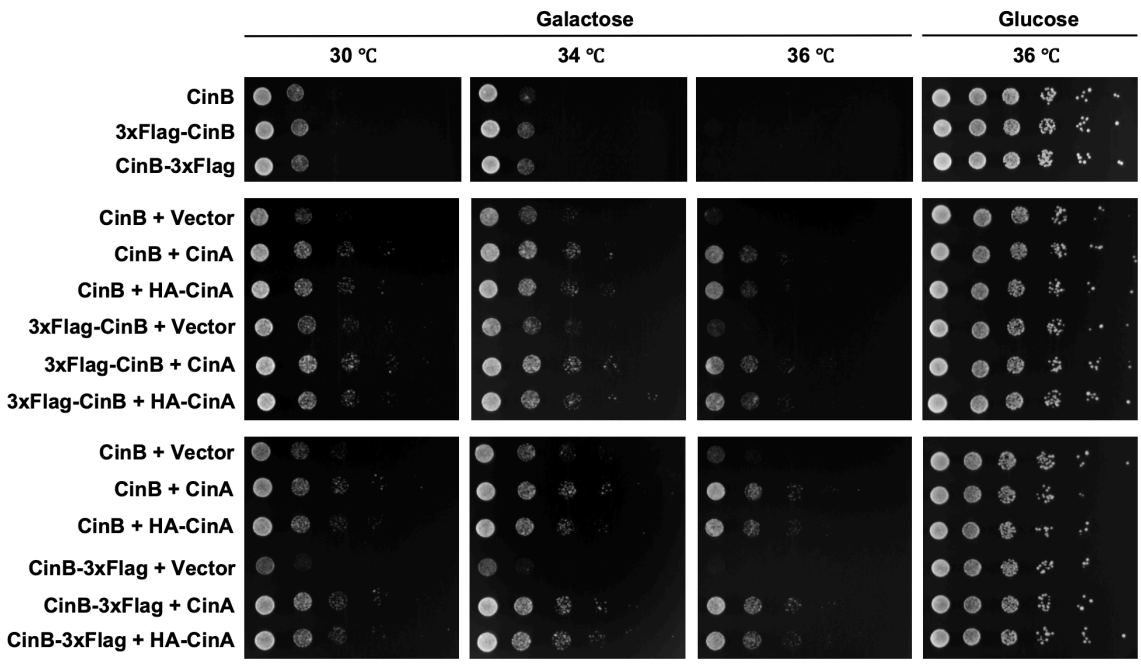

Figure 29. Effect of 3xFlag-tagged CinB$^{w\text{Pip}}$ and HA-CinA$^{w\text{Pip}}$ on *S. cerevisiae* (BY4741) growth. Growth assay was performed as **Figure 21**. Unlabeled CinA and CinB are N-terminally Flag-tagged. Both 3xFlag-CinB and CinB-3xFlag exhibited similar temperature-dependent growth lethality as Flag-CinB. Furthermore, HA-CinA is able to rescue yeast from growth defect induced by 3xFlag-CinB, CinB-3xFlag, or Flag-CinB.

v. Discussion

Consistent with data from our *in vitro* nuclease assays, the temperature-sensitive growth defect in *S. cerevisiae* caused by CinB also requires both of its N- and C-terminal nuclease domains to be active. Furthermore, we showed that single amino acid to alanine mutations in either of its nuclease domains is sufficient for inhibiting its toxicity in yeast. These data together with our enzymatic analyses highlight CinB as a dual nuclease domain toxin whose toxicity is linked to its nuclease acitivity.

Despite the strong protein-protein interaction between CinA^{wPip} and CinB^{wPip}, pre-incubation of CinB^{wPip} with 10-fold molar excess CinA^{wPip} did not reduce DNase activity in our *in vitro* assays. Similarly, co-incubation of recombinant CidA^{wPip} and CidB^{wPip} also did not limit the DUB activity of CidB^{wPip}, suggesting that CifA rescues cells from CifB-induced toxicity through a mechanism not involving direct inhibition of enzyme activities (Beckmann, Ronau and Hochstrasser, 2017). One hypothesis we favor is that CifA binding changes the cellular localization of CifB thus hindering it from accessing its substrates and preventing toxicity to the cells. To test this hypothesis, we created CifA-mCherry fusion and CifB-eGFP fusion and examined the protein localization in yeast. We showed that N-terminal fluorescent protein fusion disrupts the proper toxin-antidote behavior of the Cif proteins while C-terminal fusions maintains their toxin-antidote-like property. Unfortunately, the expression level of these proteins was too low for live-cell imaging in yeast. Future work should exploit strategies to increase expression level of the protein or different imaging methods such as immunofluorescent imaging with fixed yeast cells.

Chapter V: *Cin* Operon in Transgenic *Drosophila Melanogaster*

Note: Portions of this chapter were published in Chen, H., Ronau, J. A., Beckmann, J. F. and Hochstrasser, M. (2019) 'A Wolbachia nuclease and its binding partner provide a distinct mechanism for cytoplasmic incompatibility', Proceedings of the National Academy of Sciences, 116(44), pp. 22314-22321.

i. Introduction

Transgenic fruit fly studies have shown that the *cid* operons from both *w*Pip and *w*Mel *Wolbachia* strains can induce embryonic lethality with early-stage developmental defects similar to CI embryos (Beckmann, Ronau and Hochstrasser, 2017; LePage *et al.*, 2017). Transgenic female flies expressing either $cidA^{wMel}$ and $cidA\text{-}cidB^{wMel}$ can rescue both transgenic CI caused by cid^{wMel} and natural CI caused by *w*Mel-infected male flies (LePage *et al.*, 2017; Shropshire *et al.*, 2018). Prior to this work, there was no direct evidence proving that the *cin* operon is also capable of inducing CI and rescue.

Sequence comparison indicated the *cin* operon was a distant paralog of the *cid* operon (Beckmann and Fallon, 2013). Similar to *cid*, the *cin* operon also induced toxicity and rescue when expressed in yeast *S. cerevisiae* (Beckmann, Ronau and Hochstrasser, 2017). Most importantly, the fact that some strong CI-inducing *Wolbachia* strains, such as the *w*No strain that infects *Drosophila simulans*, contain only *cin* but not *cid* type operons and that neither operon is present in *w*Au, a close relative of *w*Mel that does not induce CI, strongly suggested that the *cin*-type operon should also be able to induce CI independent of the *cid* operon. Here we report that expression of the *cin* operon in

transgenic male flies can indeed induce post-zygotic male sterility and embryonic defects typical of CI. Importantly, transgenic *cinA* can rescue defects in egg hatch rates when expressed in females.

ii. Hatch Rate Analysis of Transgenic Fruit Flies

To test the ability of the *cin* operon to induce CI in the absence of *Wolbachia* infection, we created transgenic *D. melanogaster* lines containing $cin^{w\text{Pip}}$ genes by site-directed PhiC31-mediated integration (Groth *et al.*, 2004). Recent studies utilized two distinct strategies to generate transgenic Cid-expressing flies (Beckmann, Ronau and Hochstrasser, 2017; LePage *et al.*, 2017; Shropshire *et al.*, 2018). Here we attempted both. In the first, $cinA^{w\text{Pip}}$ and $cinB^{w\text{Pip}}$ genes were integrated into separate chromosomes (*UAS:cinA/UAS:cinA; UAS:cinB/UAS:cinB*) while the second strategy utilized a fusion of $cinA^{w\text{Pip}}$ and $cinB^{w\text{Pip}}$ genes linked by a T2A viral peptide-coding sequence (*UAS:cinA-T2A-cinB/UAS:cinA-T2A-cinB*) that causes the ribosome to terminate and immediately restart translation on the T2A sequence, resulting in the synthesis of two separate proteins from one transcript (**Figure 30**). All fly lines were verified to be uninfected with native *Wolbachia* isolates by PCR amplification of $cidA^{w\text{Mel}}$ gene (**Figure 31**). Both the *Nanos*-Gal4-*Tubulin* (NGT) driver and maternal triple driver (MTD-Gal4) were used for specific expression of the Gal4 transcription factor in fly germline cells, stimulating transcription of the *cin* transgenes through their Gal4-responsive upstream activation sequences (UAS) (Rorth, 1998; Petrella, Smith-Leiker and Cooley, 2007; White-Cooper, 2012). The MTD driver can increase the transcript levels of $cidA^{w\text{Mel}}$ by over 1000-fold relative to expression with the NGT driver, allowing transgenic $cidA^{w\text{Mel}}$ females to rescue CI

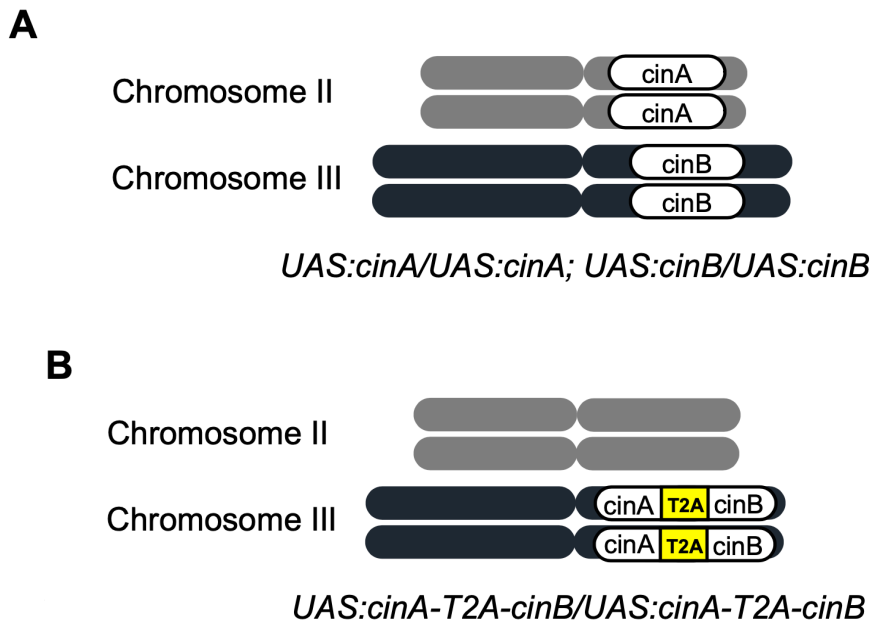

Figure 30. Two strategies were used to generate transgenic flies: (A) *cinA*$^{w\text{Pip}}$ was inserted into the second chromosome and *cinB*$^{w\text{Pip}}$ was inserted into the third chromosome (*UAS:cinA/UAS:cinA; UAS:cinB/UAS:cinB*), or (B) *cinA*$^{w\text{Pip}}$ and *cinB*$^{w\text{Pip}}$ were linked by a T2A viral sequence (yellow) and inserted into the third chromosome (*UAS:cinA-T2A-cinB/UAS:cinA-T2A-cinB*).

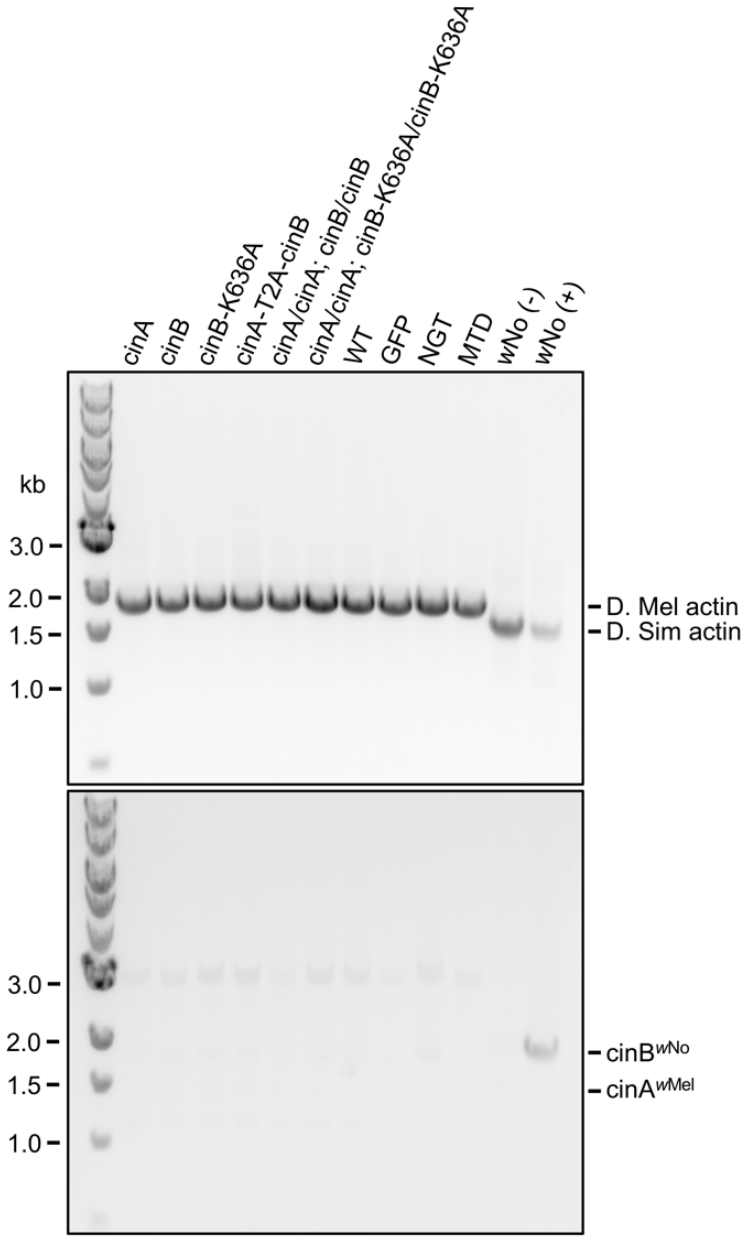

Figure 31. PCR verification of *Wolbachia* infection status in both *D. melanogaster* and *D. simulans*. Top: Positive controls for PCR amplification using the actin gene. Bottom: PCR amplifications of either $cinA^{w\text{Mel}}$ for *D. melanogaster* or $cinB^{w\text{No}}$ for *D. simulans* (last two lanes) showing that none of the *D. melanogaster* stocks used was infected by *w*Mel *Wolbachia* and only *w*No (+) stock was infected by *w*No *Wolbachia*.

induced by male flies infected with *w*Mel (Shropshire *et al.*, 2018). The level of CI was determined from the percentage of embryos that hatched into larvae.

When crossed to wild-type (WT) females, males transgenic for *cinA*$^{w\text{Pip}}$ alone under the control of NGT driver did not affect hatch rates, whereas males transgenic for *cinB*$^{w\text{Pip}}$ alone produced a ~30% hatch rate reduction (**Figure 32 Top Panel**). This reduction was partially but significantly suppressed if the catalytic lysine-636 residue was mutated to alanine. Consistent with hatch rate data for transgenic *cidA*$^{w\text{Mel}}$ and *cidB*$^{w\text{Mel}}$ (LePage *et al.*, 2017), male flies transgenic for both *cinA*$^{w\text{Pip}}$ and *cinB*$^{w\text{Pip}}$ (expressed with the NGT driver) induced a stronger reduction in hatch rates (~50-60%) when compared to males transgenic for *cinB*$^{w\text{Pip}}$ alone (**Figure 32 Middle Panel**). Both transgenic strategies generated a similar level of hatch rate reductions when using the NGT driver. Importantly, the catalytic lysine-636 to alanine mutation significantly weakened (by ~30%) the effect on hatch rates caused by transgenic *UAS:cinA/+ NGT:Gal4/+; UAS:cinB/+* males, suggesting the reduction in hatch rates depended on the nuclease activity of CinB$^{w\text{Pip}}$ (**Figure 32 Middle Panel**).

Transgenic *cinA*-T2A-*cinB* males induced a greater hatch rate reduction (nearly 90%) when under the control of the strong MTD driver. Importantly, we observed rescue of these low hatch rates by crossing transgenic *cinA*-T2A-*cinB*$^{w\text{Pip}}$ males to females that were transgenic for *cinA*$^{w\text{Pip}}$ (**Figure 32 Bottom Panel**). This strengthens and generalizes the hypothesis of *cifA* as the antidote gene in the different *cif* operon systems. Unexpectedly, transgenic *UAS:cinA/+; UAS:cinB/+* males from five independent homozygous lines all failed to lower hatch rates under the MTD-Gal4 driver when crossed to WT females; this is discussed below.

Figure 32. Expression of the *cinA-cinB*^{wPip} genes in flies induces CI-like embryo killing and rescue phenotypes. (Top panel) Crosses with flies transgenic for either *cinA*^{wPip} or *cinB*^{wPip} alone expressed using the NGT driver (highlighted in orange). Data in burgundy represents CI-inducting crosses while green represents either rescue or weakening of CI induction by the CinB-K636A mutation. All control crosses are shown in gray. n = 40-64. (Middle panel) Crosses with flies transgenic for the entire *cinA-cinB*^{wPip} operon under control of the NGT driver. n = 38-58. Error bars in (C) and (D) represent standard deviation of the mean; $^{**}P < 0.01$, $^{***}P < 0.001$, $^{****}P < 0.0001$ by ANOVA with multiple comparison between all groups. (Bottom panel) Transgenic CI in crosses with flies transgenic for the entire *cinA-cinB*^{wPip} operon expressed using the strong maternal triple driver (MTD, highlighted in red) could be rescued by transgenic *cinA*^{wPip} females. Vertical lines represent medians. n = 23-57. $^{****}P < 0.0001$ by two-tailed Mann-Whitney U test.

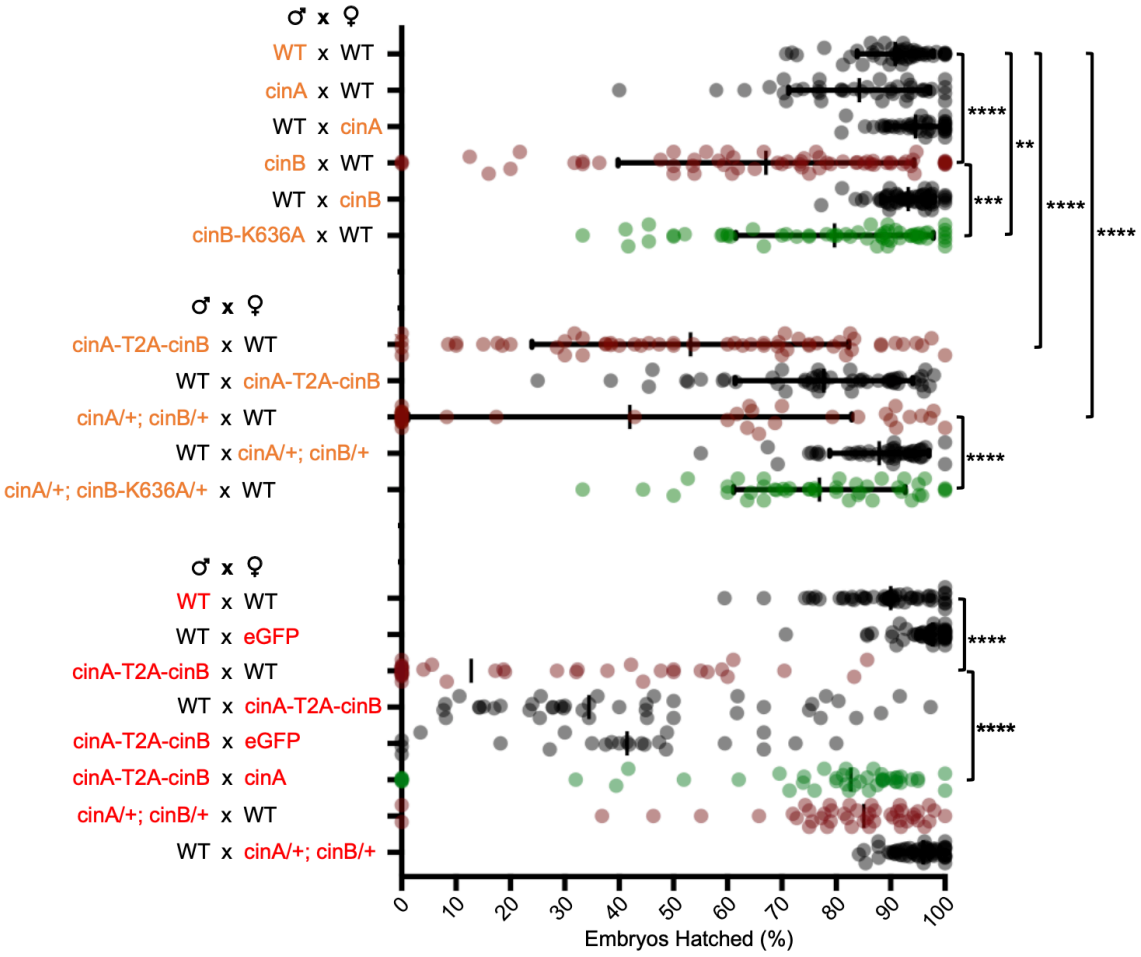
♂ x ♀
WT x WT
cinA x WT
WT x cinA
cinB x WT
WT x cinB
cinB-K636A x WT
♂ x ♀
cinA-T2A-cinB x WT
WT x cinA-T2A-cinB
cinA/+; cinB/+ x WT
WT x cinA/+; cinB/+
cinA/+; cinB-K636A/+ x WT
♂ x ♀
WT x WT
WT x eGFP
cinA-T2A-cinB x WT
WT x cinA-T2A-cinB
cinA-T2A-cinB x eGFP
cinA-T2A-cinB x cinA
cinA/+; cinB/+ x WT
WT x cinA/+; cinB/+
****
**
***
****
****
****
****
0
10
20
30
40
50
60
70
80
90
100
Embryos Hatched (%)

iii. Cytology of Transgenic and Natural CI Induced by *cin* Operon

We next determined whether the hatch-rate reduction caused by transgenic expression of the *cinA-cinB*^{wPip} genes could be traced to embryonic defects similar to those seen in natural CI. The cytology of fly embryos infected with *Wolbachia* strains known to contain only a *cin* operon has never been reported. Therefore, we first analyzed embryos from *D. simulans* infected by *w*No, a *Wolbachia* strain containing a *cin* but no *cid* operon, for comparison to the cytological analysis of our transgenic flies (**Figure 31**) (Gillespie *et al.*, 2018; Lindsey *et al.*, 2018). When mated with uninfected females, the *w*No-infected male flies induced strong embryonic hatch rate reduction similar to its previously reported CI penetrance (**Figure 33**) (Mercot *et al.*, 1995; Poinsot *et al.*, 1998). The *w*No-infected flies also exhibited a range of cytological defects similar to those previously reported for *w*Mel-induced CI with the exception that no regional mitotic failure was observed (**Figure 34**) (LePage *et al.*, 2017).

Most importantly, all transgenic crosses that resulted in reduced hatch rates induced CI-like embryonic defects in embryos collected after 1-2 h development (**Figures 35 and 36**). Similar to the *w*No infection control, about half of the embryos from the cross between transgenic *cinA*-T2A-*cinB* males under the MTD-Gal4 driver and WT females exhibited an abnormal cytological phenotype. Together, these data establish a role for the *Wolbachia cinA-cinB* genes as an independent CI-inducing gene system and support the hypothesis that *cifA* genes are specifically required for the rescue of CI, similar to their ability to suppress *cifB* toxicity in yeast.

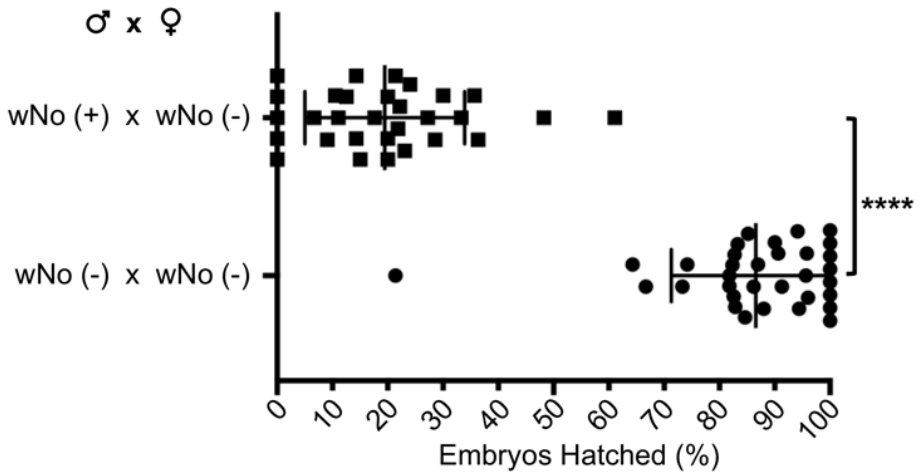

Figure 33. *w*No infected male *D. simulans* produced a ~80% hatch rate reduction when crossed to uninfected females. Error bar represents standard deviation of the mean. n = 30-33. ****$P < 0.0001$ by two-tailed Mann-Whitney U test.

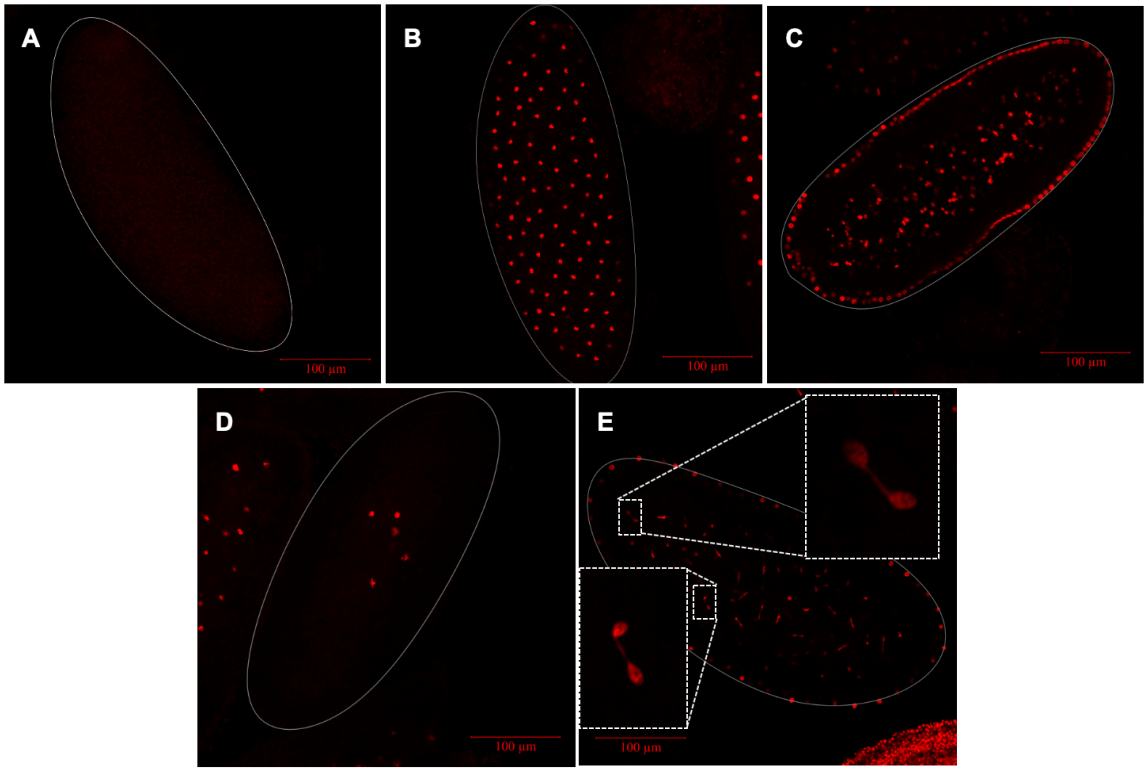

Figure 34. Representative images of propidium iodide-stained embryos from incompatible crosses between *w*No-infected males and uninfected females showing (A) an unfertilized embryo, (B) a normal embryo after 1 h development, (C) a normal embryo after 2 h development, (D) an embryo with early mitotic failure, and (E) an embryo showing anaphase chromatin bridging.

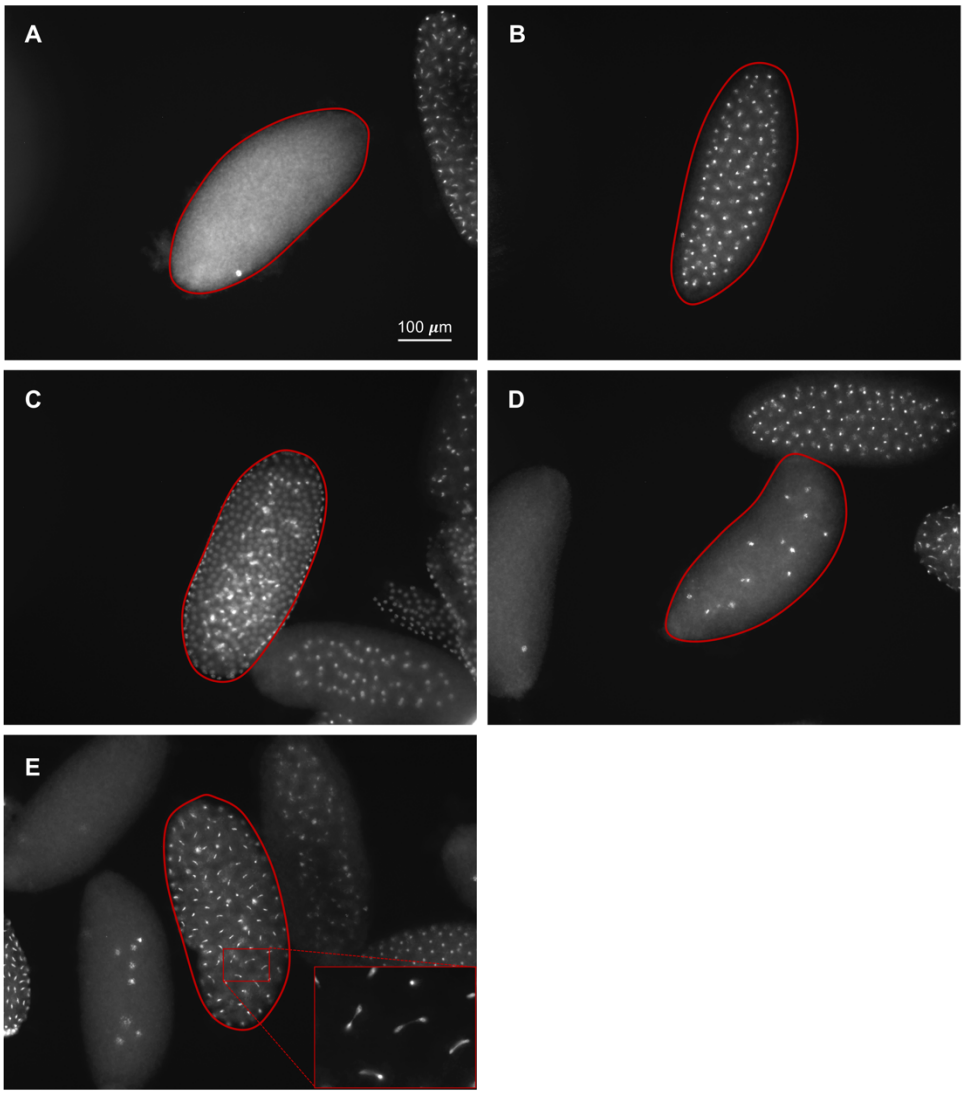

Figure 35. Embryos from crosses between transgenic *D. melanogaster* males expressing the *cinA-cinB*^{wPip} operon and wild type females show CI-like cytology. Representative images of propidium iodide-stained embryos from females showing (A) an unfertilized embryo, (B) a normal embryo after 1 h development, (C) a normal embryo after 2 h development, (D) an embryo with early mitotic failure, and (E) an embryo showing anaphase chromatin bridging.

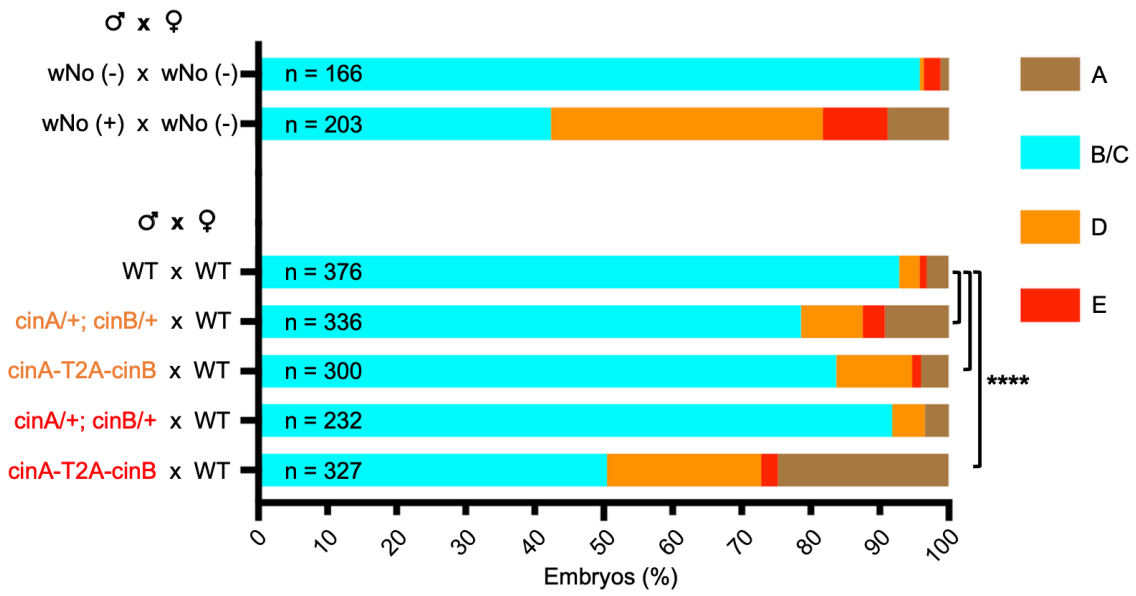

Figure 36. Quantification of embryo cytology. *w*No (-) and *w*No (+) represent *D. simulans* uninfected or infected by *w*No, respectively. *w*No infection was confirmed by PCR amplification of the *cinB*^{wNo} gene (see **Figure 31**). For the transgenic *D. melanogaster* crosses (bottom), only the *cinA*-T2A-*cinB* crosses under the MTD-Gal4 driver (highlighted in red. NGT-Gal4 driver highlighted in orange) strongly phenocopied the natural CI cytology. The number of embryos examined in each cross is shown. Embryos exhibited normal cytology after 1-2 h were grouped together and are shown in teal. ****$P < 0.0001$ by Chi-Square test comparing normal (**Figures 34B and 34C**) and abnormal (**Figures 34A, 34D and 34E**) cytological phenotypes.

iv. Discussion

Recent studies have shown that the *cidA*-*cidB* operon can induce both CI and rescue when transgenically expressed in *D. melanogaster* (Beckmann, Ronau and Hochstrasser, 2017; LePage *et al.*, 2017; Beckmann *et al.*, 2019c; Shropshire *et al.*, 2018; Shropshire and Bordenstein, 2019). Our work here demonstrates the sufficiency of the *cinA*-*cinB* operon for both inducing CI by expression in males and rescuing CI through expression (of *cinA*) in females. Cytology of CI embryos induced by the *cin*-type operon alone had not been previously characterized. Here we show that transgenic CI embryos induced by *cinA*-*cinB* operon exhibited similar cytological defect as naturally occurring CI embryos from *D. simulans* infected by *w*No *Wobachia* strain, which contains only the *cin* nuclease-type operon. Together our transgenic fruit fly data characterized the *cin*-type operon as CI-inducing genes independent to the *cid*-type operon. The rescue of transgenic CI through expression of *cinA* in females further highlights the role of *cifA* genes as the antidotes in the CI-inducing operon systems.

Surprisingly, *UAS:cinA/+; UAS:cinB/+* males did not induce embryonic lethality when under the control of the MTD-Gal4 driver, unlike *UAS:cinA-T2A-cinB/UAS:cinA-T2A-cinB* males, in our transgenic CI crosses. It is possible that the operon-like structure of *cinA*-T2A-*cinB* better mimics the natural expression ratio of the *cinA* and *cinB* genes, which was shown to be important in the *cid* operon (Bonneau *et al.*, 2018a). If relative expression of CinA were too high in *UAS:cinA/+; UAS:cinB/+* flies under the MTD-Gal4 driver, it could dampen CinB toxicity in CI crosses; alternatively, insufficient CinA during male spermiogenesis might selectively kill sperm precursors with high CinB levels. Another unexpected finding from our transgenic fly analyses was that MTD-

driven expression of *cinA*-T2A-*cinB* in females caused a high level of embryonic lethality. It is likely that such embryonic lethality is due to the toxicity from expressing the operon at a very high level.

Chapter VI: Summary and Discussion

CI is the most common form of *Wolbachia*-induced reproductive manipulations and has long been utilized in mosquito-borne disease control to reduce the spread of Dengue and Zika viruses, and other human pathogens. For many decades, the molecular basis of *Wolbachia*-induced CI had been a mystery. In 2017, the *cidA-cidB* operon was reported by two groups to be sufficient in *Wolbachia*-induced CI (Beckmann, Ronau and Hochstrasser, 2017; LePage *et al.*, 2017). The *cin* operon, a distant paralog of the *cid*-type operon, was also proposed to be another CI-inducing operon that contains putative nuclease domains. The fact that some strong CI-inducing *Wolbachia* strains contain only *cin* but not *cid* operons and that neither operon is present in *Wolbachia* strains that do not induce CI led us to hypothesize that the *cin* operon should also be able to induce CI independently of the *cid* operon.

Here we have shown that transgenic expression of the *cinA-cinB*$^{w\text{Pip}}$ operon in male *D. melanogaster* indeed recapitulates CI-like embryonic lethality when these males are mated with wild-type uninfected females. Importantly, such transgenic CI can be rescued by expression of *cinA*$^{w\text{Pip}}$ in uninfected female flies. The rescue of transgenic CI by *cinA*$^{w\text{Pip}}$ alone is fully consonant with our earlier finding that *cinA*$^{w\text{Pip}}$ suppresses *cinB*$^{w\text{Pip}}$-induced toxicity in yeast (Beckmann, Ronau and Hochstrasser, 2017). These results validated the role of the *cin*-type operon in inducing CI and of *cinA* in rescue in CI-inducing *Wolbachia* strains lacking *cid* operons.

Interestingly, when mated with wild-type uninfected females, transgenic males expressing *cinB*$^{w\text{Pip}}$ alone only induced a weak embryonic hatch rate reduction compared

to transgenic *cinA-cinB*$^{w\text{Pip}}$ males. This result is, however, similar to previously reported study with *cid* operon from *w*Mel *Wolbachia* strain where expression of neither *cidA*$^{w\text{Mel}}$ or *cidB*$^{w\text{Mel}}$ alone in transgenic males was sufficient in inducing CI (LePage *et al.*, 2017; Shropshire *et al.*, 2018; Shropshire and Bordenstein, 2019). It is intriguing how in both cases the *cifA* gene can contribute to CI while expressed in males and rescue while expressed in females. One possibility is that CifA and CifB protein complex forms a toxin that targets male-specific host factor in sperms and can be reversed later by CifB binding to maternally-supplied CifA. One way to test this hypothesis is by creating mutations in the CifA-CifB interface to disrupt protein-protein interaction. If the hypothesis holds true, one can expect such mutations to abolish the ability of CifA-CifB transgenic males to induce CI and the rescue effect of CifA in transgenic females.

Our transgenic *cin*$^{w\text{Pip}}$-induced CI embryos showed the same cytological defects as embryos from CI crosses between *w*No-infected male *D. simulans* and uninfected females, further highlighting the central role of the *cin*-type operon in inducing CI in *Wolbachia* strains, such as *w*No, that lack *cid* operons. The embryonic defects caused by *cin* operon are similar to previously reported cytological defects induced by *cid*-type operons with the exception that regional mitotic failure was only observed in *cid*- but not *cin*-induced CI embryos (LePage *et al.*, 2017). Such differences can potentially be related to different underlying molecular mechanisms in how the two types of toxin induce CI. To unravel the exact molecular mechanism of CI, it will be important to identify the substrates of both the DUB and the nuclease toxins in both *Wolbachia*-infected flies and transgenic flies expressing the *cif* operons.

Our *in vitro* nuclease activity assay confirmed CinB to be a DNase that contains two nuclease domains and has activity towards both single- and double-stranded DNAs. The nuclease activity of CinB is also essential for its toxicity in yeast and its ability to induce CI in when transgenically expressed in fruit flies. Though not detected in our study, it remains possible that CinB has RNase activity against certain RNAs. Importantly, the DNase activity of CinB requires a fully functional catalytic D-E-K triad in both of its nuclease domains. It is possible that the two domains combine in a mechanism where one domain is involved in substrate recognition while the other is responsible for the actual phosphodiester bond cleavage. Another possibility is that both nuclease domains recognize and cleave DNA substrates in a cooperative manner such that mutation in one nuclease domain is sufficient to inhibit the overall function of the protein. Many PD-(D/E)xK nucleases function as homodimers, which also brings together a pair of PD-(D/E)xK domains (Knizewski *et al.*, 2007). Structural analysis will be needed to gain a deeper understanding of the exact CinB reaction mechanism.

We have also measured a tight physical association between CinA and CinB (**Figure 20**). Nevertheless, this interaction did not inhibit the catalytic activity of the nuclease, a result similar to our finding with CidA and CidB where association of the cognate pair failed to suppress the DUB activity of CidB against model substrates such as ubiquitin polymers (Beckmann, Ronau and Hochstrasser, 2017). The rescue mechanism might instead be caused by CinA or CidA association changing the cellular localization of the cognate B toxins or their ability to bind their critical targets *in vivo*. A recent study found that the catalytic inactive CidB protein interacts with both karyopherin-α (Kap-α), a nuclear import receptor, and the P32 histone chaperone from *Drosophila melanogaster*

protein extracts (Beckmann *et al.*, 2019c). These data suggest that CidB could potentially localize in the nuclei and CidA binding might hinder CidB from entering nuclei and accessing its target substrates. Nonetheless, future work should focus on examining the localization of CifAs and CifBs proteins in fruit flies infected by *Wolbachia* or that are transgenic for *cif* operons. It would also be worthwhile to look at the yeast localization of CifA-CifB protein pairs that are capable of inducing both toxicity and rescue.

While details of the CinB nuclease's mode of action remain to be worked out, our results highlight a novel mechanism for CI that is likely to be broadly relevant to *Wolbachia*-induced CI in many different arthropods. An interesting question is why some *Wolbachia* carry both *cin* and *cid* loci, as is true for *w*Pip, or have B genes predicted to encode active nuclease and DUB activities in the same polypeptide (CndB class) (**Figure 2**) (Gillespie *et al.*, 2018; Beckmann *et al.*, 2019b). The CI loci are usually part of WO prophage regions, and repeats or partial repeats are common. Thus, these paralogs may be subject to rapid evolutionary changes that allow shifts between DUB-dominated and nuclease-dominated CI mechanisms in response to host adaptations to the endosymbiont. Finally, PD-(D/E)xK nucleases may have roles in other host-parasite interactions. The selfish genetic element *Medea*, for instance, which kills embryos expressing *Medea* maternally but lacking the gene in the zygote, also encodes a putative nuclease of this class (Lorenzen *et al.*, 2008).

Appendix I: Plasmids Used in This Study

Plasmid Names	Description	Source
JFB_BX1	KpnI-FLAG-cinB-SacI in pYes2	Beckman *et al.*, 2017
JFB_CE1	KpnI-FLAG-cinB(D614A, E634A, K636A)-SacI in pYes2	Beckman *et al.*, 2017
JAR_1.9.7	BamHI-cinA-XhoI in pCOLD-GST	Judith Ronau, this study
JAR_2.2.9	BamHI-cinB-XhoI in pGEX6P1	Judith Ronau, this study
JAR_2.7.1	BamHI-cinB(K636A)-XhoI in pGEX6P1	Judith Ronau, this study
JAR_2.8.2	BamHI-cidB(V686E, R688K)-XhoI in pCOLD-GST	Judith Ronau, this study
HC_AA1	KpnI-FLAG-cinB-HA-SacI in pYES2 vector	Hongli Chen, this study
HC_AK1	KpnI-FLAG-cinB(K279A)-SacI in pYes2	Hongli Chen, this study
HC_AL2	KpnI-FLAG-cinB(E277A, K279A)-SacI in pYes2	Hongli Chen, this study
HC_BB1	KpnI-FLAG-cinB(D257A, E277A, K279A)-SacI in pYes2	Hongli Chen, this study
HC_BS2	BamHI-FLAG-cinB(K279A)-XhoI in pGEX6P1	Hongli Chen, this study
HC_BU1	BamHI-FLAG-cinB(K279A, K636A)-XhoI in pGEX6P1	Hongli Chen, this study
HC_D5	KpnI-FLAG-cinB(D614A)-SacI in pYes2	Hongli Chen, this study
HC_E1	KpnI-FLAG-cinB(E634A)-SacI in pYes2	Hongli Chen, this study
HC_K1	KpnI-FLAG-cinB(K636A)-SacI in pYes2	Hongli Chen, this study

Plasmid Names	Description	Source
HC_K2	KpnI-FLAG-cinB(K636A)-HA-SacI in pYES2 vector	Hongli Chen, this study
HC_cinT2A-wPip	NotI-cinA-T2A-cinB-BamHI in pUASp-attb	Hongli Chen, this study
HC_cin*T2A-wPip	NotI-cinA-T2A-cinB(K636A)-BamHI in pUASp-attb	Hongli Chen, this study
HC_cinA-wPip	NotI-cinA-BamHI in pUASp-attb	Hongli Chen, this study
HC_cinB-wPip	NotI-cinB-BamHI in pUASp-attb	Hongli Chen, this study
HC_cinB*-wPip	NotI-cinB(K636A)-BamHI in pUASp-attb	Hongli Chen, this study
HC_AB6	eGFP-FLAG-cinA in pRS425	Hongli Chen, this study
HC_AD1	eGFP-FLAG-cidA in pRS425	Hongli Chen, this study
HC_AY1	SpeI-eGFP-BamHI-cinB-SalI in pRS416 gal1	Hongli Chen, this study
HC_AZ13	SpeI-eGFP-BamHI-cidB-SalI in pRS416 gal1	Hongli Chen, this study
HC_BA1	SpeI-mCherry-BamHI-cinA-SalI in pRS425 gal1	Hongli Chen, this study
HC_BC1	SpeI-mCherry-BamHI-cidA-SalI in pRS425 gal1	Hongli Chen, this study
HC_BD3	SpeI-cinB-BamHI-eGFP-SalI in pRS416 gal1	Hongli Chen, this study
HC_BJ2	NotI-cinA-T2A-cinB*(K636A)-BamHI in pUASp-attb	Hongli Chen, this study
HC_BO2	BamHI-HA-cinA-Sal1 in pRS425gal1	Hongli Chen, this study
HC_BQ1	BamHI-cinB-SpeI-3xFLAG-Sal1 in pRS416gal1	Hongli Chen, this study

Plasmid Names	Description	Source
HC_BV1	BamHI-3xFLAG-SpeI-cinB-SalI in pRS416gal1	Hongli Chen, this study
HC_BX1	SpeI-cidB-BamHI-eGFP-SalI in pRS416 gal1	Hongli Chen, this study
HC_BY5	SpeI-cinA-BamHI-mCherry-SalI in pRS425 gal1	Hongli Chen, this study
HC_BZ3	SpeI-cidA-BamHI-mCherry-SalI in pRS425 gal1	Hongli Chen, this study
HC_CA1	NotI-gal1-SpeI-cidB_wPip-BamHI-eGFP-SalI-cyc1-KpnI in pRS306	Hongli Chen, this study
HC_CB1	NotI-gal1-SpeI-cinB_wPip-BamHI-eGFP-SalI-cyc1-KpnI in pRS306	Hongli Chen, this study
HC_CC2	SpeI-cidA_wMel-BamHI-mCherry-SalI in pRS425	Hongli Chen, this study
HC_CX1	NotI-gal1-SpeI-cidB_wPip (C1024A)-BamHI-eGFP-SalI-cyc1-KpnI in pRS306	Hongli Chen, this study
HC_CY1	NotI-gal1-SpeI-cinB_wPip (K636A)-BamHI-eGFP-SalI-cyc1-KpnI in pRS306	Hongli Chen, this study

Appendix II: Drosophila Lines Used in This Study

Strain	Chromosome			Background	Source
	1	2	3		
EC2-1-1M			EGFPC1	#9744	Beckmann *et al.*, 2017
NGT-4442	y[1] w[*]	P(w[+mC]=GAL4-nos.NGT)40			Rorth, 1998
MTD-31777	P(w[+mC]=otu-GAL4::VP16.R)1, w[*]	P(w[+mC]=GAL4-nos.NGT)40	P(w[+mC]=GAL4::VP16-nos.UTR)CG6325[MVD1]		Petrella *et al.*, 2007
wCS-189				wCS	Beckmann *et al.*, 2017
HC1.1			wPip CinA	#9744	Hongli Chen, this study
HC1.2			wPip CinA	#9744	Hongli Chen, this study
HC1.3			wPip CinA	#9744	Hongli Chen, this study
HC1.4			wPip CinA	#9744	Hongli Chen, this study
HC1.5			wPip CinA	#9744	Hongli Chen, this study
HC2.1			wPip CinB	#9744	Hongli Chen, this study
HC2.2			wPip CinB	#9744	Hongli Chen, this study
HC2.3			wPip CinB	#9744	Hongli Chen, this study
HC2.4			wPip CinB	#9744	Hongli Chen, this study

Strain	Chromosome			Background	Source
	1	2	3		
HC2.5			wPip CinB	#9744	Hongli Chen, this study
HC3.1			wPip CinA-T2A-CinB	#9744	Hongli Chen, this study
HC3.2			wPip CinA-T2A-CinB	#9744	Hongli Chen, this study
HC3.3			wPip CinA-T2A-CinB	#9744	Hongli Chen, this study
HC3.4			wPip CinA-T2A-CinB	#9744	Hongli Chen, this study
HC3.5			wPip CinA-T2A-CinB	#9744	Hongli Chen, this study
HC4.1		wPip CinA		#9723	Hongli Chen, this study
HC4.2		wPip CinA		#9723	Hongli Chen, this study
HC4.3		wPip CinA		#9723	Hongli Chen, this study
HC4.4		wPip CinA		#9723	Hongli Chen, this study
HC5.1			wPip CinB (K636A)	#9744	Hongli Chen, this study
HC5.2			wPip CinB (K636A)	#9744	Hongli Chen, this study
HC5.3			wPip CinB (K636A)	#9744	Hongli Chen, this study
HC5.4			wPip CinB (K636A)	#9744	Hongli Chen, this study
HC5.5			wPip CinB (K636A)	#9744	Hongli Chen, this study

Strain	Chromosome			Background	Source
	1	2	3		
AB1		wPip CinA	wPip CinB		Hongli Chen, this study
AB2		wPip CinA	wPip CinB		Hongli Chen, this study
AB3		wPip CinA	wPip CinB		Hongli Chen, this study
AB4		wPip CinA	wPip CinB		Hongli Chen, this study
AB5		wPip CinA	wPip CinB		Hongli Chen, this study
AB1*		wPip CinA	wPip CinB (K636A)		Hongli Chen, this study
AB2*		wPip CinA	wPip CinB (K636A)		Hongli Chen, this study
AB3*		wPip CinA	wPip CinB (K636A)		Hongli Chen, this study
AB4*		wPip CinA	wPip CinB (K636A)		Hongli Chen, this study
AB5*		wPip CinA	wPip CinB (K636A)		Hongli Chen, this study

Appendix III: Primers Used in This Study

Primer name	Forward/ Reverse	Sequence 5' to 3'	Description
JFB058	F	GAGAAGTTGGCGGTT-ATGTTGGTTATAAAT-GCTACTGATC	Site-directed mutagenesis to change Aspartate (D) to Alanine (A) at the DEK site of CinB^{wPip}
JFB059	R	CATAACCGCCAACTT-CTCTCCACCACCTAT-TTGAAATTC	
HC004	F	GAATAGCGCTAAAAT-TTGCTAAGAAAGGAG-AATTGG	Site-directed mutagenesis to change Glutamate (E) to Alanine (A) at the DEK site of CinB^{wPip}
HC005	R	CAAATTTTAGCGCTA-TTCCAACTGGGGGGT-ATTC	
HC006	F	GAGCTAGCGTTTGCT-AAGAAAGGAGAATTG-GATAAAAAAG	Site-directed mutagenesis to change Lysine (K) to Alanine (A) at the DEK site of CinB^{wPip}
HC007	R	GCAAACGCTAGCTCT-ATTCCAACTGGGGGG-TATTC	
JFB060	F	GGAATAGCGCTAGCG-TTTGCTAAGAAAGGA-GAATTGG	Site-directed mutagenesis to change both E and K to Alanine (A) at the DEK site of CinB^{wPip}
JFB061	R	CTTAGCAAACGCTAG-CGCTATTCCAACTGG-GGGGTATTC	

Primer name	Forward/ Reverse	Sequence 5' to 3'	Description
JFB146	R	TAAGTTGGGTAACGC-CAGGG	Sequencing primers for genomic tiling library plasmids pGP564
JFB147	F	GAGCGGATAACAATT-TCACACAGG	
HC200	F	GAGCTTGCAGCAGGT-ACTGGTGAGATAAGT-ACAGTG	Primers to make quickchange CinB K279 => A
HC201	R	GTACCTGCTGCAAGC-TCAATAATAATAGGA-ATAGAGC	
HC202	F	CCTATTATTATTGCG-CTTGCAGCAGGTACT-GGTGAG	Primers to quickchange CinB E277 K279 => AA
HC203	R	GCTGCAAGCGCAATA-ATAATAGGAATAGAG-CTTAGCGAC	
HC204	F	GGTTACGCAGCCATT-ATTTTGCTTGTGCGC-GGTTCTG	Primers to quickchange CinB D257 => A
HC205	R	GCAAAATAATGGCTG-CGTAACCTTTTCCAG-CAAATAATTC	

Primer name	Forward/ Reverse	Sequence 5' to 3'	Description
HC230	1	CCTGCAGGATGGTAGGACGG-CCTCGCAATCGGCTTCGACC-GAGCACGCGAGATGTCAACG-ATCGAATTGC	Four-way junction sequences (4J, 1+2+3+4; 4Jh, 2+5+6+7; 4Jhs, 5+7+8+9); sequence 2 and 5 have Cy5 label versions
HC231	2	GCAATTCGATCGTTGACATC-TCGCGTGCTCGGTCAATCGG-CAGATGCGGAGTGAAGTTCC-AACGTTCGGC	
HC232	3	GCCGAACGTTGGAACTTCAC-TCCGCATCTGCCGATTCTGG-CTGTGGCGTGTTTCTGGTGG-TTCCTAGGTC	
HC233	4	GACCTAGGAACCACCAGAA-ACACGCCACAGCCAGGAAG-CCGATTGCGAGGCCGTCCTA-CCATCCTGCAGG	
HC234	5	CCTGCAGGATGGTAGGACGG-CCTCGCAATCCCGATTGACC-GAGCACGCGAGATGTCAACG-ATCGAATTGC	
HC235	6	GCCGAACGTTGGAACTTCAC-TCCGCATCTGCCGATTGACC-GAGTGGCGTGTTTCTGGTGG-TTCCTAGGTC	
HC236	7	GACCTAGGAACCACCAGAAA-CACGCCACTCGGTCAATCGG-GATTGCGAGGCCGTCCTACC-ATCCTGCAGG	
HC237	8	GCAATTCGATCGTTGACATC-TCGCGTGCTCGGTCAATCGG-CAGATGCGGAGTGAAGTTC	
HC238	9	GAACTTCACTCCGCATCTGC-CGATTGACCGAGTGGCGTGT-TTCTGGTGGTTCCTAGGTC	

Primer name	Forward/ Reverse	Sequence 5' to 3'	Description
HC239	10	GCCGAACGTTGGAACTTCAC-TCCGCATCTGCCGATTGACC-GAGCACGCGAGATGTCAACG-ATCGAATTGC	Sequences for duplex (D, 2+10), looped-out (L10, 2+11), mismatched (G/A, 2+12) and half duplex DNAs (Hd1, 2+5; Hd2, 2+6)
HC240	11	GCCGAACGTTGGAACTTCAC-TCCGCATCTGGAGCACGCGA-GATGTCAACGATCGAATTGC	
HC241	12	GCCGAACGTTGGAACTTCAC-TCCGCATCTGCCGATGGACC-GAGCACGCGAGATGTCAACG-ATCGAATTGC	
HC242	13	GACCTAGGAACCACCAGAAA-CACGCCACAGCCAGGACCGA-GCACGCGAGATGTCAACGAT-CGAATTGC	Three-way junction sequences (3J, 2+3+13; 3Jh, 2+6+14)
HC243	14	GACCTAGGAACCACCAGAAA-CACGCCACTCGGTCGACCGA-GCACGCGAGATGTCAACGAT-CGAATTGC	
HC365	F	GTAAAACGACGGCCAG	M13 forward sequencing primer
HC366	R	CAGGAAACAGCTATGAC	M13 reverse sequencing primer
HC367	F	TAGGGAAGAGAAGGACATA-TGAT	SELEX forward PCR primer
HC368	R	TCAAGTGGTCATGTACTAGT-CAA	SELEX reverse PCR primer

Primer name	Forward/ Reverse	Sequence 5' to 3'	Description
HC210	F	TGGGAACTCGAGATGCCAAT-AGAAACAAAACGTC	Primers to PCR cidA_wMel gene
HC211	R	TGGGAACTGCAGCTAAGACC-AGAAAAACCACTC	
HC214	F	AAAAGGATCCATGCATGGTA-ATAATGAAGATCGTG	Primers to PCR cidB_wNo gene
HC215	R	AAAACTCGAGTCATCTAGAA-AACCCAGATGCTCTACG	
HC373	F	CAAGTCACTAATCGGTCTTC-GAAAGTTCAATATC	Primers to PCR D.Mel act88F gene
HC374	R	GCACAGCCACGACTCTTACG-ATTAGTTCTTC	
HC377	F	GTCTAGTCGTCAACAGGAAT-CGAACGTGCG	Primers to PCR D.Sim act88F gene
HC378	R	GCCACCGATCCAGACGGAG-TACTTCCTC	

References

Arakaki, N., Miyoshi, T. and Noda, H. (2001) 'Wolbachia-mediated parthenogenesis in the predatory thrips Franklinothrips vespiformis (Thysanoptera: Insecta)', *Proc Biol Sci,* 268(1471), pp. 1011-6.

Arunachalam, N. and Curtis, C. F. (1985) 'Integration of radiation with cytoplasmic incompatibility for genetic control in the Culex pipiens complex (Diptera: Culicidae)', *J Med Entomol,* 22(6), pp. 648-53.

Asgharian, H., Chang, P. L., Mazzoglio, P. J. and Negri, I. (2014) 'Wolbachia is not all about sex: male-feminizing Wolbachia alters the leafhopper Zyginidia pullula transcriptome in a mainly sex-independent manner', *Frontiers in Microbiology,* 5.

Badawi, M., Greve, P. and Cordaux, R. (2015) 'Feminization of the Isopod Cylisticus convexus after Transinfection of the wVulC Wolbachia Strain of Armadillidium vulgare', *PLoS One,* 10(6), pp. e0128660.

Balhorn, R. (2007) 'The protamine family of sperm nuclear proteins', *Genome Biol,* 8(9), pp. 227.

Beckmann, J. F., Bonneau, M., Chen, H., Hochstrasser, M., Poinsot, D., Mercot, H., Weill, M., Sicard, M. and Charlat, S. (2019a) 'Caution Does Not Preclude Predictive and Testable Models of Cytoplasmic Incompatibility: A Reply to Shropshire et al', *Trends Genet,* 35(6), pp. 399-400.

Beckmann, J. F., Bonneau, M., Chen, H., Hochstrasser, M., Poinsot, D., Mercot, H., Weill, M., Sicard, M. and Charlat, S. (2019b) 'The Toxin-Antidote Model of Cytoplasmic

Incompatibility: Genetics and Evolutionary Implications', *Trends Genet,* 35(3), pp. 175-185.

Beckmann, J. F. and Fallon, A. M. (2012) 'Decapitation improves detection of Wolbachia pipientis (Rickettsiales: Anaplasmataceae) in Culex pipiens (Diptera: Culicidae) mosquitoes by the polymerase chain reaction', *J Med Entomol,* 49(5), pp. 1103-8.

Beckmann, J. F. and Fallon, A. M. (2013) 'Detection of the Wolbachia protein WPIP0282 in mosquito spermathecae: implications for cytoplasmic incompatibility', *Insect Biochem Mol Biol,* 43(9), pp. 867-78.

Beckmann, J. F., Ronau, J. A. and Hochstrasser, M. (2017) 'A Wolbachia deubiquitylating enzyme induces cytoplasmic incompatibility', *Nat Microbiol,* 2, pp. 17007.

Beckmann, J. F., Sharma, G. D., Mendez, L., Chen, H. and Hochstrasser, M. (2019c) 'The Wolbachia cytoplasmic incompatibility enzyme CidB targets nuclear import and protamine-histone exchange factors', *Elife,* 8.

Bhatt, S., Gething, P. W., Brady, O. J., Messina, J. P., Farlow, A. W., Moyes, C. L., Drake, J. M., Brownstein, J. S., Hoen, A. G., Sankoh, O., Myers, M. F., George, D. B., Jaenisch, T., Wint, G. R., Simmons, C. P., Scott, T. W., Farrar, J. J. and Hay, S. I. (2013) 'The global distribution and burden of dengue', *Nature,* 496(7446), pp. 504-7.

Blagrove, M. S., Arias-Goeta, C., Failloux, A. B. and Sinkins, S. P. (2012) 'Wolbachia strain wMel induces cytoplasmic incompatibility and blocks dengue transmission in Aedes albopictus', *Proc Natl Acad Sci U S A,* 109(1), pp. 255-60.

Bogart, K. and Andrews, J. (2006) 'Extraction of Total RNA from *Drosophila*', *CGB Technical Report 2006-10*. The Center for Genomics and Bioinformatics, Indiana University, Bloomington, Indiana.

Bonneau, M., Atyame, C., Beji, M., Justy, F., Cohen-Gonsaud, M., Sicard, M. and Weill, M. (2018a) 'Culex pipiens crossing type diversity is governed by an amplified and polymorphic operon of Wolbachia', *Nat Commun,* 9(1), pp. 319.

Bonneau, M., Caputo, B., Ligier, A., Caparros, R., Unal, S., Perriat-Sanguinet, M., Arnoldi, D., Sicard, M. and Weill, M. (2019) 'Variation in Wolbachia cidB gene, but not cidA, is associated with cytoplasmic incompatibility mod phenotype diversity in Culex pipiens', *Mol Ecol,* 28(21), pp. 4725-4736.

Bonneau, M., Landmann, F., Labbe, P., Justy, F., Weill, M. and Sicard, M. (2018b) 'The cellular phenotype of cytoplasmic incompatibility in Culex pipiens in the light of cidB diversity', *PLoS Pathog,* 14(10), pp. e1007364.

Bowman, L. R., Donegan, S. and McCall, P. J. (2016) 'Is Dengue Vector Control Deficient in Effectiveness or Evidence?: Systematic Review and Meta-analysis', *PLoS Negl Trop Dis,* 10(3), pp. e0004551.

Brachmann, C. B., Davies, A., Cost, G. J., Caputo, E., Li, J., Hieter, P. and Boeke, J. D. (1998) 'Designer deletion strains derived from Saccharomyces cerevisiae S288C: a useful set of strains and plasmids for PCR-mediated gene disruption and other applications', *Yeast,* 14(2), pp. 115-32.

Bressac, C. and Rousset, F. (1993) 'The reproductive incompatibility system in Drosophila simulans: DAPI-staining analysis of the Wolbachia symbionts in sperm cysts', *J Invertebr Pathol,* 61(3), pp. 226-30.

Buathong, R., Hermann, L., Thaisomboonsuk, B., Rutvisuttinunt, W., Klungthong, C., Chinnawirotpisan, P., Manasatienkij, W., Nisalak, A., Fernandez, S., Yoon, I. K., Akrasewi, P. and Plipat, T. (2015) 'Detection of Zika Virus Infection in Thailand, 2012-2014', *Am J Trop Med Hyg,* 93(2), pp. 380-383.

Bushland, R. C., Lindquist, A. W. and Knipling, E. F. (1955) 'Eradication of Screw-Worms through Release of Sterilized Males', *Science,* 122(3163), pp. 287-8.

Callaini, G., Dallai, R. and Riparbelli, M. G. (1997) 'Wolbachia-induced delay of paternal chromatin condensation does not prevent maternal chromosomes from entering anaphase in incompatible crosses of Drosophila simulans', *J Cell Sci,* 110 (Pt 2), pp. 271-80.

Chatzispyrou, I. A., Held, N. M., Mouchiroud, L., Auwerx, J. and Houtkooper, R. H. (2015) 'Tetracycline antibiotics impair mitochondrial function and its experimental use confounds research', *Cancer Res,* 75(21), pp. 4446-9.

Chen, H., Ronau, J. A., Beckmann, J. F. and Hochstrasser, M. (2019) 'A Wolbachia nuclease and its binding partner provide a distinct mechanism for cytoplasmic incompatibility', *Proceedings of the National Academy of Sciences,* 116(44), pp. 22314-22321.

Chretien, J. P., Anyamba, A., Bedno, S. A., Breiman, R. F., Sang, R., Sergon, K., Powers, A. M., Onyango, C. O., Small, J., Tucker, C. J. and Linthicum, K. J. (2007) 'Drought-

associated chikungunya emergence along coastal East Africa', *Am J Trop Med Hyg,* 76(3), pp. 405-7.

Clark, I. E., Jan, L. Y. and Jan, Y. N. (1997) 'Reciprocal localization of Nod and kinesin fusion proteins indicates microtubule polarity in the Drosophila oocyte, epithelium, neuron and muscle', *Development,* 124(2), pp. 461-70.

Cooper, B. S., Vanderpool, D., Conner, W. R., Matute, D. R. and Turelli, M. (2019) 'Wolbachia Acquisition by Drosophila yakuba-clade Hosts and Transfer of Incompatibility Loci Between Distantly Related Wolbachia', *Genetics*.

Cordaux, R., Michel-Salzat, A., Frelon-Raimond, M., Rigaud, T. and Bouchon, D. (2004) 'Evidence for a new feminizing Wolbachia strain in the isopod Armadillidium vulgare: evolutionary implications', *Heredity (Edinb),* 93(1), pp. 78-84.

de Saint Phalle, B. and Sullivan, W. (1998) 'Spindle assembly and mitosis without centrosomes in parthenogenetic Sciara embryos', *J Cell Biol,* 141(6), pp. 1383-91.

Dyer, K. A. and Jaenike, J. (2004) 'Evolutionarily stable infection by a male-killing endosymbiont in Drosophila innubila: Molecular evidence from the host and parasite genomes', *Genetics,* 168(3), pp. 1443-1455.

Epling, L. B., Grace, C. R., Lowe, B. R., Partridge, J. F. and Enemark, E. J. (2015) 'Cancer-associated mutants of RNA helicase DDX3X are defective in RNA-stimulated ATP hydrolysis', *J Mol Biol,* 427(9), pp. 1779-1796.

Fialho, R. F. and Stevens, L. (2000) 'Male-killing Wolbachia in a flour beetle', *Proceedings of the Royal Society B-Biological Sciences,* 267(1451), pp. 1469-1473.

Flores, H. A. and O'Neill, S. L. (2018) 'Controlling vector-borne diseases by releasing modified mosquitoes', *Nat Rev Microbiol,* 16(8), pp. 508-518.

Galizi, R., Hammond, A., Kyrou, K., Taxiarchi, C., Bernardini, F., O'Loughlin, S. M., Papathanos, P. A., Nolan, T., Windbichler, N. and Crisanti, A. (2016) 'A CRISPR-Cas9 sex-ratio distortion system for genetic control', *Sci Rep,* 6, pp. 31139.

Gantz, V. M. and Bier, E. (2015) 'Genome editing. The mutagenic chain reaction: a method for converting heterozygous to homozygous mutations', *Science,* 348(6233), pp. 442-4.

Gantz, V. M., Jasinskiene, N., Tatarenkova, O., Fazekas, A., Macias, V. M., Bier, E. and James, A. A. (2015) 'Highly efficient Cas9-mediated gene drive for population modification of the malaria vector mosquito Anopheles stephensi', *Proc Natl Acad Sci U S A,* 112(49), pp. E6736-43.

Gietz, R. D. and Schiestl, R. H. (2007) 'High-efficiency yeast transformation using the LiAc/SS carrier DNA/PEG method', *Nat Protoc,* 2(1), pp. 31-4.

Gillespie, J. J., Driscoll, T. P., Verhoeve, V. I., Rahman, M. S., Macaluso, K. R. and Azad, A. F. (2018) 'A Tangled Web: Origins of Reproductive Parasitism', *Genome Biol Evol,* 10(9), pp. 2292-2309.

Grandadam, M., Caro, V., Plumet, S., Thiberge, J. M., Souares, Y., Failloux, A. B., Tolou, H. J., Budelot, M., Cosserat, D., Leparc-Goffart, I. and Despres, P. (2011) 'Chikungunya virus, southeastern France', *Emerg Infect Dis,* 17(5), pp. 910-3.

Groth, A. C., Fish, M., Nusse, R. and Calos, M. P. (2004) 'Construction of transgenic Drosophila by using the site-specific integrase from phage phiC31', *Genetics,* 166(4), pp. 1775-82.

Gubler, D. J. (2002) 'The global emergence/resurgence of arboviral diseases as public health problems', *Archives of Medical Research,* 33(4), pp. 330-342.

Hammond, A., Galizi, R., Kyrou, K., Simoni, A., Siniscalchi, C., Katsanos, D., Gribble, M., Baker, D., Marois, E., Russell, S., Burt, A., Windbichler, N., Crisanti, A. and Nolan, T. (2016) 'A CRISPR-Cas9 gene drive system targeting female reproduction in the malaria mosquito vector Anopheles gambiae', *Nat Biotechnol,* 34(1), pp. 78-83.

Hedges, L. M., Brownlie, J. C., O'Neill, S. L. and Johnson, K. N. (2008) 'Wolbachia and virus protection in insects', *Science,* 322(5902), pp. 702.

Hickey, C. M., Wilson, N. R. and Hochstrasser, M. (2012) 'Function and regulation of SUMO proteases', *Nat Rev Mol Cell Biol,* 13(12), pp. 755-66.

Hilgenboecker, K., Hammerstein, P., Schlattmann, P., Telschow, A. and Werren, J. H. (2008) 'How many species are infected with Wolbachia?--A statistical analysis of current data', *FEMS Microbiol Lett,* 281(2), pp. 215-20.

Hiroki, M., Kato, Y., Kamito, T. and Miura, K. (2002) 'Feminization of genetic males by a symbiotic bacterium in a butterfly, Eurema hecabe (Lepidoptera : Pieridae)', *Naturwissenschaften,* 89(4), pp. 167-170.

Hochedez, P., Jaureguiberry, S., Debruyne, M., Bossi, P., Hausfater, P., Brucker, G., Bricaire, F. and Caumes, E. (2006) 'Chikungunya infection in travelers', *Emerg Infect Dis,* 12(10), pp. 1565-7.

Hoffman, C. S. and Winston, F. (1987) 'A ten-minute DNA preparation from yeast efficiently releases autonomous plasmids for transformation of Escherichia coli', *Gene,* 57(2-3), pp. 267-72.

Hoffmann, A. A., Hercus, M. and Dagher, H. (1998) 'Population dynamics of the Wolbachia infection causing cytoplasmic incompatibility in Drosophila melanogaster', *Genetics,* 148(1), pp. 221-31.

Hoffmann, A. A., Iturbe-Ormaetxe, I., Callahan, A. G., Phillips, B. L., Billington, K., Axford, J. K., Montgomery, B., Turley, A. P. and O'Neill, S. L. (2014) 'Stability of the wMel Wolbachia Infection following invasion into Aedes aegypti populations', *PLoS Negl Trop Dis,* 8(9), pp. e3115.

Hoffmann, A. A., Montgomery, B. L., Popovici, J., Iturbe-Ormaetxe, I., Johnson, P. H., Muzzi, F., Greenfield, M., Durkan, M., Leong, Y. S., Dong, Y., Cook, H., Axford, J., Callahan, A. G., Kenny, N., Omodei, C., McGraw, E. A., Ryan, P. A., Ritchie, S. A., Turelli, M. and O'Neill, S. L. (2011) 'Successful establishment of Wolbachia in Aedes populations to suppress dengue transmission', *Nature,* 476(7361), pp. 454-7.

Hoffmann, A. A., Turelli, M. and Harshman, L. G. (1990) 'Factors affecting the distribution of cytoplasmic incompatibility in Drosophila simulans', *Genetics,* 126(4), pp. 933-48.

Houtman, J. C., Brown, P. H., Bowden, B., Yamaguchi, H., Appella, E., Samelson, L. E. and Schuck, P. (2007) 'Studying multisite binary and ternary protein interactions by global analysis of isothermal titration calorimetry data in SEDPHAT: application to adaptor protein complexes in cell signaling', *Protein Sci,* 16(1), pp. 30-42.

Hurst, G. D. D., Johnson, A. P., von der Schulenburg, J. H. G. and Fuyama, Y. (2000) 'Male-killing Wolbachia in Drosophila: A temperature-sensitive trait with a threshold bacterial density', *Genetics,* 156(2), pp. 699-709.

Ioos, S., Mallet, H. P., Leparc Goffart, I., Gauthier, V., Cardoso, T. and Herida, M. (2014) 'Current Zika virus epidemiology and recent epidemics', *Med Mal Infect,* 44(7), pp. 302-7.

Jaenike, J. (2007) 'Spontaneous emergence of a new wolbachia phenotype', *Evolution,* 61(9), pp. 2244-2252.

Jiggins, F. M., Hurst, G. D. D., Schulenburg, J. H. G. V. D. and Majerus, M. E. N. (2001) 'Two male-killing Wolbachia strains coexist within a population of the butterfly Acraea encedon', *Heredity,* 86, pp. 161-166.

Jones, D. T. (1999) 'Protein secondary structure prediction based on position-specific scoring matrices', *J Mol Biol,* 292(2), pp. 195-202.

Jones, G. M., Stalker, J., Humphray, S., West, A., Cox, T., Rogers, J., Dunham, I. and Prelich, G. (2008) 'A systematic library for comprehensive overexpression screens in Saccharomyces cerevisiae', *Nat Methods,* 5(3), pp. 239-41.

Joubert, D. A. and O'Neill, S. L. (2017) 'Comparison of Stable and Transient Wolbachia Infection Models in Aedes aegypti to Block Dengue and West Nile Viruses', *PLoS Negl Trop Dis,* 11(1), pp. e0005275.

Kageyama, D., Nishimura, G., Hoshizaki, S. and Ishikawa, Y. (2002) 'Feminizing Wolbachia in an insect, Ostrinia furnacalis (Lepidoptera : Crambidae)', *Heredity,* 88, pp. 444-449.

Kageyama, D. and Traut, W. (2004) 'Opposite sex-specific effects of Wolbachia and interference with the sex determination of its host Ostrinia scapulalis', *Proceedings of the Royal Society B-Biological Sciences,* 271(1536), pp. 251-258.

Kambris, Z., Cook, P. E., Phuc, H. K. and Sinkins, S. P. (2009) 'Immune activation by life-shortening Wolbachia and reduced filarial competence in mosquitoes', *Science,* 326(5949), pp. 134-6.

Kanz, C., Aldebert, P., Althorpe, N., Baker, W., Baldwin, A., Bates, K., Browne, P., van den Broek, A., Castro, M., Cochrane, G., Duggan, K., Eberhardt, R., Faruque, N., Gamble, J., Diez, F. G., Harte, N., Kulikova, T., Lin, Q., Lombard, V., Lopez, R., Mancuso, R., McHale, M., Nardone, F., Silventoinen, V., Sobhany, S., Stoehr, P., Tuli, M. A., Tzouvara, K., Vaughan, R., Wu, D., Zhu, W. and Apweiler, R. (2005) 'The EMBL Nucleotide Sequence Database', *Nucleic Acids Res,* 33(Database issue), pp. D29-33.

Keller, S., Vargas, C., Zhao, H., Piszczek, G., Brautigam, C. A. and Schuck, P. (2012) 'High-precision isothermal titration calorimetry with automated peak-shape analysis', *Anal Chem,* 84(11), pp. 5066-73.

Knizewski, L., Kinch, L. N., Grishin, N. V., Rychlewski, L. and Ginalski, K. (2007) 'Realm of PD-(D/E)XK nuclease superfamily revisited: detection of novel families with modified transitive meta profile searches', *BMC Struct Biol,* 7, pp. 40.

Komori, K., Sakae, S., Fujikane, R., Morikawa, K., Shinagawa, H. and Ishino, Y. (2000) 'Biochemical characterization of the hjc holliday junction resolvase of Pyrococcus furiosus', *Nucleic Acids Res,* 28(22), pp. 4544-51.

Kushnirov, V. V. (2000) 'Rapid and reliable protein extraction from yeast', *Yeast,* 16(9), pp. 857-60.

Lanciotti, R. S., Kosoy, O. L., Laven, J. J., Panella, A. J., Velez, J. O., Lambert, A. J. and Campbell, G. L. (2007) 'Chikungunya virus in US travelers returning from India, 2006', *Emerg Infect Dis,* 13(5), pp. 764-7.

Landmann, F., Orsi, G. A., Loppin, B. and Sullivan, W. (2009) 'Wolbachia-mediated cytoplasmic incompatibility is associated with impaired histone deposition in the male pronucleus', *PLoS Pathog,* 5(3), pp. e1000343.

Lassy, C. W. and Karr, T. L. (1996) 'Cytological analysis of fertilization and early embryonic development in incompatible crosses of Drosophila simulans', *Mechanisms of Development,* 57(1), pp. 47-58.

Laven, H. (1953) 'Reziprok unterschiedliche Kreuzbarkeit von Stechmücken (Culicidae) und ihre Deutung als plasmatische Vererbung', *Zeitschrift für Induktive Abstammungs- und Vererbungslehre,* 85(1), pp. 118-136.

Laven, H. (1967) 'Eradication of Culex pipiens fatigans through cytoplasmic incompatibility', *Nature,* 216(5113), pp. 383-4.

LePage, D. P., Metcalf, J. A., Bordenstein, S. R., On, J., Perlmutter, J. I., Shropshire, J. D., Layton, E. M., Funkhouser-Jones, L. J., Beckmann, J. F. and Bordenstein, S. R. (2017) 'Prophage WO genes recapitulate and enhance Wolbachia-induced cytoplasmic incompatibility', *Nature,* 543(7644), pp. 243-247.

Leparc-Goffart, I., Nougairede, A., Cassadou, S., Prat, C. and de Lamballerie, X. (2014) 'Chikungunya in the Americas', *Lancet,* 383(9916), pp. 514.

Li, S. J. and Hochstrasser, M. (1999) 'A new protease required for cell-cycle progression in yeast', *Nature,* 398(6724), pp. 246-51.

Lindsey, A. R. I., Rice, D. W., Bordenstein, S. R., Brooks, A. W., Bordenstein, S. R. and Newton, I. L. G. (2018) 'Evolutionary Genetics of Cytoplasmic Incompatibility Genes cifA and cifB in Prophage WO of Wolbachia', *Genome Biol Evol,* 10(2), pp. 434-451.

Livak, K. J. (1984) 'Organization and mapping of a sequence on the Drosophila melanogaster X and Y chromosomes that is transcribed during spermatogenesis', *Genetics,* 107(4), pp. 611-34.

Loppin, B., Bonnefoy, E., Anselme, C., Laurencon, A., Karr, T. L. and Couble, P. (2005) 'The histone H3.3 chaperone HIRA is essential for chromatin assembly in the male pronucleus', *Nature,* 437(7063), pp. 1386-90.

Loppin, B., Dubruille, R. and Horard, B. (2015) 'The intimate genetics of Drosophila fertilization', *Open Biol,* 5(8).

Lorenzen, M. D., Gnirke, A., Margolis, J., Garnes, J., Campbell, M., Stuart, J. J., Aggarwal, R., Richards, S., Park, Y. and Beeman, R. W. (2008) 'The maternal-effect, selfish genetic element Medea is associated with a composite Tc1 transposon', *Proc Natl Acad Sci U S A,* 105(29), pp. 10085-9.

Mains, J. W., Brelsfoard, C. L., Rose, R. I. and Dobson, S. L. (2016) 'Female Adult Aedes albopictus Suppression by Wolbachia-Infected Male Mosquitoes', *Sci Rep,* 6, pp. 33846.

Mains, J. W., Kelly, P. H., Dobson, K. L., Petrie, W. D. and Dobson, S. L. (2019) 'Localized Control of Aedes aegypti (Diptera: Culicidae) in Miami, FL, via Inundative Releases of Wolbachia-Infected Male Mosquitoes', *J Med Entomol,* 56(5), pp. 1296-1303.

Mayer, S. V., Tesh, R. B. and Vasilakis, N. (2017) 'The emergence of arthropod-borne viral diseases: A global prospective on dengue, chikungunya and zika fevers', *Acta Trop,* 166, pp. 155-163.

Meany, M. K., Conner, W. R., Richter, S. V., Bailey, J. A., Turelli, M. and Cooper, B. S. (2019) 'Loss of cytoplasmic incompatibility and minimal fecundity effects explain

relatively low Wolbachia frequencies in Drosophila mauritiana', *Evolution,* 73(6), pp. 1278-1295.

Mercot, H., Llorente, B., Jacques, M., Atlan, A. and Montchamp-Moreau, C. (1995) 'Variability within the Seychelles cytoplasmic incompatibility system in Drosophila simulans', *Genetics,* 141(3), pp. 1015-23.

Moreira, L. A., Iturbe-Ormaetxe, I., Jeffery, J. A., Lu, G., Pyke, A. T., Hedges, L. M., Rocha, B. C., Hall-Mendelin, S., Day, A., Riegler, M., Hugo, L. E., Johnson, K. N., Kay, B. H., McGraw, E. A., van den Hurk, A. F., Ryan, P. A. and O'Neill, S. L. (2009) 'A Wolbachia symbiont in Aedes aegypti limits infection with dengue, Chikungunya, and Plasmodium', *Cell,* 139(7), pp. 1268-78.

Mruk, D. D. and Cheng, C. Y. (2011) 'Enhanced chemiluminescence (ECL) for routine immunoblotting: An inexpensive alternative to commercially available kits', *Spermatogenesis,* 1(2), pp. 121-122.

Musso, D. (2015) 'Zika Virus Transmission from French Polynesia to Brazil', *Emerg Infect Dis,* 21(10), pp. 1887.

Musso, D., Nilles, E. J. and Cao-Lormeau, V. M. (2014) 'Rapid spread of emerging Zika virus in the Pacific area', *Clin Microbiol Infect,* 20(10), pp. O595-6.

Negri, I., Franchini, A., Mandrioli, M., Mazzoglio, P. J. and Almai, A. (2008) 'The gonads of Zyginidia pullula males feminized by Wolbachia pipientis', *Bulletin of Insectology,* 61(1), pp. 213-214.

Nishino, T., Komori, K., Tsuchiya, D., Ishino, Y. and Morikawa, K. (2001) 'Crystal structure of the archaeal holliday junction resolvase Hjc and implications for DNA recognition', *Structure,* 9(3), pp. 197-204.

O'Connor, L., Plichart, C., Sang, A. C., Brelsfoard, C. L., Bossin, H. C. and Dobson, S. L. (2012) 'Open release of male mosquitoes infected with a wolbachia biopesticide: field performance and infection containment', *PLoS Negl Trop Dis,* 6(11), pp. e1797.

O'Neill, S. L. (2018) 'The Use of Wolbachia by the World Mosquito Program to Interrupt Transmission of Aedes aegypti Transmitted Viruses', *Adv Exp Med Biol,* 1062, pp. 355-360.

O'Neill, S. L., Ryan, P. A., Turley, A. P., Wilson, G., Retzki, K., Iturbe-Ormaetxe, I., Dong, Y., Kenny, N., Paton, C. J., Ritchie, S. A., Brown-Kenyon, J., Stanford, D., Wittmeier, N., Anders, K. L. and Simmons, C. P. (2018) 'Scaled deployment of Wolbachia to protect the community from dengue and other Aedes transmitted arboviruses', *Gates Open Res,* 2, pp. 36.

Pang, T., Mak, T. K. and Gubler, D. J. (2017) 'Prevention and control of dengue-the light at the end of the tunnel', *Lancet Infect Dis,* 17(3), pp. e79-e87.

Perlmutter, J. I., Bordenstein, S. R., Unckless, R. L., LePage, D. P., Metcalf, J. A., Hill, T., Martinez, J., Jiggins, F. M. and Bordenstein, S. R. (2019) 'The phage gene wmk is a candidate for male killing by a bacterial endosymbiont', *Plos Pathogens,* 15(9).

Perlmutter, J. I., Meyers, J. E. and Bordenstein, S. R. (2020) 'Transgenic Testing Does Not Support a Role for Additional Candidate Genes in Wolbachia Male Killing or Cytoplasmic Incompatibility', *mSystems,* 5(1).

Petrella, L. N., Smith-Leiker, T. and Cooley, L. (2007) 'The Ovhts polyprotein is cleaved to produce fusome and ring canal proteins required for Drosophila oogenesis', *Development,* 134(4), pp. 703-12.

Pingoud, A., Fuxreiter, M., Pingoud, V. and Wende, W. (2005) 'Type II restriction endonucleases: structure and mechanism', *Cell Mol Life Sci,* 62(6), pp. 685-707.

Poinsot, D., Bourtzis, K., Markakis, G., Savakis, C. and Mercot, H. (1998) 'Wolbachia transfer from Drosophila melanogaster into D. simulans: Host effect and cytoplasmic incompatibility relationships', *Genetics,* 150(1), pp. 227-37.

Powers, A. M., Brault, A. C., Tesh, R. B. and Weaver, S. C. (2000) 'Re-emergence of Chikungunya and O'nyong-nyong viruses: evidence for distinct geographical lineages and distant evolutionary relationships', *J Gen Virol,* 81(Pt 2), pp. 471-9.

Reed, K. M. and Werren, J. H. (1995) 'Induction of paternal genome loss by the paternal-sex-ratio chromosome and cytoplasmic incompatibility bacteria (Wolbachia): a comparative study of early embryonic events', *Mol Reprod Dev,* 40(4), pp. 408-18.

Rezza, G., Nicoletti, L., Angelini, R., Romi, R., Finarelli, A. C., Panning, M., Cordioli, P., Fortuna, C., Boros, S., Magurano, F., Silvi, G., Angelini, P., Dottori, M., Ciufolini, M. G., Majori, G. C., Cassone, A. and group, C. s. (2007) 'Infection with chikungunya virus in Italy: an outbreak in a temperate region', *Lancet,* 370(9602), pp. 1840-6.

Richardson, K. M., Schiffer, M., Griffin, P. C., Lee, S. F. and Hoffmann, A. A. (2016) 'Tropical Drosophila pandora carry Wolbachia infections causing cytoplasmic incompatibility or male killing', *Evolution,* 70(8).

Riparbelli, M. G., Giordano, R., Ueyama, M. and Callaini, G. (2012) 'Wolbachia-Mediated Male Killing Is Associated with Defective Chromatin Remodeling', *Plos One,* 7(1).

Roe, D. R. and Cheatham, T. E., 3rd (2013) 'PTRAJ and CPPTRAJ: Software for Processing and Analysis of Molecular Dynamics Trajectory Data', *J Chem Theory Comput,* 9(7), pp. 3084-95.

Ronau, J. A., Beckmann, J. F. and Hochstrasser, M. (2016) 'Substrate specificity of the ubiquitin and Ubl proteases', *Cell Res,* 26(4), pp. 441-56.

Rorth, P. (1998) 'Gal4 in the Drosophila female germline', *Mech Dev,* 78(1-2), pp. 113-8.

Sasaki, T., Kubo, T. and Ishikawa, H. (2002) 'Interspecific transfer of Wolbachia between two lepidopteran insects expressing cytoplasmic incompatibility: A Wolbachia variant naturally infecting Cadra cautella causes male killing in Ephestia kuehniella', *Genetics,* 162(3), pp. 1313-1319.

Serbus, L. R., Casper-Lindley, C., Landmann, F. and Sullivan, W. (2008) 'The genetics and cell biology of Wolbachia-host interactions', *Annu Rev Genet,* 42, pp. 683-707.

Shahid, M. A. and Curtis, C. F. (1987) 'Radiation sterilization and cytoplasmic incompatibility in a "tropicalized" strain of the Culex pipiens complex (Diptera: Culicidae)', *J Med Entomol,* 24(2), pp. 273-4.

Shropshire, J. D. and Bordenstein, S. R. (2019) 'Two-By-One model of cytoplasmic incompatibility: Synthetic recapitulation by transgenic expression of cifA and cifB in Drosophila', *PLoS Genet,* 15(6), pp. e1008221.

Shropshire, J. D., Leigh, B., Bordenstein, S. R., Duplouy, A., Riegler, M., Brownlie, J. C. and Bordenstein, S. R. (2019) 'Models and Nomenclature for Cytoplasmic Incompatibility: Caution over Premature Conclusions - A Response to Beckmann et al', *Trends Genet,* 35(6), pp. 397-399.

Shropshire, J. D., On, J., Layton, E. M., Zhou, H. and Bordenstein, S. R. (2018) 'One prophage WO gene rescues cytoplasmic incompatibility in Drosophila melanogaster', *Proc Natl Acad Sci U S A,* 115(19), pp. 4987-4991.

Steczkiewicz, K., Muszewska, A., Knizewski, L., Rychlewski, L. and Ginalski, K. (2012) 'Sequence, structure and functional diversity of PD-(D/E)XK phosphodiesterase superfamily', *Nucleic Acids Res,* 40(15), pp. 7016-45.

Stouthamer, R., Breeuwer, J. A. J. and Hurst, G. D. D. (1999) 'Wolbachia pipientis: Microbial manipulator of arthropod reproduction', *Annual Review of Microbiology,* 53, pp. 71-102.

Stouthamer, R. and Kazmer, D. J. (1994) 'Cytogenetics of Microbe-Associated Parthenogenesis and Its Consequences for Gene Flow in Trichogramma Wasps', *Heredity,* 73, pp. 317-327.

Stouthamer, R., Luck, R. F. and Hamilton, W. D. (1990) 'Antibiotics cause parthenogenetic Trichogramma (Hymenoptera/Trichogrammatidae) to revert to sex', *Proc Natl Acad Sci U S A,* 87(7), pp. 2424-7.

Sullivan, W., Ashburner, M. and Hawley, R. S. (2000) '*Drosophila Protocols* (Cold Spring Harbor Laboratory Press)'.

Sutton, E. R., Harris, S. R., Parkhill, J. and Sinkins, S. P. (2014) 'Comparative genome analysis of Wolbachia strain wAu', *BMC Genomics,* 15, pp. 928.

Taubitz, W., Cramer, J. P., Kapaun, A., Pfeffer, M., Drosten, C., Dobler, G., Burchard, G. D. and Loscher, T. (2007) 'Chikungunya fever in travelers: clinical presentation and course', *Clin Infect Dis,* 45(1), pp. e1-4.

Teixeira, L., Ferreira, A. and Ashburner, M. (2008) 'The bacterial symbiont Wolbachia induces resistance to RNA viral infections in Drosophila melanogaster', *PLoS Biol,* 6(12), pp. e2.

Tirmarche, S., Kimura, S., Sapey-Triomphe, L., Sullivan, W., Landmann, F. and Loppin, B. (2014) 'Drosophila protamine-like Mst35Ba and Mst35Bb are required for proper sperm nuclear morphology but are dispensable for male fertility', *G3 (Bethesda),* 4(11), pp. 2241-5.

Tram, U., Fredrick, K., Werren, J. H. and Sullivan, W. (2006) 'Paternal chromosome segregation during the first mitotic division determines Wolbachia-induced cytoplasmic incompatibility phenotype', *Journal of Cell Science,* 119(17), pp. 3655-3663.

Tram, U. and Sullivan, W. (2002) 'Role of delayed nuclear envelope breakdown and mitosis in Wolbachia-induced cytoplasmic incompatibility', *Science,* 296(5570), pp. 1124-6.

Turelli, M. (2010) 'Cytoplasmic incompatibility in populations with overlapping generations', *Evolution,* 64(1), pp. 232-41.

Turelli, M. and Hoffmann, A. A. (1995) 'Cytoplasmic incompatibility in Drosophila simulans: dynamics and parameter estimates from natural populations', *Genetics,* 140(4), pp. 1319-38.

Walker, T., Johnson, P. H., Moreira, L. A., Iturbe-Ormaetxe, I., Frentiu, F. D., McMeniman, C. J., Leong, Y. S., Dong, Y., Axford, J., Kriesner, P., Lloyd, A. L., Ritchie, S. A., O'Neill, S. L. and Hoffmann, A. A. (2011) 'The wMel Wolbachia strain blocks dengue and invades caged Aedes aegypti populations', *Nature,* 476(7361), pp. 450-3.

Wang, S., Li, W., Liu, S. and Xu, J. (2016) 'RaptorX-Property: a web server for protein structure property prediction', *Nucleic Acids Res,* 44(W1), pp. W430-5.

Weeks, A. R. and Breeuwer, J. A. (2001) 'Wolbachia-induced parthenogenesis in a genus of phytophagous mites', *Proc Biol Sci,* 268(1482), pp. 2245-51.

Werren, J. H., Baldo, L. and Clark, M. E. (2008) 'Wolbachia: master manipulators of invertebrate biology', *Nat Rev Microbiol,* 6(10), pp. 741-51.

White-Cooper, H. (2012) 'Tissue, cell type and stage-specific ectopic gene expression and RNAi induction in the Drosophila testis', *Spermatogenesis,* 2(1), pp. 11-22.

Wilson, A. L., Boelaert, M., Kleinschmidt, I., Pinder, M., Scott, T. W., Tusting, L. S. and Lindsay, S. W. (2015) 'Evidence-based vector control? Improving the quality of vector control trials', *Trends Parasitol,* 31(8), pp. 380-90.

Yamada, R., Floate, K. D., Riegler, M. and O'Neill, S. L. (2007) 'Male development time influences the strength of Wolbachia-induced cytoplasmic incompatibility expression in Drosophila melanogaster', *Genetics,* 177(2), pp. 801-8.

Yamaguchi, Y., Park, J. H. and Inouye, M. (2011) 'Toxin-antitoxin systems in bacteria and archaea', *Annu Rev Genet,* 45, pp. 61-79.

Yen, J. H. and Barr, A. R. (1973) 'The etiological agent of cytoplasmic incompatibility in Culex pipiens', *J Invertebr Pathol,* 22(2), pp. 242-50.

Zanluca, C., Melo, V. C., Mosimann, A. L., Santos, G. I., Santos, C. N. and Luz, K. (2015) 'First report of autochthonous transmission of Zika virus in Brazil', *Mem Inst Oswaldo Cruz,* 110(4), pp. 569-72.

Zeh, D. W., Zeh, J. A. and Bonilla, M. M. (2005) 'Wolbachia, sex ratio bias and apparent male killing in the harlequin beetle riding pseudoscorpion', *Heredity,* 95(1), pp. 41-49.

Zhang, D., Lees, R. S., Xi, Z., Gilles, J. R. and Bourtzis, K. (2015a) 'Combining the Sterile Insect Technique with Wolbachia-Based Approaches: II--A Safer Approach to Aedes albopictus Population Suppression Programmes, Designed to Minimize the Consequences of Inadvertent Female Release', *PLoS One,* 10(8), pp. e0135194.

Zhang, D., Zheng, X., Xi, Z., Bourtzis, K. and Gilles, J. R. (2015b) 'Combining the sterile insect technique with the incompatible insect technique: I-impact of wolbachia infection on the fitness of triple- and double-infected strains of Aedes albopictus', *PLoS One,* 10(4), pp. e0121126.

Zheng, X., Zhang, D., Li, Y., Yang, C., Wu, Y., Liang, X., Liang, Y., Pan, X., Hu, L., Sun, Q., Wang, X., Wei, Y., Zhu, J., Qian, W., Yan, Z., Parker, A. G., Gilles, J. R. L., Bourtzis, K., Bouyer, J., Tang, M., Zheng, B., Yu, J., Liu, J., Zhuang, J., Hu, Z., Zhang, M., Gong, J. T., Hong, X. Y., Zhang, Z., Lin, L., Liu, Q., Hu, Z., Wu, Z., Baton, L. A., Hoffmann, A. A. and Xi, Z. (2019) 'Incompatible and sterile insect techniques combined eliminate mosquitoes', *Nature,* 572(7767), pp. 56-61.